ALMA MATER STUDIORUM
UNIVERSITÀ DI BOLOGNA

DOTTORATO DI RICERCA IN

SCIENZE E TECNOLOGIE AGRARIE, AMBIENTALI E ALIMENTARI

Ciclo 38

Settore Concorsuale: 07/C1 - INGEGNERIA AGRARIA, FORESTALE E DEI BIOSISTEMI

Settore Scientifico Disciplinare: AGR/08 - IDRAULICA AGRARIA E SISTEMAZIONI IDRAULICO-FORESTALI

ADVANCING THE MONITORING OF SOIL-PLANT-ATMOSPHERE INTERACTIONS: INSIGHTS INTO COSMIC-RAY NEUTRON SENSING AND MULTI-SENSOR MONITORING IN VINEYARDS AND ORCHARDS.

Presentata da: Riccardo Mazzoleni

Coordinatore Dottorato

Diana Di Gioia

Supervisore

Gabriele Baroni

Co-supervisore

Ilaria Filippetti

Esame finale anno 2026

Synopsis

The sustainable management of water resources in agriculture demands accurate and continuous monitoring of soil and plant water status across multiple spatial and temporal scales. As climate crisis intensifies and irrigation becomes an increasingly dominant component of agricultural water use, the ability to quantify soil water content (SWC) and understand its interaction with plant physiology and atmospheric drivers is essential. In this context, innovative sensing technologies and integrative approaches capable of characterizing the full soil-plant-atmosphere continuum (SPAC) are crucial.

This thesis develops and validates an integrated monitoring framework combining Cosmic-Ray Neutron Sensing (CRNS) and plant physiological measurements to enhance the quantification of SWC and its influence in agricultural fields. The work spans three experimental chapters, each addressing a key dimension of the problem, from CRNS-derived SWC detection under diverse irrigation systems (Chapter 2), to the eco-physiological interpretation of soil and atmospheric drivers in vineyards (Chapter 3), and finally, to the integration of continuous soil, plant, and atmospheric data for modelling SPAC dynamics (Chapter 4).

The first objective was to evaluate the performance of CRNS for irrigation monitoring in different agricultural systems. The research was conducted at two commercial sites in northern Italy: a vineyard employing subsurface drip irrigation (SDI) and a walnut orchard using micro-sprinkler irrigation (MSI). At both sites, CRNS sensors were calibrated following a consistent procedure through soil sampling, and corrections were applied to compensate for atmospheric pressure, humidity, and incoming neutron intensity, including both the classical correction based on neutron monitoring data base (NMDB) and a muon-based in situ approach.

At the vineyard site, CRNS-derived SWC showed a consistent and sensitive response to irrigation events, with statistically significant increases in SWC during irrigation periods ($p < 0.001$). The 2023 dataset confirmed that CRNS effectively captured short-term variations in the main root zone (~50 cm), while subsequent measurements in 2024 suggested that SWC remained above the critical threshold of the wilting point (WP). Comparisons with point-scale (PS) sensors demonstrated that CRNS provided smoother temporal patterns and a more stable representation of SWC, while PS sensors recorded sharper fluctuations that tended to overestimate SWC. In the walnut orchard, the heterogeneous irrigation layout had a clear effect on CRNS performance. During the uniformly irrigated 2022 season, SWC showed a significant increase ($p < 0.001$), while in 2023, when irrigation was applied alternately across three sectors, the sensor response was weaker and correlations were lower ($p < 0.05$), consistent with the reduced spatial extent of water application. These findings confirmed CRNS sensitivity to the spatial extent and proximity of water application. Overall, Chapter 2 demonstrated that CRNS is a robust, non-invasive tool for detecting irrigation-induced SWC variations and that local calibration combined with atmospheric correction improves its applicability in managed agricultural systems.

Building on these results, Chapter 3 investigated how CRNS-derived SWC interacts with plant physiological responses and atmospheric demand in a commercial vineyard (*Vitis vinifera* L.) cultivated with local grape varieties Pignoletto (PG) and Trebbiano Romagnolo (TR). The study integrated continuous CRNS data, normalized into extractable soil water (ESW) to represent plant-available water, with periodic measurements of midday stem water potential (Ψ_{stem}), berry composition traits (total soluble solids, TSS, and titratable acidity, TA), vapor pressure deficit (VPD), and canopy vigour derived from remote sensing NDVI observations.

The two growing seasons provided contrasting hydrological conditions. In 2023, abundant rainfall produced generally non-limiting water availability, reflected in Ψ_{stem} values between -0.66 and -1.06 MPa. Under these conditions, vines exhibited uniform ripening and weak coupling with atmospheric demand. In contrast, the drier 2024 season induced more negative Ψ_{stem} (-0.95 to -1.12 MPa) and faster sugar accumulation, especially in TR. Principal Component Analysis (PCA) explained 65 % of variance in 2023 and 81.5 % in 2024, revealing that environmental drivers (ESW, VPD) became increasingly aligned with physiological and compositional parameters under more negative Ψ_{stem}. These results highlighted the dynamic relationship between ESW and atmospheric demand, showing that CRNS-derived ESW acts as a reliable integrator of vineyard water status. The chapter established the value of CRNS for eco-physiological interpretation, linking SWC dynamics to plant behaviour and grapes development.

The final stage of the research, presented in Chapter 4, extended this integrative approach to a semi-arid environment in Renmark, South Australia, where viticulture depends almost entirely on irrigation. Here, the study implemented a continuous multi-sensor monitoring system to characterize the SPAC interactions under daily drip irrigation. The setup included CRNS for field-scale SWC, stem psychrometers for determining Ψ_{stem} (MPa), sap flow sensors for measuring the total flow rate (TFR, L h^{-1}), and meteorological instrumentation for VPD and related variables. The analysis focused on quantifying the relative influence of soil and atmospheric drivers on vine hydraulics using both exploratory statistics and Linear Mixed-Effects Models (LMMs).

Daytime Ψ_{stem} values remained above -1.5 MPa throughout the study period, indicating non-stressed conditions, while sap flow displayed consistent diurnal patterns corresponding to VPD cycles. Correlation and PCA analyses identified a dominant atmospheric axis (VPD-TFR-Ψ_{stem}) explaining roughly 85 % of total variance, with SWC contributing independently on an orthogonal axis. LMMs confirmed VPD as the main predictor of vine water status ($p < 0.001$), whereas SWC exerted a significant positive effect only on the nighttime Ψ_{stem} ($p < 0.05$), indicating enhanced stem rehydration under higher SWC. Model fits were stronger during daytime (R^2 = 0.55-0.71) than at night (R^2 = 0.22-0.38), reflecting the predominance of evaporative control over transpiration. These findings demonstrated that combining continuous sensing with statistical modelling provides an effective framework for quantifying real-time SPAC dynamics and for supporting adaptive irrigation strategies in water-limited viticulture.

Taken together, the three experimental chapters provided a coherent narrative that advances both the methodology and interpretation of CRNS-based SWC monitoring. The results confirmed that CRNS can serve as a physically meaningful bridge between PS and remote sensing observations, delivering spatially integrated information essential for monitoring the soil water status. The inclusion of atmospheric and physiological data allowed the thesis to move beyond sensor validation toward a functional understanding of SPAC interactions, where the relative contributions of SWC and VPD can be disentangled and quantified.

In addition, this thesis contributed to the development of a multi-sensor framework for hydrological monitoring and modelling, demonstrating its feasibility under contrasting climatic and management conditions, from temperate to semi-arid systems, and from drip, below and above the soil, to micro-sprinkler irrigation. The methodological innovations included improved CRNS calibration and correction procedures, standardized approaches for integrating soil and plant data, and the application of mixed-effects modelling to continuous SPAC observations and interpretations.

In conclusion, this thesis contributed to establish an operational and conceptual foundation for large-scale, non-invasive monitoring of SWC and plant water relations. It confirms the robustness of CRNS under uniformly irrigated conditions, demonstrates its compatibility with advanced physiological and meteorological sensing, and illustrates how such integration enables a holistic understanding of agricultural water dynamics. The results contribute to define a road map towards the future development of data-driven agricultural water governance in Mediterranean and semi-arid regions alike and a sustainable irrigation management.

Acknowledgements

This work would not have been possible without the vision, trust, and invaluable contributions of the people I met and had the honour of collaborating with over these years. My deepest gratitude goes to Finapp S.p.A., whose contribution shaped the foundation of this study. My special thanks go to Luca Stevanato, Stefano Gianessi, and Enrico Gazzola for their continued openness, technical insight, and encouragement.

A heartfelt thank you goes to the people I met in Australia, who inspired me and offered a renewed perspective on applied science. I am deeply grateful to the entire ICT International team for making possible the project we carried out during those months “down under.” My deepest appreciation goes to Beng Umali, for welcoming me, guiding me, and making me feel part of his family, both professionally and personally.

My sincere thanks go to all the members of the Hydrology Group at the University of Bologna, who contributed significantly to this work both in and out of the field. I wish to mention Sadra Emamalizadeh, Gunay Hasanli, Francesco Vinzio, and Marco Benfenati, brilliant colleagues with whom I had the privilege of collaborating and, in some cases, co-supervising their master’s thesis works, which represent a meaningful part of this Thesis.

I owe profound gratitude to my supervisors.

To Prof. Ilaria Filippetti and her group, for her inspiration, guidance and constant availability. She has been a fundamental presence in my personal and professional growth, shaping my approach to research and knowledge of Viticulture. A special thanks to Gianluca Allegro and Gabriele Valentini. Their vision and scientific curiosity have been a true source of inspiration and an example to follow.

To Prof. Gabriele Baroni, for his exceptional guidance, insight, and humanity. His open-mindedness has made this research path both intellectually free and personally rewarding. His ability to keep things simple while giving genuine value to the people in his group has been a constant source of inspiration.

Grazie infine alla mia famiglia, agli amici e amiche che da tempo camminano con me, condividendo pezzi di strada, scelte e momenti che hanno dato senso a questo percorso.

A Enrico e Roberta, per il loro sostegno costante, la fiducia e l’esempio che hanno saputo darmi. A Elisa, quotidiana fonte di ispirazione, forza e tenacia, e per tutto l’amore e la complicità che rendono possibile ogni mio passo.

Riccardo

Contents

1. Introduction and motivations

1.1. General context

The Mediterranean basin lends its name to the Mediterranean climate, which is identified as a subtropical to midlatitude climate with overall semiarid conditions. In the Mediterranean regions, like other Mediterranean climate zones such as California, South and southwest Australia, and parts of Southern Africa, water scarcity remains a persistent concern (Seager et al., 2014). In recent decades, the Mediterranean has been identified as a global change hot spot (Giorgi, 2006) and the past ten years have seen record-breaking summer temperatures (Büntgen et al., 2024). Nevertheless, this environment is widely recognized as strongly seasonal, with sharp fluctuations in water availability and scarcity.

Nowadays, agriculture is the largest consumer of freshwater, accounting for nearly 80%, and a major contributor to greenhouse gas emissions (Tang et al., 2021). As such, it is both highly vulnerable to climate and environmental changes and simultaneously a key driver of them (Foley et al., 2011). In the agricultural context, increasing world temperature brings to the reduction of water availability and, with its influence to precipitations trends, to the alteration of both the soil water balance and vegetation growth (Kang et al., 2009; Shukla et al., 2019). Hence, the preservation and efficient use of water in agriculture, especially through careful monitoring and management of soil water content (SWC), is essential to reduce the sector's water footprint and promote sustainable irrigation practices.

1.2. Soil water content measurements techniques

The characteristic temporal and spatial scales of SWC are highly variable and range from minutes to years and from centimeters to kilometers (Robinson et al., 2008a; Vereecken et al., 2014). Consequently, SWC information is needed across multiple spatial and temporal scales. It has long been recognized that the characterization of SWC data depends on three key attributes: the volume of a single measurement, the spatial resolution between measurements and the overall area covered by the dataset (Blöschl and Sivapalan, 1995). For a comprehensible representation of the scales of SWC measurement techniques, simplifications are necessary, and the volume, spatial and temporal resolutions are often mixed (Bogena et al., 2015) (Figure 1).

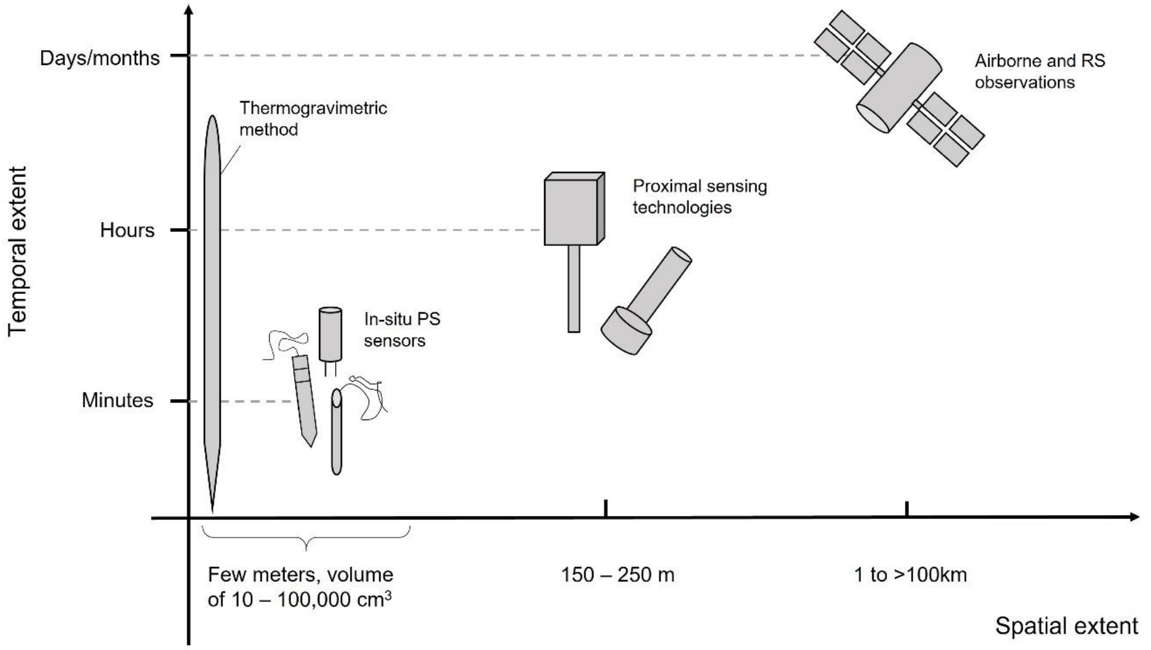

Figure 1: Scales of various SWC measurement techniques and technologies. Adapted and modified following Bogena et al. (2015) and Robinson et al. (2008).

The reference standard for SWC measurements is the direct thermogravimetric method, commonly based on the weight loss from drying a soil sample at 105 °C. Such determination is laborious, destructive and generally inconvenient, which limits both the temporal and spatial resolution of observations (Marshall et al., 1996).

To overcome this, a range of in-situ point-scale (PS) sensor types based on various electromagnetic techniques can be used to continuously measure SWC, e.g., time domain reflectometry (TDR), time domain transmission (TDT), impedance or capacitance sensors and electromagnetic induction (EMI) (Bogena et al., 2017; Brogi et al., 2019). These sensors typically have measurement volumes in the order of ~10 - 1000 cm^3, which strongly depends on the length of the measurement rod, and their efficacy mostly relies on the success of their deployment (Babaeian et al., 2019). However, geostatistical methods nowadays allow for the integration of these measurements, enabling the comparisons with other SWC measurement techniques and the generation of spatial maps (Bogena et al., 2010).

As an alternative, non-invasive SWC measurement techniques are active neutron probes (ANP) and nuclear magnetic resonance (NMR). ANP provide large-volume measurements (> 100,000 cm^3) of undisturbed soil but are semi-invasive, costly, and require regulatory approval (Evett, 2000). NMR is fully non-destructive and enables deep profiling, though it is expensive and less accurate (Walsh et al., 2011). Both are suited for time-lapse monitoring but not for large-scale sensor networks.

SWC can also be determined from a wide variety of air and spaceborne remote sensing (RS) techniques. These can be categorized based on their measurement principles: optical sensors operating in the near-infrared and shortwave infrared ranges, thermal sensors, active microwave sensors, and passive microwave sensors (Babaeian et al., 2019). Airborne SWC surveys, though limited in temporal and spatial extent (≤100 km), offer high spatial resolution (1-100 m) and are often used for satellite mission validation (Mengen et al., 2021). In contrast, spaceborne RS observations, despite their increasing popularity due to their capacity to cover large areas and inaccessible regions, provide a coarser resolution (>25 km), shallower sensing depth (~5 cm) (Loew et al., 2017). Besides, both methods require in-situ or intermediate-scale data for the assessment and the understanding of the value of the signal in the different applications (Emamalizadeh et al., 2024).

In most cases, SWC measurement techniques exhibit a trade-off between spatial and temporal resolution, with larger spatial scales typically corresponding to lower temporal resolution (Bogena et al., 2015). However, research advancements on proximal sensing technologies ultimately showed potential to overcome this limitation (Hardie, 2020). Notably, global navigation satellite system (GNSS) reflectometry, gamma ray monitoring, and cosmic ray neutron sensing (CRNS) have emerged as promising approaches for capturing SWC at intermediate spatial and temporal scales. GNSS reflectometry, by analyzing changes in signal amplitude and phase caused by soil permittivity, measures topsoil moisture (2-5 cm depth) with sub-daily resolution and maximum 200 m footprint extent, but is limited by station placement in urban areas (Larson et al., 2010; Rodriguez-Alvarez et al., 2009). Gamma ray monitoring using naturally occurring radionuclides (^{232}Th, ^{238}U, ^{40}K), provides near-continuous data over ~25 m radius and ~30 cm depth, with existing ground stations offering scalable coverage, unlike costly airborne surveys (Baldoncini et al., 2018; Bogena et al., 2015). Lastly, CRNS has emerged as a reliable approach for non-invasive and continuous monitoring of SWC (Zreda et al., 2008). As CRNS represents a key methodological component of this thesis, the next section provides a targeted discussion of its theoretical basis and practical implications.

1.2.1. Cosmic-ray neutron sensing

Primary cosmic rays (~1 GeV) entering Earth's atmosphere generate secondary particle showers, including neutrons, mostly generated from protons by the splitting of nitrogen and oxygen (Köhli et al., 2015). As high-energy neutrons lose energy, interactions shift toward scattering, with hydrogen being the dominant moderator in the epithermal range (~0.5 eV-

100 keV). Most of the near-surface hydrogen in terrestrial environments is stored in soil water. Therefore, the measurement of epithermal neutrons, thus the counting of epithermal neutrons, allows for the measurement of SWC (Desilets et al., 2010; Köhli et al., 2021; Zreda et al., 2012). Besides, near the soil surface, epithermal neutron density is inversely related to environmental hydrogen content (Köhli et al., 2015; Zreda et al., 2008; Zreda et al., 2012). However, neutron intensity is also influenced by air pressure (Desilets and Zreda, 2003), air humidity (Rosolem et al., 2013), and incoming cosmic ray flux (Desilets and Zreda, 2001), which must be corrected for accurate hydrogen estimation, and thus SWC.

CRNS are nowadays operated above the ground surface, at ~1-2 m height. In this configuration, the derived signal is representative for 120 to 250 m radius and soil depths of 15 to 70 cm, depending on SWC (Köhli et al., 2015; Schrön et al., 2017).

New-generation commercial CRNS devices adopt advanced detection materials, enabling neutron conversion through solid ^{6}Li (Fersch et al., 2020), solid ^{10}B (Weimar et al., 2020), or scintillator-based technologies (Stevanato et al., 2019). To measure epithermal neutrons, the bare neutron sensors are shielded with high density polyethylene (HDPE), which contains large amounts of hydrogen and is very efficient in moderating neutrons to lower energy levels (Zreda et al., 2012). While neutron density may be affected by changes in the cosmic ray intensity and by additional hydrogen sources, such as biomass and lattice water (Andreasen et al., 2017; Baatz et al., 2015), SWC can be estimated from the epithermal neutron intensity through a conversion function (Desilets et al., 2010).

Among various hydrological applications, CRNS has been ultimately assessed for monitoring SWC variations on agricultural field scales, particularly under irrigation (Baroni et al., 2018; Brogi et al., 2022, 2023; Gianessi et al., 2021; Han et al., 2016; Li et al., 2019). However, the relatively large footprint of the CRNS limits its ability to detect localized water applications and for this reason it is generally not well-suited for small irrigation research plots. Besides, the performance of the CRNS might be significantly affected by the choice of irrigation methods, provided that appropriate calibration and correction strategies are employed (Hawdon et al., 2014; Iwema et al., 2021; Schrön et al., 2017). Considering this, the debate regarding the suitability of CRNS in irrigated agricultural fields is still ongoing. Latest studies emphasized the need to integrate multiple methods and technologies for a more robust assessment of field-scale SWC (Emamalizadeh et al., 2024; Robinson et al., 2008a). This ongoing debate should not be seen as a limitation of the technology, but rather as the core scientific motivation of this Thesis, which aims to critically assess and expand the applicability of CRNS under irrigated agricultural conditions. This point will be further addressed in the dedicated paragraph (Section 1.4) outlining the study's objectives, where the role of CRNS within the broader research framework will be examined.

1.3. Towards an integrated monitoring approach

It is known that irrigation control systems based solely on SWC monitoring present several limitations, as plant water demand is regulated by the dynamic balance of all three components of the soil-plant-atmosphere continuum (SPAC) (Bwambale et al., 2022). Besides, plant growth is tightly linked to SWC, as this water is not only needed for evapotranspiration, but also controls the mobilization and availability of nutrients (Rodriguez-Iturbe, 2000). Thus, especially in arid and semi-arid regions, SWC is considered a driving force of agricultural productivity, with irrigation being often essential (Siebert et al., 2005). In response, plants often develop distinct adaptations to the hydrological cycle (Jacobsen et al., 2008). The diverse ways in which water interacts with vegetation across hydroclimatic gradients give rise to markedly different plant-water relationships and functional responses (Jackson and Colmer, 2005).

Within this broader context, viticulture represents a particularly relevant and sensitive agricultural sector. Water use in vineyards is a function of available water content of the soil (Lebon et al., 2003), and the co-occurrence of low SWC and high vapor pressure deficit (VPD) may trigger reductions in vegetation productivity driven by drought and heat (Zhou et al., 2019). Grapevine (*Vitis vinifera* L.), although is considered to be highly adaptable to water restrictions (Lovisolo et al., 2010), exhibits complex physiological responses to water deficits that can influence both vegetative growth and fruit development (Chaves et al., 2010; Valentini et al., 2022; Valentini at al., 2025). In this context, the ability to monitor plant water use and to understand water dynamics within the SPAC has become crucial for advancing both agricultural productivity and sustainability. Water movement from the soil to the atmosphere is driven by gradients in water potential (Ψ), traversing a series of hydraulic conductances, or resistances, along its pathway from bulk soil to the leaves (Delval et al., 2025). Rather than being static, these conductances often vary with Ψ, leading to complex, often nonlinear relationships between Ψ gradients and the resulting fluxes within the SPAC (Suter et al., 2019; Williamson et al., 2024). Accurately quantifying these hydraulic properties, especially under drought conditions, is fundamental to improving our understanding of plant water status and developing more resilient agricultural systems (Yu et al., 2020).

One of the key challenges lies in understanding the processes involved and capturing the variability that occurs across multiple spatial scales within agricultural fields. However, it is logistically a constraint to measure a large number of plants to address the question of *"how to tell the forest from the trees"* (Denmead, 1984), and research in the last decades has been oriented towards building scalable approaches (Asbjornsen et al., 2011). Driven by this, detailed spatial information on grapevine water status can be particularly useful for providing guidelines on viticultural management to optimize grape production (Gambetta et al., 2020). Measuring Ψ relative to the leaf (Ψ_{leaf}) or stem (Ψ_{stem}) is an effective method to assess grapevine water status (Choné, 2001). Vine water use is closely linked to stomatal conductance (g_s), a key physiological parameter regulating transpiration (Bota et al., 2001; Gambetta et al., 2020). Several studies have shown that stomatal aperture is co-regulated by SWC and VPD (Gowdy et al., 2022; Lavoie-Lamoureux et al., 2017; Liu et al., 2020; Prieto et al., 2010). The g_s responds to variations in water potential, particularly Ψ_{leaf}. However, defining reliable water stress thresholds based on Ψ_{leaf} remains challenging, as it is influenced by several factors, including the genotype (Schultz, 2003), prevailing environmental conditions at the time of measurement, such as VPD and SWC, and the specific type of measurement used (e.g., pre-dawn Ψ, midday Ψ_{leaf}, or midday Ψ_{stem}) (Choné, 2001). Grapevine water status, and thus stress, can also be assessed through chlorophyll fluorescence. At the leaf level, measurements are typically performed using handheld fluorometers, which provide a wide range of parameters commonly employed in plant stress physiology research (Galat Giorgi et al., 2019; Murchie and Lawson, 2013), and the correlation with standard indicators of plant water status (i.e., g_s, Ψ) have been described in different studies (Cifre et al., 2005; Medrano, 2002).

Understanding the complex interactions between plant water status and other functional physiological variables within the SPAC remains challenging, as conventional correlation analyses often fall short in capturing their dynamic and nonlinear nature. Furthermore, most commonly used plant water status indicators rely on discontinuous measurements, providing only isolated acquisitions at specific times during the season (Benyahia et al., 2023). This highlights the critical need for continuous monitoring systems and integrated data approaches to obtain a more comprehensive and temporally resolved understanding of plant-environment interactions (Brillante et al., 2016). Other technologies, such as the sap flow sensors and psychrometers, are also able to provide continuous and direct information about the plant water uptake and plant Ψ (Dainese et al., 2022; Mancha et al., 2021; Martinez et al., 2011).

It has been documented that sap flow rates are affected, other than by the genotype, by the SWC and changes in the environmental conditions over time (Dragoni et al., 2006; Zhang et al., 2011).

As such, integrating multiple, complementary sensors offers a more holistic and temporally resolved view of vine water status. This integrated approach could not only improve the accuracy of plant stress detection but also enhance our capacity to interpret plant-environment interactions under varying hydroclimatic conditions. In the long term, such multi-sensor frameworks hold great potential for the development of site-specific, model-driven irrigation strategies.

1.4. Objectives of the study

Building on the discussion above, this thesis aims to tackle current challenges in agricultural water monitoring, particularly in viticulture, by developing an integrated approach that combines large-scale sensing technologies with high-resolution, plant-level measurements. The specific objectives of the study are as follows:

i. Evaluation and assessment of CRNS for irrigation monitoring in agricultural systems.

The primary goal was to assess the performance of the CRNS in two commercial irrigated agricultural environments, with the intent of reducing the uncertainty surrounding its applicability under such conditions. The study focused on validating large-scale CRNS data over a network of PS sensors to determine how accurately the sensor can detect irrigation-induced variations in SWC. Achieving this objective is essential for establishing calibration protocols and signal correction strategies that enhance the reliability of CRNS as a tool for irrigation monitoring.

ii. Integration of CRNS-derived SWC with grapevine physiological and environmental variables.

The research investigated the interactions between SWC dynamics, as continuously monitored by CRNS, and grapevine physiological responses, specifically Ψ_{stem} and grape berries maturation traits. By incorporating VPD as a key driver of atmospheric water demand, the study evaluated vine responses not only to water availability but also to evaporative demand. This multidimensional analysis helped to overcome the limitations of SWC-based interpretations alone, providing a more holistic understanding of grapevine water status and its adaptive capacity.

iii. Integration of SWC, VPD, vine Ψ, and sap flow into a continuous advanced sensor monitoring system.

The final objective was the design and demonstration of an integrated monitoring system that combines CRNS and VPD data with continuous measurements from additional advanced sensors for monitoring vine Ψ via psychrometers, and sap flow sensors. Merging these variables into a single, real-time sensing framework represented a crucial step in this research. Such an approach may be an indication for the development of more precise and dynamic irrigation management models, informed by comprehensive data that reflects the full complexity of water dynamics within the vineyard system.

1.5. References

Andreasen, M., Jensen, K. H., Desilets, D., Franz, T. E., Zreda, M., Bogena, H. R., & Looms, M. C. (2017). Status and Perspectives on the Cosmic-Ray Neutron Method for Soil Moisture Estimation and Other Environmental Science Applications. *Vadose Zone Journal*, *16*(8), vzj2017.04.0086. https://doi.org/10.2136/vzj2017.04.0086

Asbjornsen, H., Goldsmith, G. R., Alvarado-Barrientos, M. S., Rebel, K., Van Osch, F. P., Rietkerk, M., Chen, J., Gotsch, S., Tobón, C., Geissert, D. R., Gómez-Tagle, A., Vache, K., & Dawson, T. E. (2011). Ecohydrological advances and applications in plant–water relations research: A review. *Journal of Plant Ecology*, *4*(1–2), 3–22. https://doi.org/10.1093/jpe/rtr005

Baatz, R., Bogena, H. R., Hendricks Franssen, H.-J., Huisman, J. A., Montzka, C., & Vereecken, H. (2015). An empirical vegetation correction for soil water content quantification using cosmic ray probes. *Water Resources Research*, *51*(4), 2030–2046. https://doi.org/10.1002/2014WR016443

Babaeian, E., Sadeghi, M., Jones, S. B., Montzka, C., Vereecken, H., & Tuller, M. (2019). Ground, Proximal, and Satellite Remote Sensing of Soil Moisture. *Reviews of Geophysics*, *57*(2), 530–616. https://doi.org/10.1029/2018RG000618

Baldoncini, M., Albéri, M., Bottardi, C., Chiarelli, E., Raptis, K. G. C., Strati, V., & Mantovani, F. (2018). Investigating the potentialities of Monte Carlo simulation for assessing soil water content via proximal gamma-ray spectroscopy. *Journal of Environmental Radioactivity*, *192*, 105–116. https://doi.org/10.1016/j.jenvrad.2018.06.001

Baroni, G., Scheiffele, L. M., Schrön, M., Ingwersen, J., & Oswald, S. E. (2018). Uncertainty, sensitivity and improvements in soil moisture estimation with cosmic-ray neutron sensing. *Journal of Hydrology*, *564*, 873–887. https://doi.org/10.1016/j.jhydrol.2018.07.053

Benyahia, F., Bastos Campos, F., Ben Abdelkader, A., Basile, B., Tagliavini, M., Andreotti, C., & Zanotelli, D. (2023). Assessing Grapevine Water Status by Integrating Vine Transpiration, Leaf Gas Exchanges, Chlorophyll Fluorescence and Sap Flow Measurements. *Agronomy*, *13*(2), 464. https://doi.org/10.3390/agronomy13020464

Blöschl, G., & Sivapalan, M. (1995). Scale issues in hydrological modelling: A review. *Hydrological Processes*, *9*(3–4), 251–290. https://doi.org/10.1002/hyp.3360090305

Bogena, H. R., Herbst, M., Huisman, J. A., Rosenbaum, U., Weuthen, A., & Vereecken, H. (2010). Potential of Wireless Sensor Networks for Measuring Soil Water Content VariabilityAll rights reserved. No part of this periodical may be reproduced or transmitted in any form or by any means, electronic or mechanical, including photocopying, recording, or any information storage and retrieval system, without permission in writing from the publisher. *Vadose Zone Journal*, *9*(4), 1002–1013. https://doi.org/10.2136/vzj2009.0173

Bogena, H. R., Huisman, J. A., Güntner, A., Hübner, C., Kusche, J., Jonard, F., Vey, S., & Vereecken, H. (2015). Emerging methods for noninvasive sensing of soil moisture dynamics from field to catchment scale: A review. *WIREs Water*, *2*(6), 635–647. https://doi.org/10.1002/wat2.1097

Bogena, H. R., Huisman, J. A., Schilling, B., Weuthen, A., & Vereecken, H. (2017). Effective Calibration of Low-Cost Soil Water Content Sensors. *Sensors*, *17*(1), 208. https://doi.org/10.3390/s17010208

Bota, B. J., Flexas, J., & Medrano, H. (2001). Genetic variability of photosynthesis and water use in Balearic grapevine cultivars. *Annals of Applied Biology*, *138*(3), 353–361. https://doi.org/10.1111/j.1744-7348.2001.tb00120.x

Brillante, L., Bois, B., Lévêque, J., & Mathieu, O. (2016). Variations in soil-water use by grapevine according to plant water status and soil physical-chemical characteristics—A 3D spatio-temporal analysis. *European Journal of Agronomy*, *77*, 122–135. https://doi.org/10.1016/j.eja.2016.04.004

Brogi, C., Bogena, H. R., Köhli, M., Huisman, J. A., Hendricks Franssen, H.-J., & Dombrowski, O. (2022). Feasibility of irrigation monitoring with cosmic-ray neutron sensors. *Geoscientific Instrumentation, Methods and Data Systems*, *11*(2), 451–469. https://doi.org/10.5194/gi-11-451-2022

Brogi, C., Huisman, J. A., Pätzold, S., von Hebel, C., Weihermüller, L., Kaufmann, M. S., van der Kruk, J., & Vereecken, H. (2019). Large-scale soil mapping using multi-configuration EMI and supervised image classification. *Geoderma*, *335*, 133–148. https://doi.org/10.1016/j.geoderma.2018.08.001

Brogi, C., Pisinaras, V., Köhli, M., Dombrowski, O., Hendricks Franssen, H.-J., Babakos, K., Chatzi, A., Panagopoulos, A., & Bogena, H. R. (2023). Monitoring Irrigation in Small Orchards with Cosmic-Ray Neutron Sensors. *Sensors*, *23*(5), Article 5. https://doi.org/10.3390/s23052378

Büntgen, U., Reinig, F., Verstege, A., Piermattei, A., Kunz, M., Krusic, P., Slavin, P., Štěpánek, P., Torbenson, M., del Castillo, E. M., Arosio, T., Kirdyanov, A., Oppenheimer, C., Trnka, M., Palosse, A., Bebchuk, T., Camarero, J. J., & Esper, J. (2024). Recent summer warming over the western Mediterranean region is unprecedented since medieval times. *Global and Planetary Change*, *232*, 104336. https://doi.org/10.1016/j.gloplacha.2023.104336

Bwambale, E., Abagale, F. K., & Anornu, G. K. (2022). Smart irrigation monitoring and control strategies for improving water use efficiency in precision agriculture: A review. *Agricultural Water Management*, *260*, 107324. https://doi.org/10.1016/j.agwat.2021.107324

Chaves, M. M., Zarrouk, O., Francisco, R., Costa, J. M., Santos, T., Regalado, A. P., Rodrigues, M. L., & Lopes, C. M. (2010). Grapevine under deficit irrigation: Hints from physiological and molecular data. *Annals of Botany*, *105*(5), 661–676. https://doi.org/10.1093/aob/mcq030

Choné, X. (2001). Stem Water Potential is a Sensitive Indicator of Grapevine Water Status. *Annals of Botany*, *87*(4), 477–483. https://doi.org/10.1006/anbo.2000.1361

Cifre, J., Bota, J., Escalona, J. M., Medrano, H., & Flexas, J. (2005). Physiological tools for irrigation scheduling in grapevine (*Vitis vinifera* L.). *Agriculture, Ecosystems & Environment*, *106*(2), 159–170. https://doi.org/10.1016/j.agee.2004.10.005

Dainese, R., Lopes, B. de C. F. L., Fourcaud, T., & Tarantino, A. (2022). Evaluation of instruments for monitoring the soil–plant continuum. *Geomechanics for Energy and the Environment*, *30*, 100256. https://doi.org/10.1016/j.gete.2021.100256

Delval, L., Vanderborght, J., & Javaux, M. (2025). Combination of plant and soil water potential monitoring and modelling demonstrates soil-root hydraulic disconnection during drought. *Plant and Soil*, *511*(1), 1449–1472. https://doi.org/10.1007/s11104-024-07062-2

Denmead, O. T. (1984). Plant Physiological Methods for Studying Evapotranspiration: Problems of Telling the Forest from the Trees. In M. L. Sharma (Ed.), *Developments in Agricultural and Managed Forest Ecology* (Vol. 13, pp. 167–189). Elsevier. https://doi.org/10.1016/B978-0-444-42250-7.50014-8

Desilets, D., & Zreda, M. (2001). On scaling cosmogenic nuclide production rates for altitude and latitude using cosmic-ray measurements. *Earth and Planetary Science Letters*, *193*(1–2), 213–225. https://doi.org/10.1016/S0012-821X(01)00477-0

Desilets, D., & Zreda, M. (2003). Spatial and temporal distribution of secondary cosmic-ray nucleon intensities and applications to in situ cosmogenic dating. *Earth and Planetary Science Letters*, *206*(1), 21–42. https://doi.org/10.1016/S0012-821X(02)01088-9

Desilets, D., Zreda, M., & Ferré, T. P. A. (2010). Nature's neutron probe: Land surface hydrology at an elusive scale with cosmic rays. *Water Resources Research*, *46*(11). https://doi.org/10.1029/2009WR008726

Dragoni, D., Lakso, A. N., Piccioni, R. M., & Tarara, J. M. (2006). Transpiration of Grapevines in the Humid Northeastern United States. *American Journal of Enology and Viticulture*, *57*(4), 460–467. https://doi.org/10.5344/ajev.2006.57.4.460

Emamalizadeh, S., Pirola, A., Alessandrini, C., Balenzano, A., & Baroni, G. (2024). Comparison of Soil Water Content from SCATSAR-SWI and Cosmic Ray Neutron Sensing at Four Agricultural Sites in Northern Italy: Insights from Spatial Variability and Representativeness. *Remote Sensing*, *16*(18), Article 18. https://doi.org/10.3390/rs16183384

Evett, S. R. (2000). Exploits and endeavours in soil water management and conservation using nuclear techniques. *Nuclear Techniques in Integrated Plant Nutrient, Water and Soil Management*, *16*, 151.

Fersch, B., Francke, T., Heistermann, M., Schrön, M., Döpper, V., Jakobi, J., Baroni, G., Blume, T., Bogena, H., Budach, C., Gränzig, T., Förster, M., Güntner, A., Hendricks Franssen, H.-J., Kasner, M., Köhli, M., Kleinschmit, B., Kunstmann, H., Patil, A., … Oswald,

S. (2020). A dense network of cosmic-ray neutron sensors for soil moisture observation in a highly instrumented pre-Alpine headwater catchment in Germany. *Earth System Science Data*, *12*(3), 2289–2309. https://doi.org/10.5194/essd-12-2289-2020

Foley, J. A., Ramankutty, N., Brauman, K. A., Cassidy, E. S., Gerber, J. S., Johnston, M., Mueller, N. D., O'Connell, C., Ray, D. K., West, P. C., Balzer, C., Bennett, E. M., Carpenter, S. R., Hill, J., Monfreda, C., Polasky, S., Rockström, J., Sheehan, J., Siebert, S., … Zaks, D. P. M. (2011). Solutions for a cultivated planet. *Nature*, *478*(7369), 337–342. https://doi.org/10.1038/nature10452

Galat Giorgi, E., Sadras, V. O., Keller, M., & Perez Peña, J. (2019). Interactive effects of high temperature and water deficit on Malbec grapevines. *Australian Journal of Grape and Wine Research*, *25*(3), 345–356. https://doi.org/10.1111/ajgw.12398

Gambetta, G. A., Herrera, J. C., Dayer, S., Feng, Q., Hochberg, U., & Castellarin, S. D. (2020). The physiology of drought stress in grapevine: Towards an integrative definition of drought tolerance. *Journal of Experimental Botany*, *71*(16), 4658–4676. https://doi.org/10.1093/jxb/eraa245

Gianessi, S., Polo, M., Stevanato, L., Lunardon, M., Ahmed, H. S., Weltin, G., Toloza, A., Budach, C., Bíró, P., Francke, T., Heistermann, M., Oswald, S. E., Fulajtar, E., Dercon, G., Heng, L. K., & Baroni, G. (2021). Assessment of a new non-invasive soil moisture sensor based on cosmic-ray neutrons. *2021 IEEE International Workshop on Metrology for Agriculture and Forestry (MetroAgriFor)*, 290–294. https://doi.org/10.1109/MetroAgriFor52389.2021.9628451

Giorgi, F. (2006). Climate change hot-spots. *Geophysical Research Letters*, *33*(8). https://doi.org/10.1029/2006GL025734

Gowdy, M., Pieri, P., Suter, B., Marguerit, E., Destrac-Irvine, A., Gambetta, G., & van Leeuwen, C. (2022). Estimating Bulk Stomatal Conductance in Grapevine Canopies. *Frontiers in Plant Science*, *13*. https://doi.org/10.3389/fpls.2022.839378

Han, X., Hendricks Franssen, H.-J., Jiménez Bello, M. Á., Rosolem, R., Bogena, H., Alzamora, F. M., Chanzy, A., & Vereecken, H. (2016). Simultaneous soil moisture and properties estimation for a drip irrigated field by assimilating cosmic-ray neutron intensity. *Journal of Hydrology*, *539*, 611–624. https://doi.org/10.1016/j.jhydrol.2016.05.050

Hardie, M. (2020). Review of Novel and Emerging Proximal Soil Moisture Sensors for Use in Agriculture. *Sensors*, *20*(23), Article 23. https://doi.org/10.3390/s20236934

Hawdon, A., McJannet, D., & Wallace, J. (2014). Calibration and correction procedures for cosmic-ray neutron soil moisture probes located across Australia. *Water Resources Research*, *50*(6), 5029–5043. https://doi.org/10.1002/2013WR015138

Iwema, J., Schrön, M., Koltermann Da Silva, J., Schweiser De Paiva Lopes, R., & Rosolem, R. (2021). Accuracy and precision of the cosmic-ray neutron sensor for soil moisture estimation at humid environments. *Hydrological Processes*, *35*(11), e14419. https://doi.org/10.1002/hyp.14419

Jackson, M. B., & Colmer, T. D. (2005). Response and Adaptation by Plants to Flooding Stress. *Annals of Botany*, *96*(4), 501–505. https://doi.org/10.1093/aob/mci205

Jacobsen, A. L., Pratt, R. B., Davis, S. D., & Ewers, F. W. (2008). Comparative community physiology: Nonconvergence in water relations among three semi-arid shrub communities. *New Phytologist*, *180*(1), 100–113. https://doi.org/10.1111/j.1469-8137.2008.02554.x

Kang, Y., Khan, S., & Ma, X. (2009). Climate change impacts on crop yield, crop water productivity and food security – A review. *Progress in Natural Science*, *19*(12), 1665–1674. https://doi.org/10.1016/j.pnsc.2009.08.001

Köhli, M., Schrön, M., Zreda, M., Schmidt, U., Dietrich, P., & Zacharias, S. (2015). Footprint characteristics revised for field-scale soil moisture monitoring with cosmic-ray neutrons. *Water Resources Research*, *51*(7), 5772–5790. https://doi.org/10.1002/2015WR017169

Köhli, M., Weimar, J., Schrön, M., Baatz, R., & Schmidt, U. (2021). Soil Moisture and Air Humidity Dependence of the Above-Ground Cosmic-Ray Neutron Intensity. *Frontiers in Water*, *2*. https://www.frontiersin.org/articles/10.3389/frwa.2020.544847

Larson, K. M., Braun, J. J., Small, E. E., Zavorotny, V. U., Gutmann, E. D., & Bilich, A. L. (2010). GPS Multipath and Its Relation to Near-Surface Soil Moisture Content. *IEEE Journal of Selected Topics in Applied Earth Observations and Remote Sensing*, *3*(1), 91–99. https://doi.org/10.1109/JSTARS.2009.2033612

Lavoie-Lamoureux, A., Sacco, D., Risse, P., & Lovisolo, C. (2017). Factors influencing stomatal conductance in response to water availability in grapevine: A meta-analysis. *Physiologia Plantarum*, *159*(4), 468–482. https://doi.org/10.1111/ppl.12530

Lebon, E., Dumas, V., Pieri, P., & Schultz, H. R. (2003). Modelling the seasonal dynamics of the soil water balance of vineyards. *Functional Plant Biology*, *30*(6), 699. https://doi.org/10.1071/FP02222

Li, D., Schrön, M., Köhli, M., Bogena, H., Weimar, J., Jiménez Bello, M. A., Han, X., Martínez Gimeno, M. A., Zacharias, S., Vereecken, H., & Hendricks Franssen, H.-J. (2019). Can Drip Irrigation be Scheduled with Cosmic-Ray Neutron Sensing? *Vadose Zone Journal*, *18*(1), 190053. https://doi.org/10.2136/vzj2019.05.0053

Liu, L., Gudmundsson, L., Hauser, M., Qin, D., Li, S., & Seneviratne, S. I. (2020). Soil moisture dominates dryness stress on ecosystem production globally. *Nature Communications*, *11*(1), 4892. https://doi.org/10.1038/s41467-020-18631-1

Loew, A., Bell, W., Brocca, L., Bulgin, C. E., Burdanowitz, J., Calbet, X., Donner, R. V., Ghent, D., Gruber, A., Kaminski, T., Kinzel, J., Klepp, C., Lambert, J.-C., Schaepman-Strub, G., Schröder, M., & Verhoelst, T. (2017). Validation practices for satellite-based Earth observation data across communities. *Reviews of Geophysics*, *55*(3), 779–817. https://doi.org/10.1002/2017RG000562

Lovisolo, C., Perrone, I., Carra, A., Ferrandino, A., Flexas, J., Medrano, H., & Schubert, A. (2010). Drought-induced changes in development and function of grapevine (Vitis spp.) organs and in their hydraulic and non-hydraulic interactions at the whole-plant level: A physiological and molecular update. *Functional Plant Biology*, *37*(2), 98–116. https://doi.org/10.1071/FP09191

Mancha, L. A., Uriarte, D., & Prieto, M. del H. (2021). Characterization of the Transpiration of a Vineyard under Different Irrigation Strategies Using Sap Flow Sensors. *Water*, *13*(20), 2867. https://doi.org/10.3390/w13202867

Marshall, T. J., Holmes, J. W., & Rose, C. W. (1996). *Soil Physics* (3rd ed.). Cambridge University Press. https://doi.org/10.1017/CBO9781139170673

Martinez, E., Cancela, J. J., Cuesta, T., & Neira, X. (2011). Review. Use of psychrometers in field measurements of plant material: Accuracy and handling difficulties. *SPANISH JOURNAL OF AGRICULTURAL RESEARCH*, *9*, 313–328.

Medrano, H. (2002). Regulation of Photosynthesis of C3 Plants in Response to Progressive Drought: Stomatal Conductance as a Reference Parameter. *Annals of Botany*, *89*(7), 895–905. https://doi.org/10.1093/aob/mcf079

Mengen, D., Montzka, C., Jagdhuber, T., Fluhrer, A., Brogi, C., Baum, S., Schüttemeyer, D., Bayat, B., Bogena, H., Coccia, A., Masalias, G., Trinkel, V., Jakobi, J., Jonard, F., Ma, Y., Mattia, F., Palmisano, D., Rascher, U., Satalino, G., … Vereecken, H. (2021). The SARSense Campaign: Air- and Space-Borne C- and L-Band SAR for the Analysis of Soil and Plant Parameters in Agriculture. *Remote Sensing*, *13*(4), 825. https://doi.org/10.3390/rs13040825

Murchie, E. H., & Lawson, T. (2013). Chlorophyll fluorescence analysis: A guide to good practice and understanding some new applications. *Journal of Experimental Botany*, *64*(13), 3983–3998. https://doi.org/10.1093/jxb/ert208

Prieto, J. A., Lebon, É., & Ojeda, H. (2010). Stomatal behavior of different grapevine cultivars in response to soil water status and air water vapor pressure deficit. *OENO One*, *44*(1), 9. https://doi.org/10.20870/oeno-one.2010.44.1.1459

Robinson, D. A., Campbell, C. S., Hopmans, J. W., Hornbuckle, B. K., Jones, S. B., Knight, R., Ogden, F., Selker, J., & Wendroth, O. (2008a). Soil Moisture Measurement for Ecological and Hydrological Watershed-Scale Observatories: A Review. *Vadose Zone Journal*, *7*(1), 358–389. https://doi.org/10.2136/vzj2007.0143

Robinson, D. A., Campbell, C. S., Hopmans, J. W., Hornbuckle, B. K., Jones, S. B., Knight, R., Ogden, F., Selker, J., & Wendroth, O. (2008b). Soil Moisture Measurement for Ecological and Hydrological Watershed-Scale Observatories: A Review. *Vadose Zone Journal*, *7*(1), 358–389. https://doi.org/10.2136/vzj2007.0143

Rodriguez-Alvarez, N., Bosch-Lluis, X., Camps, A., Vall-llossera, M., Valencia, E., Marchan-Hernandez, J. F., & Ramos-Perez, I. (2009). Soil Moisture Retrieval Using GNSS-R Techniques: Experimental Results Over a Bare Soil Field. *IEEE Transactions on*

Geoscience and Remote Sensing, *47*(11), 3616–3624. https://doi.org/10.1109/TGRS.2009.2030672

Rodriguez-Iturbe, I. (2000). Ecohydrology: A hydrologic perspective of climate-soil-vegetation dynamies. *Water Resources Research*, *36*(1), 3–9. https://doi.org/10.1029/1999WR900210

Rosolem, R., Shuttleworth, W. J., Zreda, M., Franz, T. E., Zeng, X., & Kurc, S. A. (2013). The Effect of Atmospheric Water Vapor on Neutron Count in the Cosmic-Ray Soil Moisture Observing System. *Journal of Hydrometeorology*, *14*(5), 1659–1671. https://doi.org/10.1175/JHM-D-12-0120.1

Schrön, M., Köhli, M., Scheiffele, L., Iwema, J., Bogena, H. R., Lv, L., Martini, E., Baroni, G., Rosolem, R., Weimar, J., Mai, J., Cuntz, M., Rebmann, C., Oswald, S. E., Dietrich, P., Schmidt, U., & Zacharias, S. (2017). Improving calibration and validation of cosmic-ray neutron sensors in the light of spatial sensitivity. *Hydrology and Earth System Sciences*, *21*(10), 5009–5030. https://doi.org/10.5194/hess-21-5009-2017

Schultz, H. R. (2003). Differences in hydraulic architecture account for near-isohydric and anisohydric behaviour of two field-grown Vitis vinifera L. cultivars during drought. *Plant, Cell & Environment*, *26*(8), 1393–1405. https://doi.org/10.1046/j.1365-3040.2003.01064.x

Seager, R., Liu, H., Henderson, N., Simpson, I., Kelley, C., Shaw, T., Kushnir, Y., & Ting, M. (2014). Causes of Increasing Aridification of the Mediterranean Region in Response to Rising Greenhouse Gases. *Journal of Climate*, *27*(12), 4655–4676. https://doi.org/10.1175/JCLI-D-13-00446.1

Shukla, P. R., Skeg, J., Buendia, E. C., Masson-Delmotte, V., Pörtner, H.-O., Roberts, D. C., Zhai, P., Slade, R., Connors, S., Diemen, S. van, Ferrat, M., Haughey, E., Luz, S., Pathak, M., Petzold, J., Pereira, J. P., Vyas, P., Huntley, E., Kissick, K., … Malley, J. (2019). *Climate Change and Land: An IPCC special report on climate change, desertification, land degradation, sustainable land management, food security, and greenhouse gas fluxes in terrestrial ecosystems*. https://philpapers.org/rec/SHUCCA-2

Siebert, S., Döll, P., Hoogeveen, J., Faures, J.-M., Frenken, K., & Feick, S. (2005). Development and validation of the global map of irrigation areas. *Hydrology and Earth System Sciences*, *9*(5), 535–547. https://doi.org/10.5194/hess-9-535-2005

Stevanato, L., Baroni, G., Cohen, Y., Fontana, C. L., Gatto, S., Lunardon, M., Marinello, F., Moretto, S., & Morselli, L. (2019). A Novel Cosmic-Ray Neutron Sensor for Soil Moisture Estimation over Large Areas. *Agriculture*, *9*(9), Article 9. https://doi.org/10.3390/agriculture9090202

Suter, B., Triolo, R., Pernet, D., Dai, Z., & Van Leeuwen, C. (2019). Modeling Stem Water Potential by Separating the Effects of Soil Water Availability and Climatic Conditions on Water Status in Grapevine (Vitis vinifera L.). *Frontiers in Plant Science*, *10*. https://www.frontiersin.org/articles/10.3389/fpls.2019.01485

Tang, Y., Luan, X., Sun, J., Zhao, J., Yin, Y., Wang, Y., & Sun, S. (2021). Impact assessment of climate change and human activities on GHG emissions and agricultural water use. *Agricultural and Forest Meteorology*, *296*, 108218. https://doi.org/10.1016/j.agrformet.2020.108218

Valentini, G., Allegro, G., Pastore, C., Zanini, A., Moffa, A., Gottardi, D., Gomez-Urios, C., Patrignani, F., & Filippetti, I. (2025). An Automatic Cooling System to Cope with the Thermal–Radiative Stresses in the Pignoletto White Grape. *Horticulturae*, *11*(9), 1128. https://doi.org/10.3390/horticulturae11091128

Valentini, G., Pastore, C., Allegro, G., Mazzoleni, R., Chinnici, F., & Filippetti, I. (2022). Vine Physiology, Yield Parameters and Berry Composition of Sangiovese Grape under Two Different Canopy Shapes and Irrigation Regimes. *Agronomy*, *12*(8), Article 8. https://doi.org/10.3390/agronomy12081967

Vereecken, H., Huisman, J. A., Pachepsky, Y., Montzka, C., van der Kruk, J., Bogena, H., Weihermüller, L., Herbst, M., Martinez, G., & Vanderborght, J. (2014). On the spatio-temporal dynamics of soil moisture at the field scale. *Journal of Hydrology*, *516*, 76–96. https://doi.org/10.1016/j.jhydrol.2013.11.061

Walsh, D. O., Grunewald, E., Turner, P., Hinnell, A., & Ferre, P. (2011). Practical limitations and applications of short dead time surface NMR. *Near Surface Geophysics*, *9*(2), 103–113. https://doi.org/10.3997/1873-0604.2010073

Weimar, J., Köhli, M., Budach, C., & Schmidt, U. (2020). Large-Scale Boron-Lined Neutron Detection Systems as a 3He Alternative for Cosmic Ray Neutron Sensing. *Frontiers in Water*, *2*. https://doi.org/10.3389/frwa.2020.00016

Williamson, J. A., Petrone, R. M., Valentini, R., Macrae, M. L., & Reynolds, A. (2024). Assessing the influence of climate controls on grapevine biophysical responses: A review of Ontario viticulture in a changing climate. *Canadian Journal of Plant Science*, *104*(5), 394–409. https://doi.org/10.1139/cjps-2023-0161

Yu, R., Brillante, L., Martínez-Lüscher, J., & Kurtural, S. K. (2020). Spatial Variability of Soil and Plant Water Status and Their Cascading Effects on Grapevine Physiology Are Linked to Berry and Wine Chemistry. *Frontiers in Plant Science*, *11*. https://doi.org/10.3389/fpls.2020.00790

Zhang, Y., Kang, S., Ward, E. J., Ding, R., Zhang, X., & Zheng, R. (2011). Evapotranspiration components determined by sap flow and microlysimetry techniques of a vineyard in northwest China: Dynamics and influential factors. *Agricultural Water Management*, *98*(8), 1207–1214. https://doi.org/10.1016/j.agwat.2011.03.006

Zhou, S., Zhang, Y., Park Williams, A., & Gentine, P. (2019). Projected increases in intensity, frequency, and terrestrial carbon costs of compound drought and aridity events. *Science Advances*, *5*(1), eaau5740. https://doi.org/10.1126/sciadv.aau5740

Zreda, M., Desilets, D., Ferré, T. P. A., & Scott, R. L. (2008). Measuring soil moisture content non-invasively at intermediate spatial scale using cosmic-ray neutrons. *Geophysical Research Letters*, *35*(21). https://doi.org/10.1029/2008GL035655

Zreda, M., Shuttleworth, W. J., Zeng, X., Zweck, C., Desilets, D., Franz, T., & Rosolem, R. (2012). COSMOS: The COsmic-ray Soil Moisture Observing System. *Hydrology and Earth System Sciences*, *16*(11), 4079–4099. https://doi.org/10.5194/hess-16-4079-2012

2. Cosmic-ray neutron sensing to monitor soil moisture across various irrigation methods

Riccardo Mazzoleni[1], Sadra Emamalizadeh[1], Gabriele Baroni[1]

[1]University of Bologna, Department of Agricultural and Food Sciences (DISTAL), Viale Giuseppe Fanin 50, 40127 Bologna, Italy.

Note of the Candidate: this chapter is based on a manuscript prepared for submission to Vadose Zone Journal, under the Special Issue "Advances in Monitoring Soil Water Content." It is reproduced here in its original format.

Abbreviations: CRNS, Cosmic-Ray Neutron Sensing; FC, Field Capacity; LW, Lattice Water; MSI, Micro Sprinklers Irrigation; SAT, Soil Saturated Water Content; SDI, Subsurface Drip Irrigation; SHP, Static Hydrogen Pool; SOC, Soil Organic carbon; SWC, Soil Water Content; PS, Point-Scale; PSD, Particle Size Density; PTF, Pedotransfer Function; WP, Wilting Point.

Core ideas:

- CRNS effectively detected irrigation-driven SWC changes under both SDI and MSI systems across field conditions.
- Statistical analysis confirmed CRNS sensitivity to irrigation, with significant SWC increases under uniform wetting.
- The extent of irrigation influenced CRNS response, offering insights into its vertical and horizontal spatial sensitivity.
- Muon-based correction shows some agreement and potential as an alternative to incoming neutron correction but needs further investigation.

Abstract

Accurate and continuous monitoring of soil water content (SWC) is critical for efficient irrigation management, particularly under variable irrigation systems. This study investigated the use of Cosmic-Ray Neutron Sensing (CRNS) to monitor SWC in two agricultural contexts in Italy: a vineyard employing subsurface drip irrigation (SDI) in Imola and a walnut orchard with micro-sprinkler irrigation (MSI) in Bondeno. The analysis included site-specific calibration, CRNS signal correction using both traditional atmospheric and local muon-based methods, and a statistical assessment of SWC dynamics during irrigation events. At the Imola site, CRNS-derived SWC showed a consistent and sensitive response to irrigation, with strong agreement between the two correction approaches. A significant increase in

SWC was observed during irrigation events in 2023 ($p < 0.001$), confirming the sensor's ability to detect short-term moisture changes in the main root zone (50 cm). SWC values tended to be higher also after irrigation periods in 2024. However, these differences were not statistically significant ($p > 0.05$). At the Bondeno site, uniform irrigation in 2022 gave a high statistically significant increase in SWC ($p < 0.001$), while in 2023 only the sector nearest to the sensor showed a modest response ($p < 0.05$), with no significant changes detected in other sectors. This highlights CRNS sensitivity to the spatial extent and proximity of water application. Comparisons with point-scale (PS) sensors at Imola revealed that CRNS provided smoother SWC dynamics, whereas PS sensors captured sharper fluctuations but often overestimated SWC. These findings validate CRNS as a robust, non-invasive tool for SWC monitoring and emphasize the value of combining multiple sensing approaches to improve the spatial and temporal assessment of field-scale SWC.

2.1. Introduction

The climate change effects on agricultural environments are often interconnected with its impact on soil water balance and vegetation growth (Kang et al., 2009). Therefore, the efficient use of water resources is paramount nowadays and, to this end, precision agriculture and irrigation management are central to improving water use. In this context, soil water content (SWC) plays a vital role in controlling the energy and water fluxes in the continuum of soil, vegetation, and atmosphere and, consequently, affects atmospheric processes, including precipitation patterns, air temperature, and evapotranspiration (Seneviratne et al., 2010). Plant growth is tightly linked to SWC, as this water is not only needed for evapotranspiration but also controls the mobilization and availability of nutrients (Rodriguez-Iturbe, 2000). Continuously monitoring the SWC can uphold anticipating plant water stress and the onset of drought conditions (Babaeian et al., 2019). Thus, accurate monitoring of SWC is essential for managing agricultural water resources and for optimizing agricultural productivity. Numerous methods for assessing SWC, ranging from point-scale sensors to satellite remote sensing approaches, have been devised (Babaeian et al., 2019; Robinson et al., 2008; Susha Lekshmi et al., 2014). Traditional SWC techniques provide only isolated point measurements of soil water, which may lack representativeness for a field or its sub-areas. Despite recent development of wireless techniques, employing dense grids of soil water sensors for irrigation management still proves impractical in many applications due to economic, logistical, and management constraints. This poses a challenge for both conventional irrigation and site-specific irrigation (Barker et al., 2017;

Evett et al., 2009). On the other hand, satellite remote sensing is currently striving with issues such as small penetration depth and low overpass frequencies (Peng et al., 2021). Yet, the challenge in remote sensing of SWC lies in developing practical models that can effectively integrate remotely sensed measurements and validate the results (Zappa et al., 2024). In recent years, there has been significant research activity in the development of proximal sensors that aggregate data over field scales and could overcome some of the limitations discussed above (Bogena et al., 2015; Hardie, 2020).

In this perspective, cosmic-ray neutron sensing (CRNS) has emerged as a reliable approach for non-invasive and continuous monitoring of SWC (Zreda et al., 2008). This approach relies on the inverse correlation between neutrons generated by cosmic-ray fluxes and then scattered by hydrogen, primarily present in the soil as water. The part of the neutrons energy spectrum that is most sensitive to SWC is the epithermal region from energies of 0.25 eV to 100 keV (Köhli et al., 2015). While neutron density may be affected by changes in the cosmic-ray intensity and by additional hydrogen sources, such as biomass and lattice water (Andreasen et al., 2017; Baatz et al., 2015), SWC can be estimated from the epithermal neutron intensity through a conversion function (Desilets et al., 2010).

The acknowledged advantage of CRNS sensors lies in their horizontal and vertical footprint (Schrön et al., 2017). Research has proven the robustness and validity of CRNS as a proximal soil sensing method for assessing SWC at the field scale, featuring a penetration depth spanning from 10 cm to 70 cm in dry soils and a footprint radius ranging from 100 m to 200 m (Köhli et al., 2015). Among various hydrological applications, CRNS has been ultimately assessed for monitoring SWC variations on agricultural field scales, particularly under irrigation (Brogi et al., 2023; Gianessi et al., 2021; Han et al., 2016; Li et al., 2019). Nevertheless, the debate regarding the suitability of CRNS in precision irrigation applications is still ongoing. Studies on the use of CRNS for supporting water management are still limited and mainly focused on more traditional irrigation methods. The relatively large footprint of the CRNS limits its ability to detect localized water applications and for this reason it is generally not well-suited for small irrigation research plots. Besides, the performance of the CRNS might be significantly affected by the choice of irrigation methods. According to Zhu et al. (2015), under flooding irrigation, CRNS may lead to an overestimation of SWC levels due to ponding water. Conversely, CRNS application could be more suitable in arid or semi-arid environments, as suggested by Chen et al. (2022). Their study demonstrated the capability of CRNS to accurately monitor changes in average SWC, allowing the identification of flooding irrigation timings and SWC variations before and after irrigation events. Drip irrigation may also result in challenges for CRNS SWC values interpretation. Li et al. (2019) reported that the precise irrigation scheduling was not feasible in their case due to the small area wetted by drip irrigation. Their research also emphasized the potential for enhancing CRNS sensitivity to detect small-scale drip irrigation. However, its overall performance is expected to be more effective in situations where drier soils are irrigated for longer durations or with more intensive irrigation methods. The research conducted by Baroni et al. (2018) revealed a distinctive response in CRNS SWC values under sprinkler irrigation. Yet, accurately attributing changes in SWC to individual irrigation events proved difficult, as adjacent fields, falling within the sensor's ~200 m footprint, exhibited variable moisture conditions that likely influenced the signal. The concept of SWC heterogeneity within the sensor footprint was ultimately well established by Schrön et al. (2023), and the research of Brogi et al. (2022) and Brogi et al. (2023). The latter studies further confirmed that a considerable fraction of the detected neutrons can originate from areas beyond the irrigated zone, and this proportion exhibits substantial variation based on the size of the irrigated areas. In agreement with previous studies, further progress is necessary to implement practical applications of CRNS across various irrigation methods and in site-specific heterogeneity.

Given the circumstances, this study aims to assess CRNS signal dynamics in two agricultural test fields in Italy's Emilia-Romagna region. Each field utilizes distinct irrigation methods: a walnut orchard employing micro-sprinkler irrigation (MSI) and a vineyard using subsurface drip irrigation (SDI). While the SWC dynamics under MSI have been partially documented, there remains a critical lack of insight into SWC behavior under SDI within CRNS applications. Therefore, this study evaluates CRNS responses to SWC changes across both sites, intending to advance the understanding of CRNS signal under different irrigation regimes. Finally, the CRNS sensors that were used within the present study have the capability to measure simultaneously neutrons and muons particles. The latter has been identify to be a potential alternative for local incoming correction (Stevanato et al., 2022). This approach was also tested within the present study.

2.2. Materials and methods

2.2.1. Sites overview characteristics of investigated locations

The vineyard (*Vitis vinifera* L. cv Trebbiano romagnolo and cv Grechetto gentile) is located at Imola, Bologna, Italy (44.384954, 11.698439), covering an approximate area of 12 hectares (Figure 1, panel A). The site is characterized by fine-textured river sediments, classified as silty clay according to the USDA textural classification. Società Agricola CACI in Imola, Bologna (Italy) manages the vineyard. Irrigation is provided with an SDI system which covers uniformly the entire area.

The SDI system is installed at a depth of 25 cm along two lines parallel to each row of plants, and drip system has a water capacity of 0.008 m^3 h^{-1}.

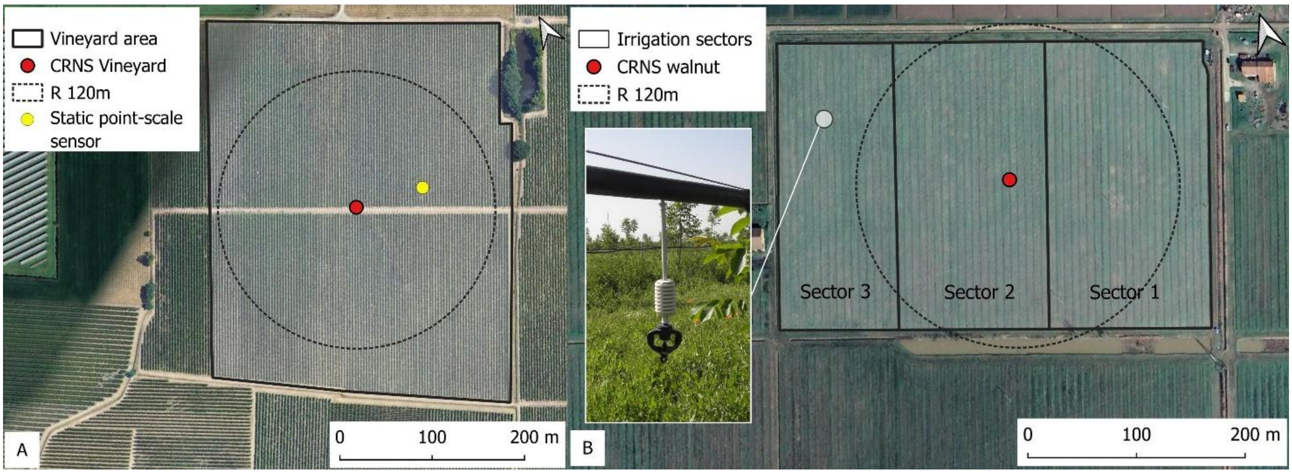

Figure 1: Overview of the experimental sites. A) The vineyard area with the sensors' setup. B) The walnut orchard, divided into three irrigation sectors and equipped with a micro-sprinkler irrigation system (detail picture on the left bottom corner). In both panels, the extent of the CRNS detection footprint (radius R 120m) is depicted.

The walnut orchard (*Juglans regia* L. cv Chandler) is situated in Bondeno, Ferrara, Italy (44.855103, 11.383767), in the flat agricultural area of Po River (Figure 1, panel B). The walnut orchard extends over approximately 160 ha and is managed by Società Agricola Agro Noce S.r.l. The investigated area, covering 10 hectares, is characterized by a silty clay loam soil texture, as per USDA classification, and is divided into three irrigated sectors, each controlled by independent valves, with micro-sprinklers system. Sprinkler nozzles are suspended at 1 m from the soil surface and positioned along polyethylene (PE) tubes at 5 m intervals. The PE tubes have a water volume capacity of 80 m^3h^{-1}, and each nozzle has a water capacity of 0.078 m^3 h^{-1}. The MSI system provides uniform irrigation coverage at the ground level across each irrigated sector, with an effective wetting radius of ~3 m.

2.2.2. Site-specific instruments and measurements

The CRNS probes, manufactured by Finapp S.r.l (Montegrotto Terme, Padova, Italy), were installed in Bondeno in August 2021 and in Imola in April 2023. Each probe is outfitted with a few centimeters of polyethylene, a material enriched with hydrogen that serves as a moderator to slow down the epithermal neutrons (Gianessi et al., 2024; Stevanato et al., 2019). This enrichment enhances the probes' sensitivity to soil moisture, as described by Köhli et al. (2015). Each sensor is individually powered by a solar panel, ensuring continuous monitoring through a backup battery for long-term use. The sensors were installed in selected areas expected to be suitable for the signal interpretation, considering the extent of the CRNS footprint. Following Schrön et al. (2017), a radius of 120 m was determined, which included the irrigated areas (Figure 1).

Within the Imola area, TEROS12 point-scale soil moisture sensors (METER Group, Pullman, WA, USA) were installed in 2023 at different depths below ground (5 cm, 15 cm and 25 cm). At each depth, the TEROS12 sensors were installed with their tines oriented horizontally to ensure measurement consistency at the target soil layer. At both sites, precipitation and weather data were sourced from the network stations of the regional environmental agency ARPAe and were processed in accordance with Antolini et al. (2016). Soil texture analyses were conducted for both sites, using composite soil samples collected during each calibration. Particle size distribution (PSD) of soil materials was determined using a PARIO™ system (METER Group, Pullman, WA, USA). The results were subsequently utilized to predict soil hydraulic parameters, including soil saturated water content (SAT), field capacity (FC), and wilting point (WP), by applying pedotransfer functions (PTFs) through the web interface of Szabó et al. (2021). Although PTFs may not accurately predict these soil properties because of their dependence on soil structure and other factors, they were applied to obtain indicative values of soil hydraulic thresholds, which served as a reference for interpreting SWC dynamics.

2.2.3. CRNS signal corrections and calibration

Neutrons measured by the CRNS sensors (N) were corrected to account for changing in air pressure (F_p), air humidity (F_v) and variability in the incoming neutron flux (F_i), based on the following equations (Zreda et al., 2012):

$$F_p = \exp(\beta(p - p_{ref})) \quad \text{Eq. 1}$$

$$F_i = \frac{I_{ref}}{I} \quad \text{Eq. 2}$$

$$F_v = 1 + \alpha(h - h_{ref}) \quad \text{Eq. 3}$$

$$N_c = N \cdot F_p \cdot F_i \cdot F_v \quad \text{Eq. 4}$$

where β = 0.0076 (mb^{-1}); α = 0.0054 (m^3 g^{-1}); p and h are air pressure (mb) and absolute humidity (g m^{-3}); I is the incoming flux of cosmic-ray neutrons induced by galactic primary particles in the Earth's atmosphere (counts per hour, cph); and h_{ref}, p_{ref} and I_{ref} are reference values of air pressure, absolute air humidity and incoming neutron flux during the measuring period, respectively. Here, the average values on the calibration days were taken. The F_i correction factor data are used from the station at Jungfraujoch (Switzerland), as adopted in many applications in central Europe, following common approaches suggested in literature (Bogena et al., 2022). Data from the network (Neutron Monitor Data Base, hereinafter NMDB, https://www.nmdb.eu/nest/) is used to correct the intensity for the variation in incoming cosmic radiation as the data are available online in real-time. In addition, the incoming correction based on the muon particles (F_i Muons) simultaneously measured by the CRNS-Finapp sensor is tested (Stevanato et al., 2022). This approach is further summarized.

Muon counting rate is first corrected for air pressure based on the following equation:

$$M = M_0 \cdot e^{-\beta_\mu(\Delta P)}$$
$$ln\left(\frac{M}{M_0}\right) = -\beta_\mu \cdot \Delta P \qquad \text{Eq. 5}$$

where M is the muon count rate at air pressure P, M_0 is the reference muon count at pressure P_0, and $\Delta P = P - P_0$ represents the deviation from the reference pressure.

The signal is further corrected for air temperature based on the following equation:

$$\frac{M}{M_0} = 1 - \alpha \cdot \Delta T \qquad \text{Eq. 6}$$

where T is the measured air temperature, T_0 is the reference temperature, and $\Delta T = T - T_0$ is the deviation from that reference. The coefficients $\beta\mu$ and α represent the barometric and temperature correction factors, respectively, derived empirically through regression fitting of local data as described in Stevanato et al. (2022).

While air temperature across the atmosphere profiles should better capture the local condition, air temperature measured at two meters height at the weather stations have been used. Despite this, additional errors may be introduced but have been shown to be a good proxy in other studies (de Mendonça et al., 2016) and it is also integrated in the present work.

Finally, the CRNS calibration took place on March 28th 2022 for the CRNS sensor installed in Bondeno and on May 8th 2023 for the sensor in Imola. The calibration procedure was consistent for both sites and allows to convert corrected neutron counts (Nc) into SWC based on the following equation (Desilets et al., 2010):

$$SWC_v(Nc) = \left(\frac{0.0808}{\frac{Nc}{N_0} - 0.372} - 0.115 - SWC_{offset}\right) \cdot \frac{\rho_{bd}}{\rho_w} \qquad \text{Eq. 7}$$

where r_{bd} and r_w are respectively the soil bulk density and water density (kg m^{-3}); SWC_{offset} is the contribution of static hydrogen pools (SHP), which is represented by the lattice water (LW) and soil organic carbon (SOC); $SWC_v (N_c)$ is the volumetric SWC average during the calibration day, N_0 is the calibration parameter. According to Franz et al. (2012), the protocol established a set of 18 sampling locations to quantify the average soil moisture content within the sensor's footprint area. Soil samples were collected at every 60° angle and at distances of 120, 35, and 3 meters from the CRNS sensor. At each location, soil samples were obtained at four depths (0-5 cm, 10-15 cm, 20-25 cm, and 30-35 cm) to assess the spatial sensitivity of the detected signal (Schrön et al., 2017). In total, 72 soil samples were collected and tested in the laboratory for gravimetric SWC (g g^{-1}) and bulk density ρ_{bd} (g m^{-3}) using a dry-oven method over a 24-hour cycle at 105°C. Based on these values, a weighted average SWC has been calculated following Schrön et al. (2017) to account for the horizontal and vertical sensitivity of the signal. A composite soil sample was also prepared to measure SOC and LW. These two parameters were determined using the loss on ignition method over a 24-hour cycle at 500°C and a 12-hour cycle at 1000°C, respectively (Scheiffele et al., 2020). Finally, SWC estimations were smoothed with a Savitzky-Golay filter to decrease the random fluctuations at a short time period, as suggested in the literature (Franz et al., 2020).

2.2.4. Statistical analysis

All the correlation and computation analysis presented in this study were conducted using the software R, in RStudio (2024.12.1).

To assess the impact of irrigation on SWC measured with the CRNS sensors, a statistical comparison was conducted between irrigated and non-irrigated time intervals. For this purpose, a binary variable was defined, where values were assigned as during irrigation events (value = 1) and for the subsequent 12 hours, and during the 12 hours preceding each event (value = 0). A 12-hour window before and after each irrigation event was chosen to adequately capture the SWC response while accounting for delayed infiltration and avoiding overlap with other external influences.

The statistical analysis was performed using a simple linear model in R, with SWC as the dependent variable and the irrigation proxy (proxy_irr) as the independent categorical predictor. The model was fit using the lm() function, and the significance of the irrigation effect was assessed via the associated p-value. A custom function was used to assign significance levels based on conventional thresholds ($p < 0.05$, 0.01, and 0.001, respectively).

2.3. Results and discussion

2.3.1. Muons and CRNS correction factors

The correlation between muon counting rates and environmental drivers, specifically atmospheric pressure and air temperature, were investigated at the two experimental sites (Figure 2).

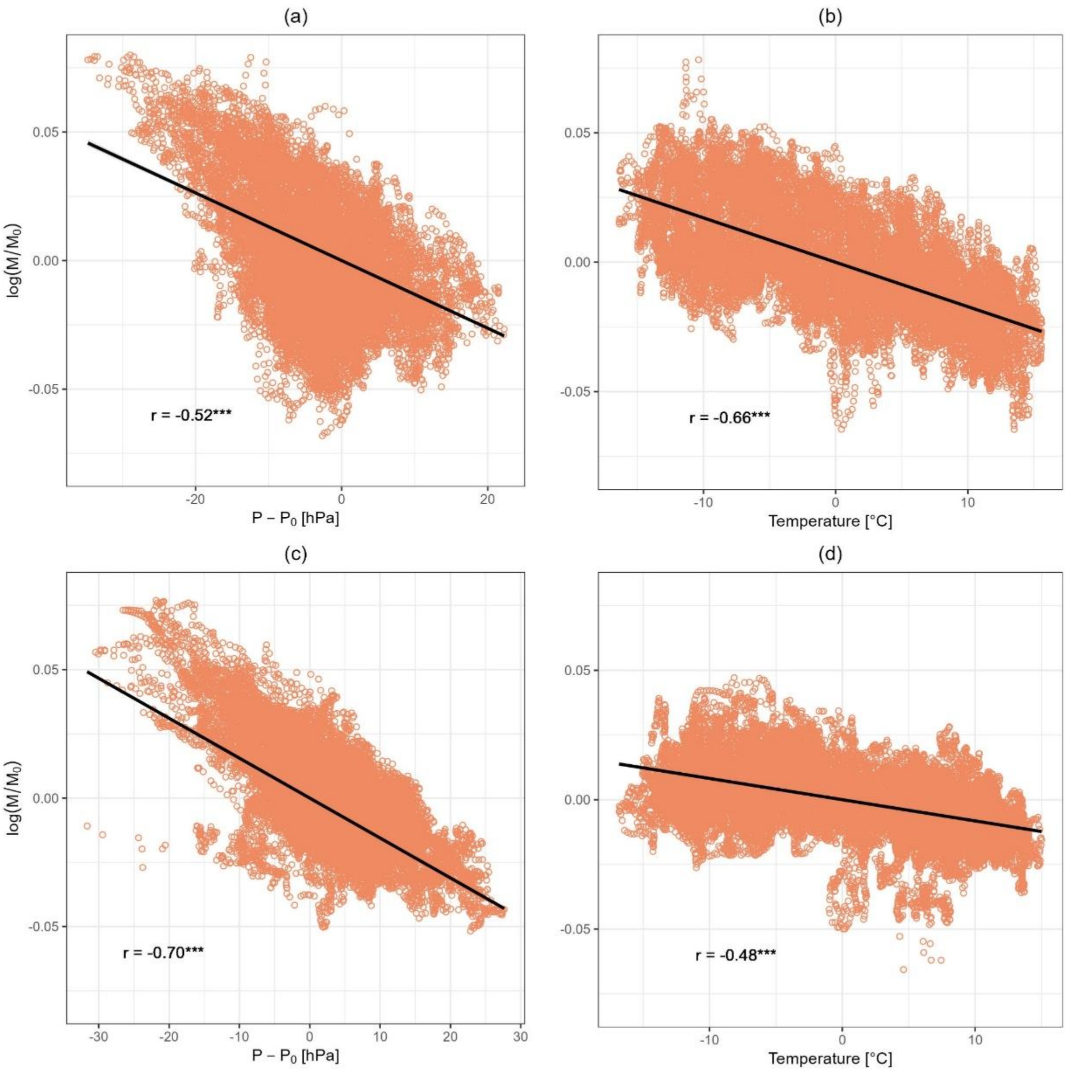

Figure 2: Correlation between normalized muon counts and environmental variables at the two experimental sites, the vineyard in Imola (panels a and b) and the walnut orchard in Bondeno (panels c and d). Panels (a) and (c) show the response to atmospheric pressure anomalies ($P – P_0$), while panels (b) and (d) depict the response to air temperature. Correlation coefficients (r) and significance levels are also indicated (* $p < 0.05$, ** $p < 0.01$, *** $p < 0.001$).

A strong and consistent negative correlation between atmospheric pressure anomalies and muon counting rates across both sites was confirmed (Figure 2, panels a and c). The correlation is statistically significant and highlights that those deviations in muon fluxes scale primarily with ΔP. In Imola (Figure 2a), the dependence is strong ($r = -0.52$, $p < 0.001$), while in Bondeno (Figure 2c) the correlation is even more pronounced ($r = -0.70$, $p < 0.001$), indicating that the walnut orchard site is slightly more sensitive to pressure variations. This behavior emphasizes that pressure corrections are essential for CRNS data processing in both environments and aligns with previous observations in nearby experimental contexts (Stevanato et al., 2022). The relationship with air temperature was also noteworthy (Figure 2, panels b and d). In Imola (Figure 2b), the correlation is significant ($r = -0.66$, $p < 0.001$), suggesting that local temperature variability plays a relevant role in shaping short-term muon fluctuations. In contrast, in Bondeno (Figure 2d) the correlation with temperature is weaker, though still significant ($r = -0.48$, $p < 0.001$). This is consistent with findings from Gianessi et al. (2024), who reported a limited influence of near-surface temperature on muon counts. It is therefore likely that the 2 m air temperature used here does not fully capture the vertical atmospheric gradients that modulate muon attenuation, particularly at the orchard site.

The corrections, based on both neutron incoming (F_i Jung) and in situ muon measurements (F_i muons) for the two experimental sites were further compared (Figure 3). The time series analysis reveals site-specific responses and varying degrees of agreement between the correction methods.

At the Imola site, Fi Jung and Fi muons show a similar pattern, with a gradual positive trend towards data in 2024. This concordance indicates that space and geomagnetic conditions influencing neutron moderation also impacted local muon fluxes, reinforcing the validity of using either correction factor at this location. The relatively strong correlation ($r = 0.67$) supports the interpretation that both neutron and muon-based corrections respond coherently to long-term variations in cosmic ray flux.

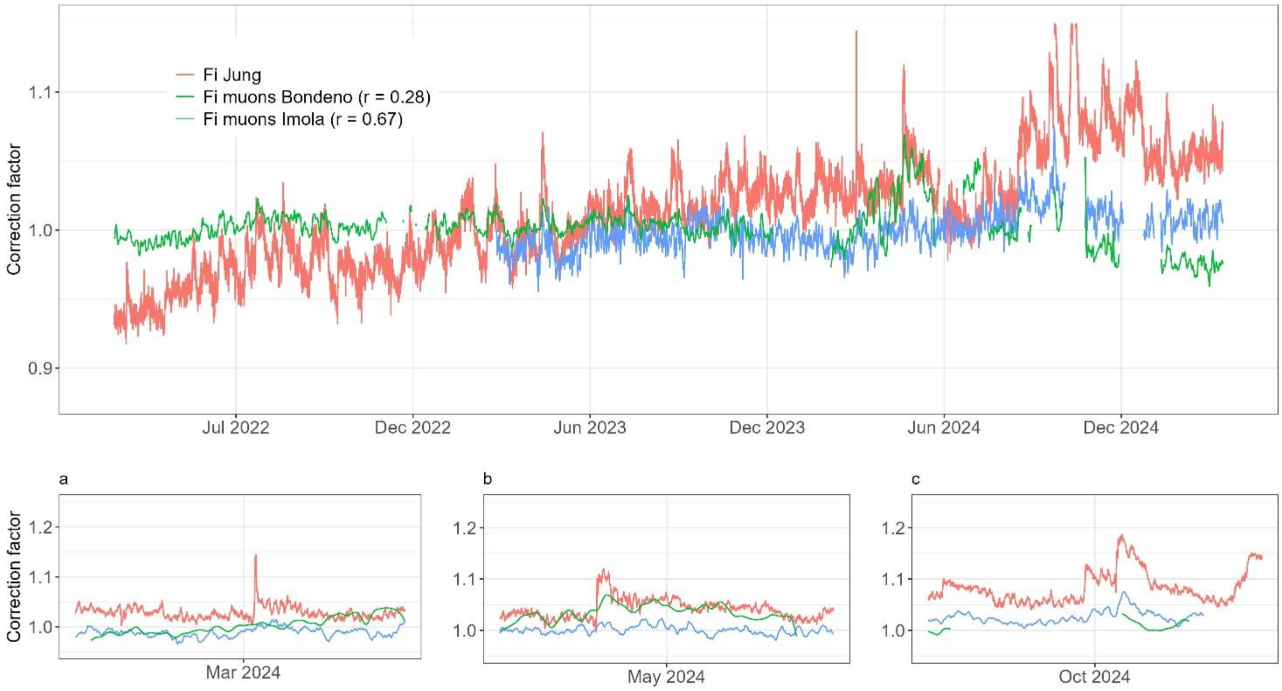

Figure 3. Comparison of neutron correction factors derived from the Jungfraujoch station (Fi Jung, red line) and from in situ muons (Fi muons) at the two study sites: Bondeno (green line) and Imola (blue line). The main plot shows the full time series, with correlation values between Fi Jung and Fi muons indicated for each site. Panels (a–c) zoom in on selected Forbush decrease events, highlighting the differential response and recovery dynamics of the correction factors.

In contrast, at the Bondeno site, Fi muons remain relatively stable over time, primarily capturing short-term fluctuations rather than broader trends. Although the overall correlation is still positive (r = 0.28), the smoothed nature of Fi muons indicates a weaker sensitivity to long-term incoming neutron variability.

Three close-up panels (Figure 3, a–c) illustrate Forbush decrease events occurred in 2024, according to what has also been reported by Riggi et al., (2025). This phenomenon caused short-term reductions in cosmic ray intensity due to solar disturbances. In our context, Fi muons also responded to such atmospheric changes, particularly visible in panel b and c, but the dynamic is more smoothed. These findings emphasize the need to assess both short and long-term agreement when applying correction factors for neutron-based SWC sensing. While Fi Jung provides a reliable global standard, in situ muon corrections may offer enhanced temporal resolution and responsiveness to localized events, contingent on site-specific conditions.

2.3.2. Comparative analysis of Jung and local muon-based SWC with CRNS

The results obtained after calibration campaigns in both sites showed some differences between the two sites, as expected (Table 1).

Table 1. Results of the soil sample analysis for CRNS calibration and soil textures at Bondeno and Imola experimental sites.

Site calibration date (yyyy /mm/dd)	**Bondeno 2022/03/28**	**Imola 2023/05/08**
SOC [a]	0.022	0.028
LW [b]	0.083	0.019
SWCg [c]	0.175 ± 0.003	0.259 ± 0.003
SWCg (wt) [d]	0.115	0.256
ρ_{bd} [e]	1.475	1.446
Nc (Fi) [f]	952	643
Nc (Fi Muons) [g]	1023	665
N_0 [h]	1420	1137
N_0 (Muons) [i]	1489	1176
Sand [j]	6	9
Silt [k]	56	42
Clay [l]	38	49

[a] Soil organic carbon (g g^{-1}); **[b]** Lattice water (g g^{-1}); **[c]** Gravimetric soil water content and relative ± standard deviation (g g^{-1}); **[d]** Weighted average gravimetric soil water content (g g^{-1}); **[e]** soil bulk density (g cm^{-3}); **[f]** Neutron counts during the calibration campaign corrected based on Jung neutron monitoring station (cph); **[g]** Neutron counts during the calibration campaign corrected using in-situ muon particles (cph); **[h]** Calibrated parameter based on Eq. 3 (cph); **[i]** Calibrated parameter based on Eq. 3 (cph) but using incoming muon correction; **[j, k, l]** Soil textural element content (%) of sand, silt and clay, respectively.

The results in Imola exhibited higher soil moisture on the day of calibration compared to Bondeno, leading to consistently lower values of Nc correction factors and N_0. The LW content in Bondeno was notably higher than in Imola, suggesting an influence from differences in mineral composition, particularly the presence of clay particles. Notably, the comparison between N_0 and N_0 (Muons) showed close agreement at Imola, while larger discrepancies were observed at Bondeno. These differences may result from a combination of site-specific soil properties, higher soil moisture variability, or potential signal instability during the muon-based calibration process at that site. These variations highlight the necessity of site-specific calibration in CRNS applications due to differences in soil properties and environmental conditions. Additionally, further investigations and soil sampling will be essential to refine calibration values and improve accuracy. Besides, it is worth noting that each CRNS sensor was calibrated on a single date only, which may introduce additional uncertainty in the absolute values under SWC conditions different from those observed during calibration (Iwema et al., 2015).

The estimated SWC at the two sites are shown in Figure 4. The results show how the CRNS signal was regularly recorded and transmitted over the first two years. Later, some gaps were experienced. The issues were attributed mainly to energy supply and were fixed by replacement of batteries and solar panel. Moreover, the outcomes of SWC patterns recorded with the CRNS sensors revealed some differences between the two experimental sites, particularly when comparing SWC and SWC muon data. At Imola (Figure 4, panel A), both the Jung and muon-corrected SWC data generally aligned well throughout the entire monitoring period. Regardless of the correction factor applied, both SWC dynamics demonstrated a clear and rapid response to rainfall events, indicating that the sensors effectively captured changes in soil moisture levels. This coherence suggests that, at Imola, the muon-based correction reflects actual soil moisture variations, confirming and reinforcing what previously observed concerning the correction factors over this site.

At the Bondeno site (Figure 4, panel B), the muon-corrected SWC measurements initially aligned reasonably well with the Jung-corrected data, particularly during the early phases following site-specific calibration. Over time, however, a progressive divergence became apparent. From July 2023 onward, the muon-corrected CRNS signal began to diverge from the Jung-corrected estimate (Figure 4B), although no interruptions or malfunctions were recorded. Despite these issues, both correction approaches generally preserved the expected temporal response to rainfall events, capturing the broad patterns of soil moisture variation. The increasing mismatch over time in the muon-based series may point to a different sensitivity to long-term modulation of solar cycle activities, highlighting the need for periodic recalibration to maintain consistency in long-term SWC monitoring. Besides, this discrepancy aligns with previous observations, indicating that site-specific conditions, such as atmospheric variables, can significantly impact the accuracy of muon-based estimates (Gianessi et al., 2024).

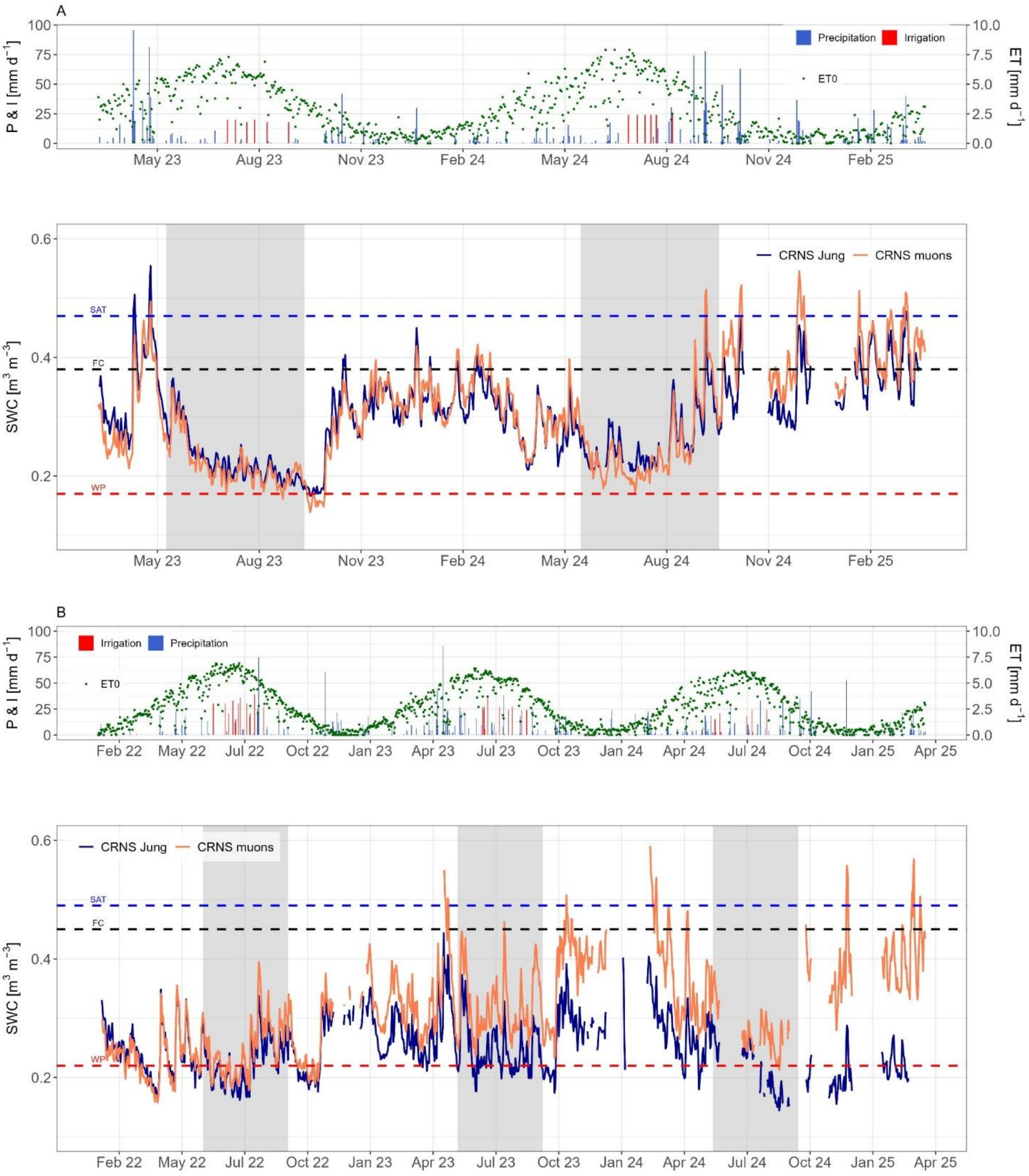

Figure 4. The SWC recorded over the time by the CRNS sensors at the two experimental sites, Imola (A) and Bondeno (B). The Jung-corrected (CRNS Jung, blue line) and muon-corrected (CRNS muon, orange line) SWC data ($m^3\ m^{-3}$), are integrated daily. Additionally, cumulative daily rainfall, evapotranspiration (ET0) and irrigations ($mm\ d^{-1}$) are shown for both sites. Grey-shaded areas in both panels highlight the irrigation occurrences during the seasons. Dashed horizontal lines indicate soil hydraulic limits: soil saturated water content (SAT, blue), field capacity (FC, black), and wilting point (WP, red).

2.3.3. Comparison with point-scale sensors

A set of PS sensors was installed at Imola site to assess the temporal variations in SWC and to compare these measurements with those from CRNS method (Figure 5). The dynamics of SWC are examined in the context of recorded precipitation and irrigation events during the irrigation seasons of 2023 and 2024 (June to September). During each year, the SDI system was consistently operated on a six-day cycle, delivering approximately 20 mm of water per irrigation event.

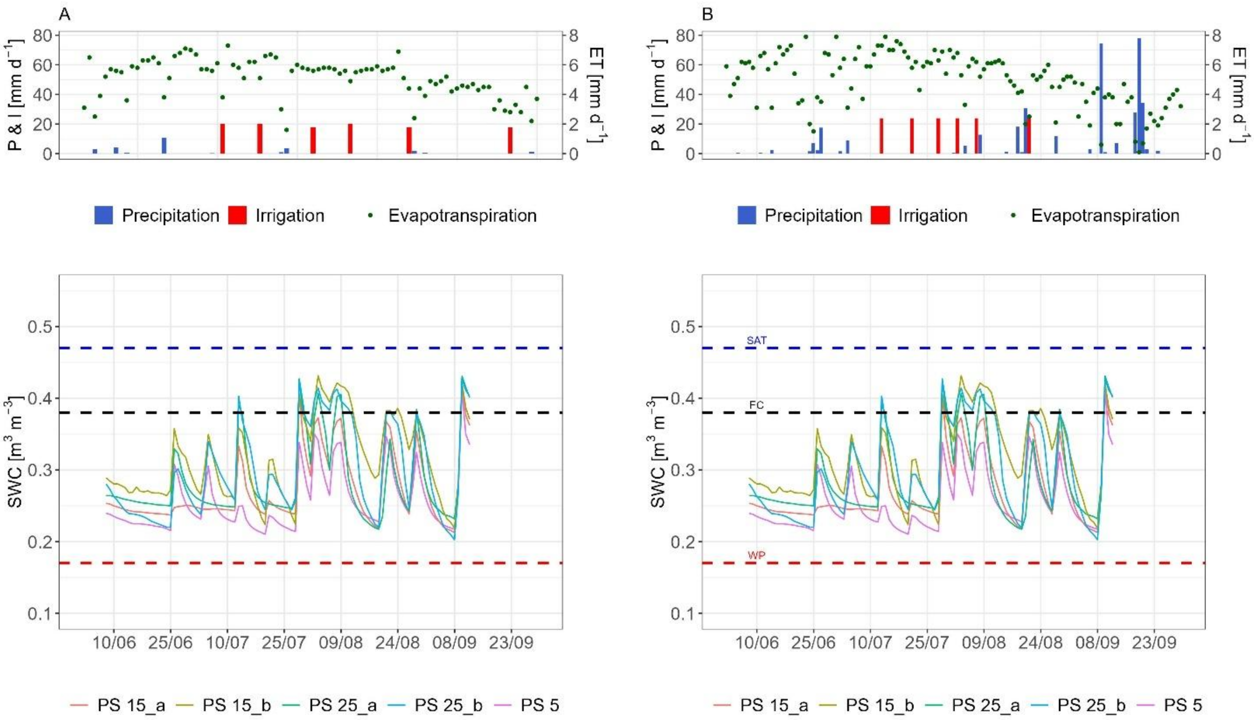

Figure 5: Data recorded in the vineyard in Imola during the 2023 (panel A) and the 2024 season (panel B) are shown. Upper panels show daily values of precipitation (blue bars), irrigation (red bars), and reference evapotranspiration (ET0, green dots). Lower panels show soil water content (SWC, $m^3\ m^{-3}$) measured at five depths (5 cm, 15a cm, 15b cm, 25a cm, 25b cm). The letters "a" and "b" denote whether the sensor was positioned close to the irrigation line (a) or 20 cm away from it (b). Dashed horizontal lines indicate soil saturated water content (SAT, blue), field capacity (FC, black), and wilting point (WP, red).

During 2023 (Figure 5, panel A), PS sensor SWC profiles show gradual declines, particularly in the deeper sensors (25a and 25b cm), with minor fluctuations in response to irrigation. Interestingly, the 5 cm and 15b cm sensors, located further from the drip line, often failed to capture clear wetting peaks following irrigation events, emphasizing the limited wetted radius and heterogeneity in water redistribution under point-source irrigation. It is also notable how the sensor placed at 15a cm showed no data alongside the investigated period. The SWC remained below FC (0.38 m^3 m^{-3}) across most of the season, especially at shallow depths, and never reached SAT (0.47 m^3 m^{-3}).

Notably, during the 2024 season (Figure 5, panel B), the PS SWC recorded at different depths align much more. This suggests that previous data could have been affected by the sensor installation while the soil disturbance decreases over time. Moreover, more frequent precipitations during the irrigation occurrences led to multiple wetting-drying cycles visible across all depths, especially near the irrigation line (15a and 25a cm). These sensors consistently recorded increases in SWC that frequently exceeded FC and occasionally approached SAT, indicating localized water accumulation.

A visual evaluation was also made to compare the SWC data obtained with PS sensors and CRNS (Figure 6).

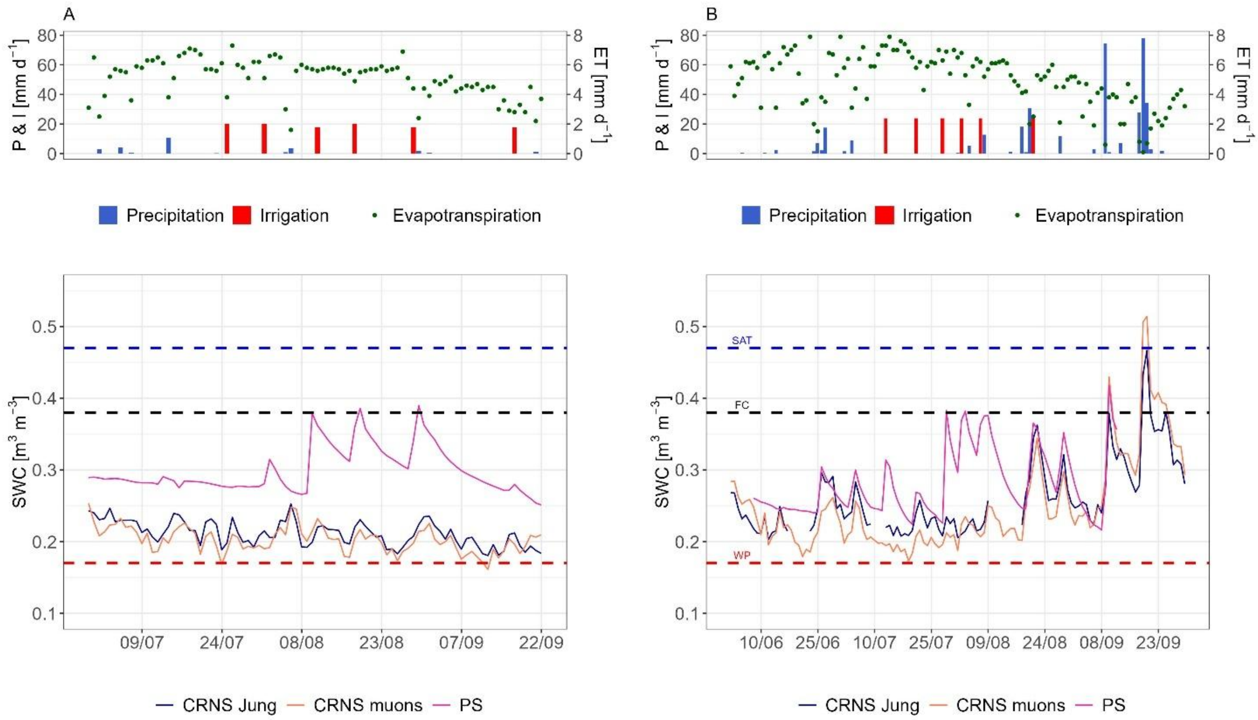

Figure 6: Data recorded in the vineyard in Imola during the 2023 (panel A) and the 2024 season (panel B) are shown. Upper panels show daily values of precipitation (blue bars), irrigation (red bars), and reference evapotranspiration (ET0, green dots). Lower panels show average soil water content (SWC, m^3 m^{-3}) measured with PS sensors, alongside measured by the CRNS sensor using both Jung-corrected (blue line) and muon-corrected (orange line). Dashed horizontal lines indicate soil hydraulic limits: soil saturated water content (SAT, blue), field capacity (FC, black), and wilting point (WP, red).

As expected, in both seasons, the PS SWC exhibited greater variability and sharper peaks in response to irrigation and rainfall events, particularly during periods of high-water input. Conversely, CRNS-derived SWC showed smoother temporal dynamics, reflecting their larger sensing integration. Despite these differences in response dynamics, all three methods generally tracked within a similar range, and remained below FC for most of the monitoring period, except during intense precipitation events during September 2024 (Figure 6, panel B). Overall, the PS data occasionally reached or exceeded FC, indicating localized saturation near emitters that is not reflected in the CRNS signals. These results highlight both the strengths and limitations of the different measurement approaches. While PS sensors are valuable for detecting sharp wetting events and assessing localized irrigation effectiveness, they may overestimate SWC at the field scale. In contrast, CRNS provides a more spatially integrated estimate, better suited for capturing broader scale trends and informing field irrigation management. Besides, while the CRNS footprint is relatively large, the data remained reliable for field-scale assessments, as the sensor was positioned to align with homogeneously managed areas. These results further highlight the inherent challenges of interpreting PS sensor data for SWC and for supporting irrigation scheduling, given that each sensor investigates only a small soil volume relative to the larger study area (Datta and Taghvaeian, 2023).

2.3.4. CRNS for irrigation assessment

CRNS-derived SWC was further analysed at hourly resolution to capture sub-daily dynamics around irrigation events, using both Jung- and muon-based corrections at each experimental site. For each irrigation date, SWC patterns are presented over a 24-hour window (12 hours before and after the event), together with the corresponding hourly irrigation and precipitation rates. To mitigate statistical noise at this temporal scale, the same smoothing procedure applied to daily data was also used here.

For Imola, data were analysed for the 2023 and 2024 seasons. This detailed examination is particularly novel given the context of the SDI system, a relatively unexplored configuration for CRNS applications. Despite the drip system delivering water below the surface, potentially limiting the signal response due to reduced direct wetting of the upper soil layers, the CRNS sensor clearly captured consistent increases in SWC in response to irrigation events, validating its vertical sensitivity and supporting irrigation scheduling even under SDI conditions. In both years, SWC remained above the WP (0.17 m^3 m^{-3}), ensuring that vines were not exposed to critical water stress conditions. During 2023 (Appendix, panel A) a moderate but visible increase in SWC followed each irrigation event. Only during the last irrigation event of 2023, a slight decrease in SWC was visible. While no conclusion can be formulated to explain this behaviour, the role of atmospheric correction or biomass changes might be potential candidates (McJannet et al., 2025). The 2024 season (Appendix, panel

B) showed a slightly higher baseline SWC, especially in the later season, where cumulative rainfall and irrigation led to a more pronounced SWC increase. These results confirm that Jung and muon-corrected SWC closely overlapped throughout most irrigation events, as reflected by correlation coefficients of $r = 0.72$ in 2023 and $r = 0.94$ in 2024. These values, computed over each irrigation (12 hours before, during, and 12 hours after the event), reinforce the reliability of both correction approaches under the relatively stable atmospheric and soil moisture conditions characteristic of the Imola site.

These findings are further supported by the statistical analysis of SWC changes in response to irrigation events (Figure 7). A possible estimation of the irrigation contribution to the SWC is also performed assuming a soil layer of 30 cm, based on average CRNS penetration depth. Concerning the Imola site, in 2023 (Figure 7, panel A) a highly significant difference in SWC was observed between irrigated and non-irrigated conditions ($p < 0.001$, ΔSWC = 3.8 mm), indicating that the CRNS sensor was able to detect a clear increase in soil moisture associated with irrigation events. During 2024, SWC values consistently tended to be higher during irrigation events than during periods without water inputs although no statistically significant difference in SWC between irrigated and non-irrigated periods was detected (Figure 7, panel B; $p > 0.05$, ΔSWC = 2.9 mm). The absence of a statistically significant response may reflect elevated baseline soil moisture conditions during the 2024 season (Appendix, panel B), potentially due to cumulative precipitation or increased frequency of irrigation events. These conditions may have reduced the relative contrast in SWC before and after irrigation, thereby diminishing the statistical relevance.

The analysis for Bondeno included the 2022 and 2023 seasons. In 2022, all sectors were irrigated simultaneously through the MSI system on the same dates, whereas in 2023 it was possible to focus on individual irrigation sectors. Due to the presence of several gaps during irrigation events in 2024, data from that period were not included in this analysis.

In 2022 (Figure 7, panel C) the CRNS sensor clearly detected a significant increase in SWC during irrigation periods ($p < 0.001$, ΔSWC = 5.5 mm), confirming the sensor's sensitivity under widespread and uniform wetting conditions. This result further demonstrates that when irrigation events affect the entire CRNS footprint evenly, the sensor is highly effective in capturing resulting changes in soil moisture, confirming what observed by Schrön et al. (2023). Overall, the ΔSWC calculated resulted lower than the actual water provided through irrigation in each site (~18mm each event). This result was in line with expectations, considering the localized wetting areas of both SDI and MSI.

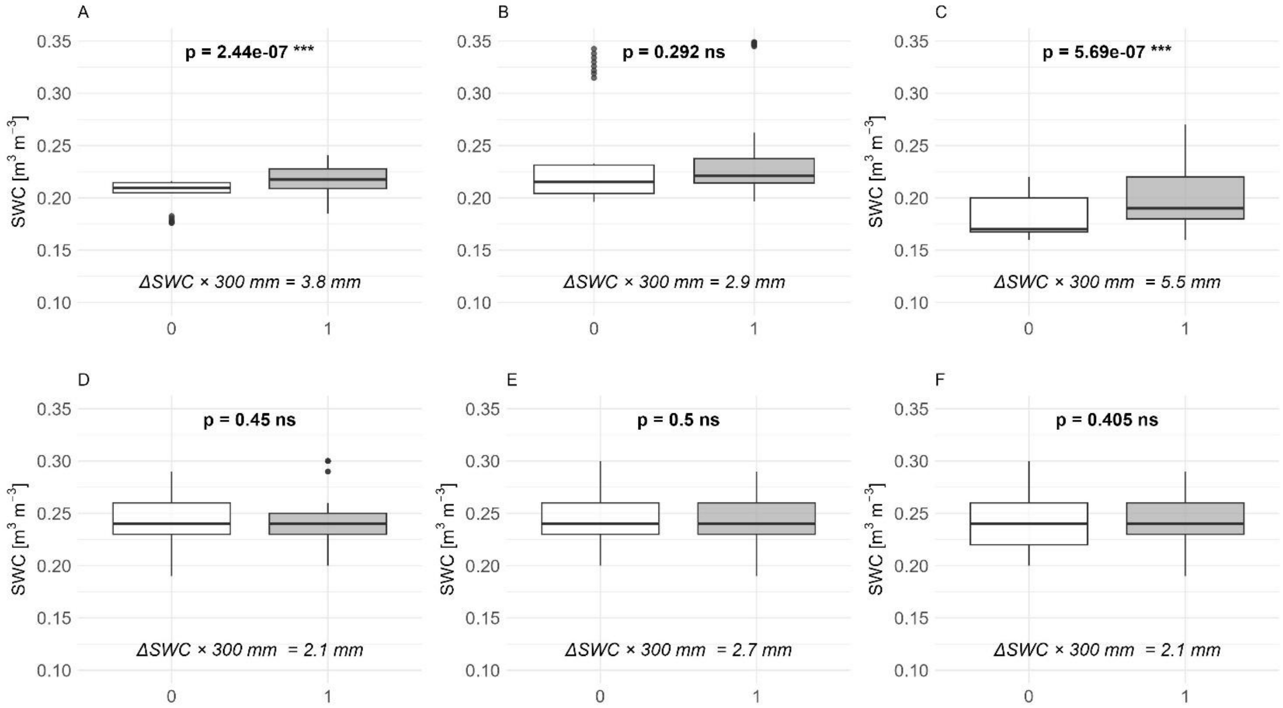

Figure 7: Boxplots showing SWC (m^3 m^{-3}) measured with CRNS under irrigated (1) and non-irrigated (0) conditions, based on a binary irrigation proxy assigned to 12 hours before and after each irrigation event. Statistical comparisons were conducted using linear models to assess the significance of SWC differences between the two conditions. Significance levels were assigned based on conventional p-values thresholds ($p < 0.05$, 0.01, and 0.001). In addition, the equivalent change in SWC was estimated as ΔSWC × 300 mm and reported within each panel to provide an integrated measure of CRNS sensitivity to irrigation in 30 cm depth. Different panels are referred to: A) Imola, 2023; B) Imola, 2024; C) Bondeno, 2022; D) Bondeno, Sector 1, 2023; E) Bondeno, Sector 2, 2023; F) Bondeno, Sector 3, 2023.

The 2022 season was marked by some of the most severe heatwaves recorded during the summer months, particularly in southern Europe (Büntgen et al., 2024). The impact of these extreme weather conditions was evident in our study as well, as shown by the SWC dynamics captured by the CRNS during irrigation-focused periods in Bondeno (Appendix, panel C). Notably, the baseline SWC in 2022 was relatively low, frequently falling below the WP (0.22 m3 m-3), reflecting the soil moisture deficit associated with the severe heatwaves. It was only towards the end of August, coinciding with rainfall events, that SWC values rose above the WP threshold. The Jung and muons-corrected SWC dynamics showed good agreement throughout the analysed period (r = 0.92), supporting earlier findings that the two correction approaches aligned well during the early phase following in situ calibration. In contrast, in 2023, the two SWC dynamics began to diverge slightly, although they continued to follow the same overall response to irrigation events (r = 0.94) (Appendix, panel D-F).

During the 2023 season, each sector had to be analysed separately, as irrigation was applied independently on most dates. Across all three sectors, no statistically significant differences in SWC were detected between irrigated and non-irrigated periods (Figure 7, panels D-F, ΔSWC < 3 mm). The absence of statistical significance may be explained by the spatial heterogeneity within the CRNS footprint and the alternating irrigation across sectors, both of which can reduce the magnitude of the sensor's response. This outcome aligns with theoretical expectations, as often detection becomes more uncertain during irrigation events with limited surface expression within the core sensitivity zone of the sensor (Schrön et al., 2017). These observations further emphasize the horizontal spatial dependency of CRNS responsiveness to irrigation, reinforcing the importance of footprint geometry and sensor positioning when interpreting soil moisture changes under localized irrigation management.

2.4. Summary and conclusions

This study investigated the application of CRNS for field-scale SWC monitoring at two agricultural fields employing different irrigation systems: a vineyard employing SDI and a walnut orchard with MSI, located at Imola and Bondeno, Italy, respectively. The research encompassed the evaluation of different CRNS signal correction methods over several years, site-specific calibration, and cross-comparison with PS soil moisture sensors, including a statistical assessment of the CRNS use under irrigation events. The study showed a positive correlation between muon and incoming neutron fluctuation detected at Jungfraujoch, confirming the potential of local muon measurements as a possible local alternative correction factor for CRNS. However, some significant discrepancies also emerged. Specifically, very short incoming fluctuation were not recorded probably due to the use of a relatively small detector, as previously discussed (Gianessi et al., 2024). Moreover, for the first time the availability of relative long time series recorded at Bondeno (three years) also showed that the local muons did not capture the long-term trend attributed to the solar cycle activities. For this reason, the results highlight the need of further investigation to better understand the use of muon-based corrections to enhance the temporal resolution and site-specific accuracy of SWC data.

Comparisons with PS sensors at the Imola site revealed clear distinctions in scale sensitivity and signal dynamics. While PS sensors effectively captured rapid wetting and drying cycles, especially near emitters, they often overestimated the SWC due to their localized nature. Conversely, CRNS data offered smoother but spatially integrated insights into SWC dynamics, proving more robust for field-scale monitoring. These results further reinforce the role of spatial variability that remains an important aspect to be further explored and the limitations of relying solely on PS data, particularly under broad irrigated areas. This also emphasizes the need to integrate multiple methods and technologies for a more robust assessment of field-scale soil moisture, as also suggested by Emamalizadeh et al. (2024) and Robinson et al. (2008), underscoring the value of combining PS measurements with other approaches to capture the spatial and temporal variability more comprehensively.

The results obtained confirmed the overall robustness of CRNS technology to capture temporal soil moisture dynamics under both irrigation systems. At the Imola site, CRNS-derived SWC, using both Jung and muon-based corrections, showed a strong and consistent response to irrigation events, even under SDI, a relatively unexplored application for CRNS. The hourly analysis clearly demonstrated the sensor's capability to detect increases in SWC due to irrigations and gave an empirical positive evaluation on the vertical spatial sensitivity of the sensor. Moreover, the statistical analysis further supported these findings: a highly significant difference ($p < 0.001$) was found in 2023 between irrigated and non-irrigated periods. In contrast, a tendency toward higher SWC values during irrigation periods was still observable during 2024 season even these differences were not statistically significant. At the Bondeno site, in 2022, when all sectors were irrigated simultaneously, the CRNS sensor recorded a clear and statistically significant increase in SWC ($p < 0.001$), affirming the sensor's sensitivity under uniform wetting conditions. The 2023 season, which involved irrigation across separate sectors, revealed a different scenario. No significant differences were detected in the all the sectors. This emphasizes the horizontal spatial sensitivity of CRNS and highlights the critical influence of irrigation footprint on the detectability of SWC changes, especially in a context in which the irrigation is delivered not uniformly over a large area.

Although in this study CRNS was primarily used to detect the occurrence of irrigation events, its potential for quantifying applied irrigation amounts deserves further investigation under different application methods and volumes. Ultimately, this work underscored the utility of CRNS as a reliable, non-invasive technique for monitoring soil moisture under varied irrigation strategies. The evidence supported its integration into the agriculture frameworks, provided that appropriate calibration and correction strategies are employed.

2.5. Appendix

A

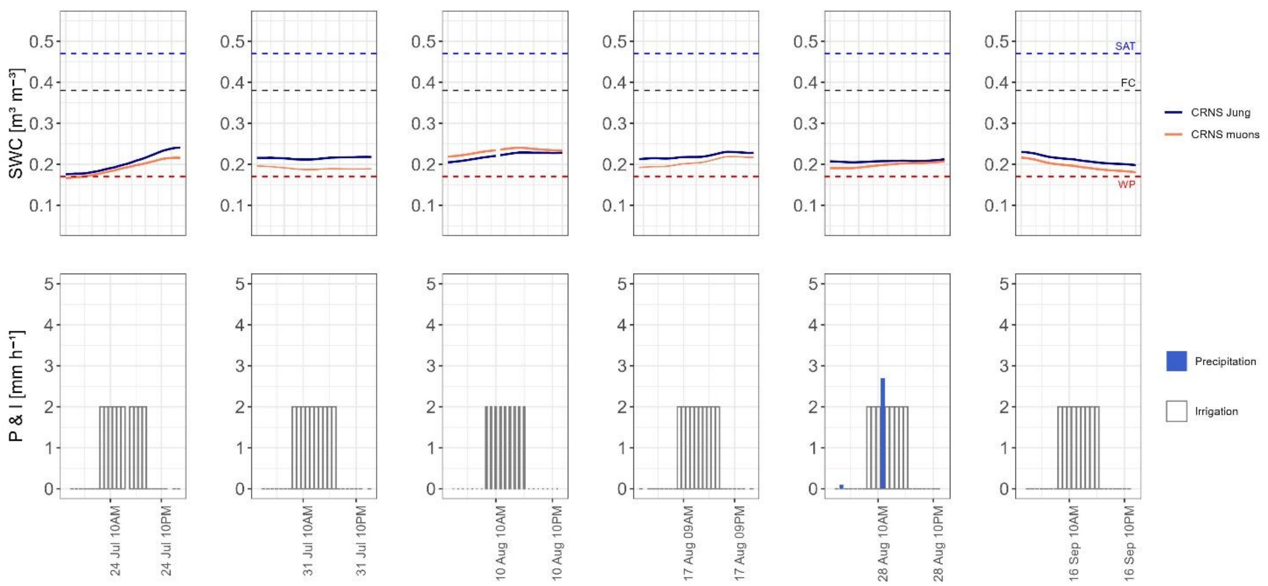

B

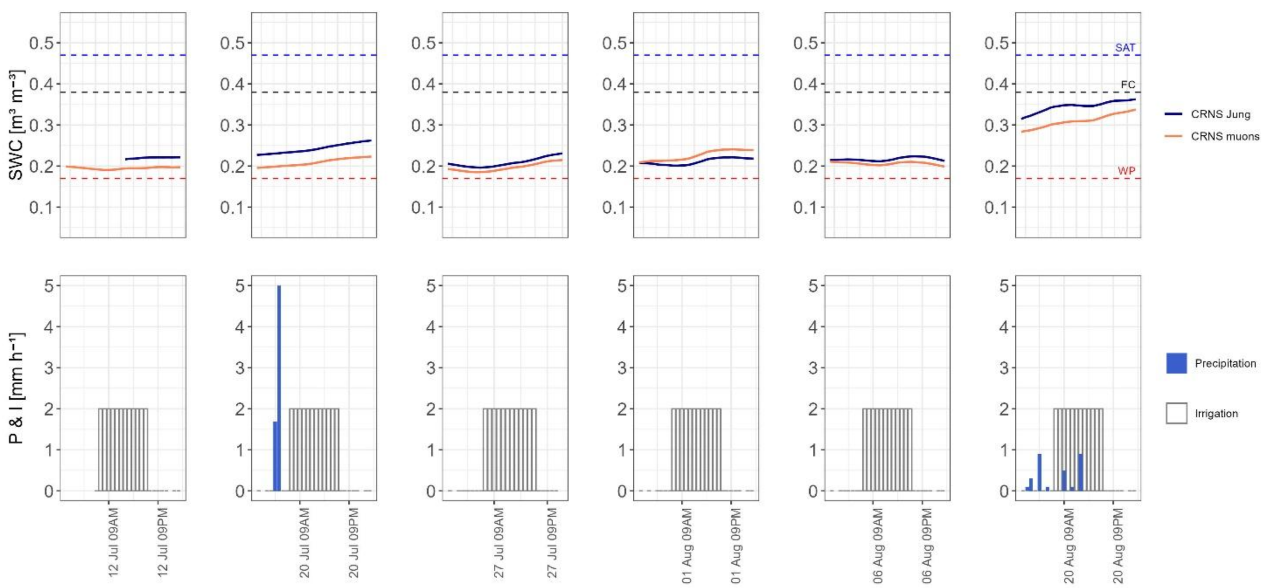

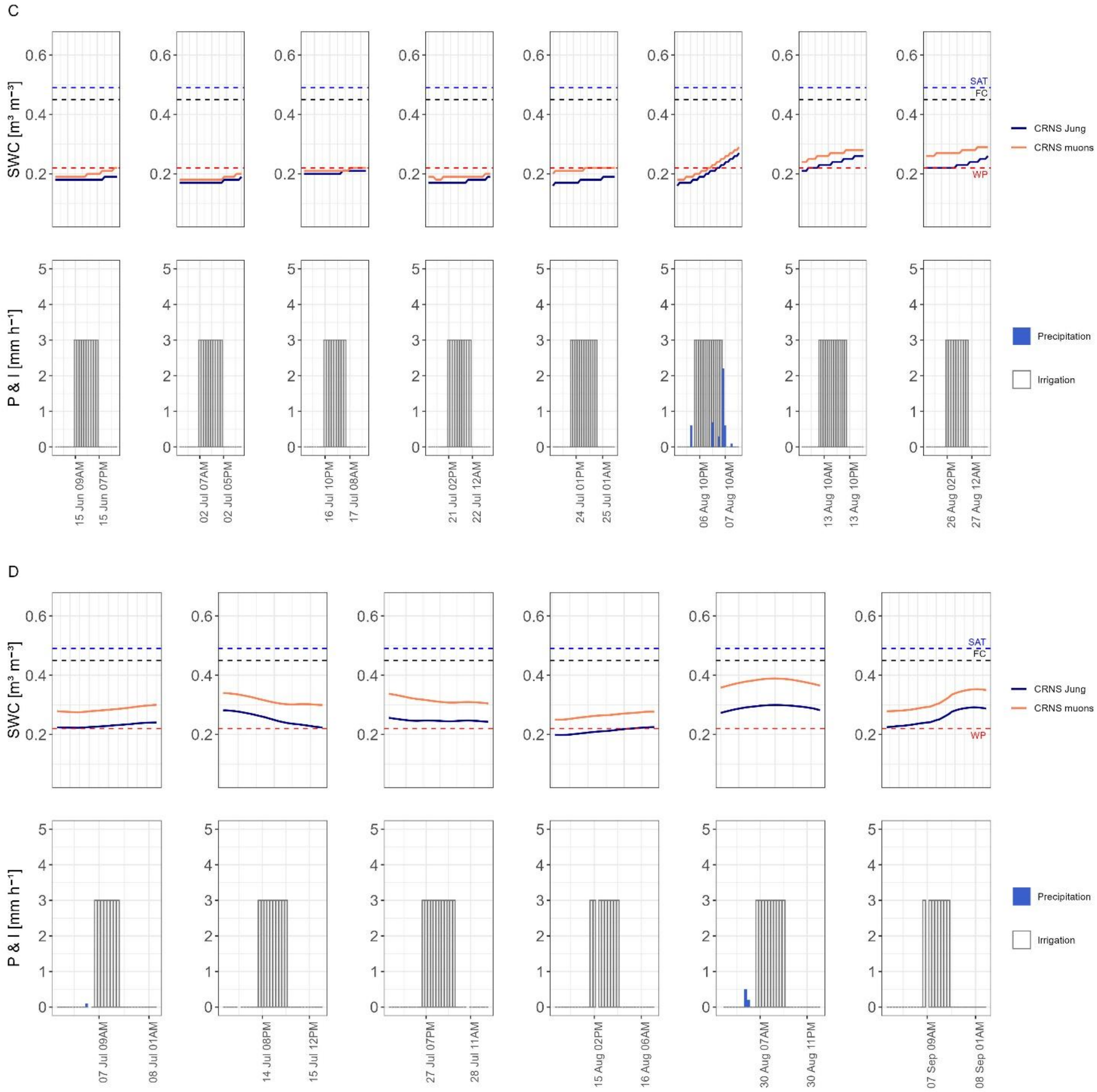
C
SWC [m³ m⁻³]
P & I [mm h⁻¹]
SAT
FC
WP
CRNS Jung
CRNS muons
Precipitation
Irrigation
15 Jun 09AM
15 Jun 07PM
02 Jul 07AM
02 Jul 05PM
16 Jul 10PM
17 Jul 08AM
21 Jul 02PM
22 Jul 12AM
24 Jul 01PM
25 Jul 01AM
06 Aug 10PM
07 Aug 10AM
13 Aug 10AM
13 Aug 10PM
26 Aug 02PM
27 Aug 12AM
D
07 Jul 09AM
08 Jul 01AM
14 Jul 08PM
15 Jul 12PM
27 Jul 07PM
28 Jul 11AM
15 Aug 02PM
16 Aug 06AM
30 Aug 07AM
30 Aug 11PM
07 Sep 09AM
08 Sep 01AM

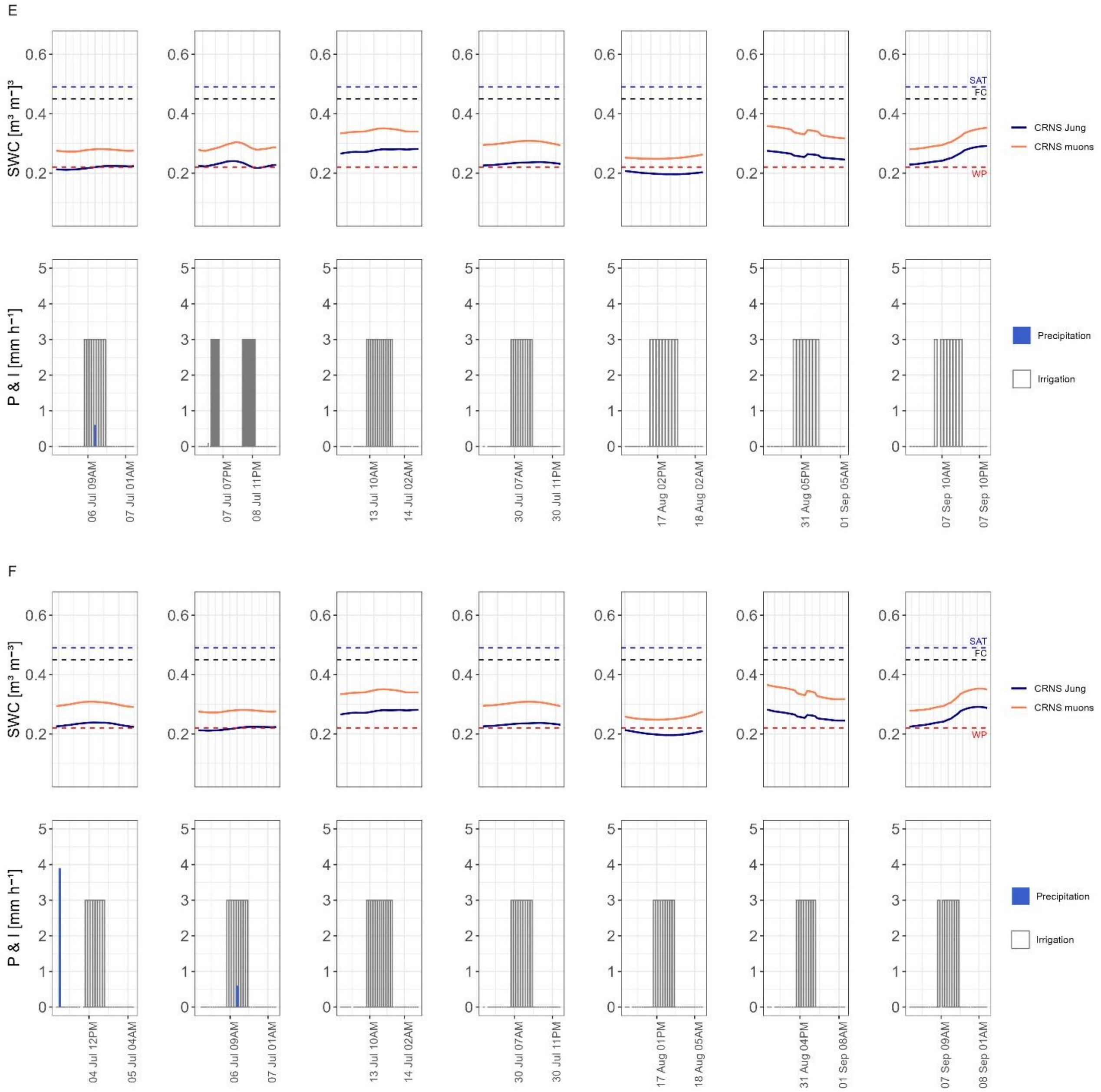

Appendix: Hourly SWC dynamics around irrigation events, as measured by CRNS using Jung-corrected (blue line) and muon-corrected (orange line) data. Each subpanel shows a 24-hour time window (12 hours before and after the irrigation event). The upper plots depict SWC variations ($m^3\ m^{-3}$), while the lower plots display the corresponding water inputs from irrigation (grey bars) and precipitation (blue bars), expressed in mm h^{-1}. Dashed horizontal lines indicate soil hydraulic limits: soil saturated water content (SAT, blue), field capacity (FC, black), and wilting point (WP, red). Different panels are referred to: A) Imola, 2023; B) Imola, 2024; C) Bondeno, 2022; D) Bondeno, Sector 1, 2023; E) Bondeno, Sector 2, 2023; F) Bondeno, Sector 3, 2023.

2.6. References

Andreasen, M., Jensen, K. H., Desilets, D., Franz, T. E., Zreda, M., Bogena, H. R., & Looms, M. C. (2017). Status and Perspectives on the Cosmic-Ray Neutron Method for Soil Moisture

Estimation and Other Environmental Science Applications. *Vadose Zone Journal*, *16*(8), vzj2017.04.0086. https://doi.org/10.2136/vzj2017.04.0086

Antolini, G., Auteri, L., Pavan, V., Tomei, F., Tomozeiu, R., & Marletto, V. (2016). A daily high-resolution gridded climatic data set for Emilia-Romagna, Italy, during 1961-2010: EMILIA-ROMAGNA DAILY GRIDDED CLIMATIC DATA SET. *International Journal of Climatology*, *36*(4), 1970–1986. https://doi.org/10.1002/joc.4473

Baatz, R., Bogena, H. R., Hendricks Franssen, H.-J., Huisman, J. A., Montzka, C., & Vereecken, H. (2015). An empirical vegetation correction for soil water content quantification using cosmic ray probes. *Water Resources Research*, *51*(4), 2030–2046. https://doi.org/10.1002/2014WR016443

Babaeian, E., Sadeghi, M., Jones, S. B., Montzka, C., Vereecken, H., & Tuller, M. (2019). Ground, Proximal, and Satellite Remote Sensing of Soil Moisture. *Reviews of Geophysics*, *57*(2), 530–616. https://doi.org/10.1029/2018RG000618

Barker, J. B., Franz, T. E., Heeren, D. M., Neale, C. M. U., & Luck, J. D. (2017). Soil water content monitoring for irrigation management: A geostatistical analysis. *Agricultural Water Management*, *188*, 36–49. https://doi.org/10.1016/j.agwat.2017.03.024

Baroni, G., Scheiffele, L. M., Schrön, M., Ingwersen, J., & Oswald, S. E. (2018). Uncertainty, sensitivity and improvements in soil moisture estimation with cosmic-ray neutron sensing. *Journal of Hydrology*, *564*, 873–887. https://doi.org/10.1016/j.jhydrol.2018.07.053

Bogena, H. R., Huisman, J. A., Güntner, A., Hübner, C., Kusche, J., Jonard, F., Vey, S., & Vereecken, H. (2015). Emerging methods for noninvasive sensing of soil moisture dynamics from field to catchment scale: A review. *WIREs Water*, *2*(6), 635–647. https://doi.org/10.1002/wat2.1097

Bogena, H. R., Schrön, M., Jakobi, J., Ney, P., Zacharias, S., Andreasen, M., Baatz, R., Boorman, D., Duygu, M. B., Eguibar-Galán, M. A., Fersch, B., Franke, T., Geris, J., González Sanchis, M., Kerr, Y., Korf, T., Mengistu, Z., Mialon, A., Nasta, P., … Vereecken, H. (2022). COSMOS-Europe: A European network of cosmic-ray neutron soil moisture sensors. *Earth System Science Data*, *14*(3), 1125–1151. https://doi.org/10.5194/essd-14-1125-2022

Brogi, C., Bogena, H. R., Köhli, M., Huisman, J. A., Hendricks Franssen, H.-J., & Dombrowski, O. (2022). Feasibility of irrigation monitoring with cosmic-ray neutron sensors.

Geoscientific Instrumentation, Methods and Data Systems, *11*(2), 451–469. https://doi.org/10.5194/gi-11-451-2022

Brogi, C., Pisinaras, V., Köhli, M., Dombrowski, O., Hendricks Franssen, H.-J., Babakos, K., Chatzi, A., Panagopoulos, A., & Bogena, H. R. (2023). Monitoring Irrigation in Small Orchards with Cosmic-Ray Neutron Sensors. *Sensors*, *23*(5), Article 5. https://doi.org/10.3390/s23052378

Büntgen, U., Reinig, F., Verstege, A., Piermattei, A., Kunz, M., Krusic, P., Slavin, P., Štěpánek, P., Torbenson, M., del Castillo, E. M., Arosio, T., Kirdyanov, A., Oppenheimer, C., Trnka, M., Palosse, A., Bebchuk, T., Camarero, J. J., & Esper, J. (2024). Recent summer warming over the western Mediterranean region is unprecedented since medieval times. *Global and Planetary Change*, *232*, 104336. https://doi.org/10.1016/j.gloplacha.2023.104336

Chen, X., Song, W., Shi, Y., Liu, W., Lu, Y., Pang, Z., & Chen, X. (2022). Application of Cosmic-Ray Neutron Sensor Method to Calculate Field Water Use Efficiency. *Water*, *14*(9), Article 9. https://doi.org/10.3390/w14091518

Datta, S., & Taghvaeian, S. (2023). Soil water sensors for irrigation scheduling in the United States: A systematic review of literature. *Agricultural Water Management*, *278*, 108148. https://doi.org/10.1016/j.agwat.2023.108148

de Mendonça, R. R. S., Braga, C. R., Echer, E., Dal Lago, A., Munakata, K., Kuwabara, T., Kozai, M., Kato, C., Rockenbach, M., Schuch, N. J., Al Jassar, H. K., Sharma, M. M., Tokumaru, M., Duldig, M. L., Humble, J. E., Evenson, P., & Sabbah, I. (2016). The temperature effect in secondary cosmic rays (muons) observed at the ground: Analysis of the global muon detector network data. *The Astrophysical Journal*, *830*(2), 88. https://doi.org/10.3847/0004-637X/830/2/88

Desilets, D., Zreda, M., & Ferré, T. P. A. (2010). Nature's neutron probe: Land surface hydrology at an elusive scale with cosmic rays. *Water Resources Research*, *46*(11). https://doi.org/10.1029/2009WR008726

Emamalizadeh, S., Pirola, A., Alessandrini, C., Balenzano, A., & Baroni, G. (2024). *Advancing soil moisture estimation across scales: Insights from the SoMMet Project *

(Nos. EGU24-11565). EGU24. Copernicus Meetings. https://doi.org/10.5194/egusphere-egu24-11565

Evett, S. R., Schwartz, R. C., Tolk, J. A., & Howell, T. A. (2009). Soil Profile Water Content Determination: Spatiotemporal Variability of Electromagnetic and Neutron Probe Sensors in Access TubesAll rights reserved. No part of this periodical may be reproduced or transmitted in any form or by any means, electronic or mechanical, including photocopying, recording, or any information storage and retrieval system, without permission in writing from the publisher. *Vadose Zone Journal*, *8*(4), 926–941. https://doi.org/10.2136/vzj2008.0146

Franz, T. E., Wahbi, A., Zhang, J., Vreugdenhil, M., Heng, L., Dercon, G., Strauss, P., Brocca, L., & Wagner, W. (2020). Practical Data Products From Cosmic-Ray Neutron Sensing for Hydrological Applications. *Frontiers in Water*, *2*. https://www.frontiersin.org/articles/10.3389/frwa.2020.00009

Franz, T. E., Zreda, M., Rosolem, R., & Ferre, T. P. A. (2012). Field Validation of a Cosmic-Ray Neutron Sensor Using a Distributed Sensor Network. *Vadose Zone Journal*, *11*(4). https://doi.org/10.2136/vzj2012.0046

Gianessi, S., Polo, M., Stevanato, L., Lunardon, M., Ahmed, H. S., Weltin, G., Toloza, A., Budach, C., Bíró, P., Francke, T., Heistermann, M., Oswald, S. E., Fulajtar, E., Dercon, G., Heng, L. K., & Baroni, G. (2021). Assessment of a new non-invasive soil moisture sensor based on cosmic-ray neutrons. *2021 IEEE International Workshop on Metrology for Agriculture and Forestry (MetroAgriFor)*, 290–294. https://doi.org/10.1109/MetroAgriFor52389.2021.9628451

Gianessi, S., Polo, M., Stevanato, L., Lunardon, M., Francke, T., Oswald, S. E., Said Ahmed, H., Toloza, A., Weltin, G., Dercon, G., Fulajtar, E., Heng, L., & Baroni, G. (2024). Testing a novel sensor design to jointly measure cosmic-ray neutrons, muons and gamma rays for non-invasive soil moisture estimation. *Geoscientific Instrumentation, Methods and Data Systems*, *13*(1), 9–25. https://doi.org/10.5194/gi-13-9-2024

Han, X., Hendricks Franssen, H.-J., Jiménez Bello, M. Á., Rosolem, R., Bogena, H., Alzamora, F. M., Chanzy, A., & Vereecken, H. (2016). Simultaneous soil moisture and properties estimation for a drip irrigated field by assimilating cosmic-ray neutron intensity. *Journal of Hydrology*, *539*, 611–624. https://doi.org/10.1016/j.jhydrol.2016.05.050

Hardie, M. (2020). Review of Novel and Emerging Proximal Soil Moisture Sensors for Use in Agriculture. *Sensors*, *20*(23), Article 23. https://doi.org/10.3390/s20236934

Iwema, J., Rosolem, R., Baatz, R., Wagener, T., & Bogena, H. R. (2015). Investigating temporal field sampling strategies for site-specific calibration of three soil moisture–neutron intensity parameterisation methods. *Hydrology and Earth System Sciences*, *19*(7), 3203–3216. https://doi.org/10.5194/hess-19-3203-2015

Kang, Y., Khan, S., & Ma, X. (2009). Climate change impacts on crop yield, crop water productivity and food security – A review. *Progress in Natural Science*, *19*(12), 1665–1674. https://doi.org/10.1016/j.pnsc.2009.08.001

Köhli, M., Schrön, M., Zreda, M., Schmidt, U., Dietrich, P., & Zacharias, S. (2015). Footprint characteristics revised for field-scale soil moisture monitoring with cosmic-ray neutrons. *Water Resources Research*, *51*(7), 5772–5790. https://doi.org/10.1002/2015WR017169

Li, D., Schrön, M., Köhli, M., Bogena, H., Weimar, J., Jiménez Bello, M. A., Han, X., Martínez Gimeno, M. A., Zacharias, S., Vereecken, H., & Hendricks Franssen, H.-J. (2019). Can Drip Irrigation be Scheduled with Cosmic-Ray Neutron Sensing? *Vadose Zone Journal*, *18*(1), 190053. https://doi.org/10.2136/vzj2019.05.0053

Mazzoleni, R., Emamalizadeh, S., & Baroni, G. (2025). *Datasets analysed within the study "Cosmic-ray neutron sensing to monitor soil moisture across various irrigation methods"* [Dataset]. Zenodo. https://doi.org/10.5281/ZENODO.17177047

McJannet, D., Rasche, D., Marano, J., Hawdon, A., Stenson, M., & Schrön, M. (2025). Over-Water Low-Energy Neutron Observations for Intensity Corrections Across Cosmic-Ray Soil Moisture Sensor Networks. *Water Resources Research*, *61*(9), e2024WR039727. https://doi.org/10.1029/2024WR039727

Peng, J., Albergel, C., Balenzano, A., Brocca, L., Cartus, O., Cosh, M. H., Crow, W. T., Dabrowska-Zielinska, K., Dadson, S., Davidson, M. W. J., de Rosnay, P., Dorigo, W., Gruber, A., Hagemann, S., Hirschi, M., Kerr, Y. H., Lovergine, F., Mahecha, M. D., Marzahn, P., … Loew, A. (2021). A roadmap for high-resolution satellite soil moisture applications – confronting product characteristics with user requirements. *Remote Sensing of Environment*, *252*, 112162. https://doi.org/10.1016/j.rse.2020.112162

Riggi, F., Hertle, L., Abbrescia, M., Avanzini, C., Baldini, L., Baldini Ferroli, R., Batignani, G., Battaglieri, M., Boi, S., Boike, J., Bossini, E., Carnesecchi, F., Cavazza, D., Cicalò, C., Cifarelli, L., Coccetti, F., Coccia, E., Corvaglia, A., De Gruttola, D., … Pinazza, O. (2025). High latitude observation of the Forbush decrease during the May 2024 solar storms with muon and neutron detectors on Svalbard. *Advances in Space Research*. https://doi.org/10.1016/j.asr.2025.05.023

Robinson, D. A., Campbell, C. S., Hopmans, J. W., Hornbuckle, B. K., Jones, S. B., Knight, R., Ogden, F., Selker, J., & Wendroth, O. (2008a). Soil Moisture Measurement for Ecological and Hydrological Watershed-Scale Observatories: A Review. *Vadose Zone Journal*, *7*(1), 358–389. https://doi.org/10.2136/vzj2007.0143

Robinson, D. A., Campbell, C. S., Hopmans, J. W., Hornbuckle, B. K., Jones, S. B., Knight, R., Ogden, F., Selker, J., & Wendroth, O. (2008b). Soil Moisture Measurement for Ecological and Hydrological Watershed-Scale Observatories: A Review. *Vadose Zone Journal*, *7*(1), 358–389. https://doi.org/10.2136/vzj2007.0143

Rodriguez-Iturbe, I. (2000). Ecohydrology: A hydrologic perspective of climate-soil-vegetation dynamies. *Water Resources Research*, *36*(1), 3–9. https://doi.org/10.1029/1999WR900210

Scheiffele, L. M., Baroni, G., Franz, T. E., Jakobi, J., & Oswald, S. E. (2020). A profile shape correction to reduce the vertical sensitivity of cosmic-ray neutron sensing of soil moisture. *Vadose Zone Journal*, *19*(1), e20083. https://doi.org/10.1002/vzj2.20083

Schrön, M., Köhli, M., Scheiffele, L., Iwema, J., Bogena, H. R., Lv, L., Martini, E., Baroni, G., Rosolem, R., Weimar, J., Mai, J., Cuntz, M., Rebmann, C., Oswald, S. E., Dietrich, P., Schmidt, U., & Zacharias, S. (2017). Improving calibration and validation of cosmic-ray neutron sensors in the light of spatial sensitivity. *Hydrology and Earth System Sciences*, *21*(10), 5009–5030. https://doi.org/10.5194/hess-21-5009-2017

Schrön, M., Köhli, M., & Zacharias, S. (2023). Signal contribution of distant areas to cosmic-ray neutron sensors – implications for footprint and sensitivity. *Hydrology and Earth System Sciences*, *27*(3), 723–738. https://doi.org/10.5194/hess-27-723-2023

Seneviratne, S. I., Corti, T., Davin, E. L., Hirschi, M., Jaeger, E. B., Lehner, I., Orlowsky, B., & Teuling, A. J. (2010). Investigating soil moisture–climate interactions in a changing climate: A review. *Earth-Science Reviews*, *99*(3), 125–161. https://doi.org/10.1016/j.earscirev.2010.02.004

Stevanato, L., Baroni, G., Cohen, Y., Fontana, C. L., Gatto, S., Lunardon, M., Marinello, F., Moretto, S., & Morselli, L. (2019). A Novel Cosmic-Ray Neutron Sensor for Soil Moisture Estimation over Large Areas. *Agriculture*, *9*(9), Article 9. https://doi.org/10.3390/agriculture9090202

Stevanato, L., Baroni, G., Oswald, S. E., Lunardon, M., Mares, V., Marinello, F., Moretto, S., Polo, M., Sartori, P., Schattan, P., & Ruehm, W. (2022a). An Alternative Incoming Correction for Cosmic-Ray Neutron Sensing Observations Using Local Muon Measurement. *Geophysical Research Letters*, *49*(6), e2021GL095383. https://doi.org/10.1029/2021GL095383

Stevanato, L., Baroni, G., Oswald, S. E., Lunardon, M., Mares, V., Marinello, F., Moretto, S., Polo, M., Sartori, P., Schattan, P., & Ruehm, W. (2022b). An Alternative Incoming Correction for Cosmic-Ray Neutron Sensing Observations Using Local Muon Measurement. *Geophysical Research Letters*, *49*(6), e2021GL095383. https://doi.org/10.1029/2021GL095383

Susha Lekshmi, S. U., Singh, D. N., & Shojaei Baghini, M. (2014). A critical review of soil moisture measurement. *Measurement*, *54*, 92–105. https://doi.org/10.1016/j.measurement.2014.04.007

Szabó, B., Weynants, M., & Weber, T. K. D. (2021). Updated European hydraulic pedotransfer functions with communicated uncertainties in the predicted variables (euptfv2). *Geoscientific Model Development*, *14*(1), 151–175. https://doi.org/10.5194/gmd-14-151-2021

Zappa, L., Dari, J., Modanesi, S., Quast, R., Brocca, L., De Lannoy, G., Massari, C., Quintana-Seguí, P., Barella-Ortiz, A., & Dorigo, W. (2024). Benefits and pitfalls of irrigation timing and water amounts derived from satellite soil moisture. *Agricultural Water Management*, *295*, 108773. https://doi.org/10.1016/j.agwat.2024.108773

Zhu, Z., Tan, L., Gao, S., & Jiao, Q. (2015). Observation on Soil Moisture of Irrigation Cropland by Cosmic-Ray Probe. *IEEE Geoscience and Remote Sensing Letters*, *12*(3), 472–476. IEEE Geoscience and Remote Sensing Letters. https://doi.org/10.1109/LGRS.2014.2346784

Zreda, M., Desilets, D., Ferré, T. P. A., & Scott, R. L. (2008). Measuring soil moisture content non-invasively at intermediate spatial scale using cosmic-ray neutrons. *Geophysical Research Letters*, *35*(21). https://doi.org/10.1029/2008GL035655

Zreda, M., Shuttleworth, W. J., Zeng, X., Zweck, C., Desilets, D., Franz, T., & Rosolem, R. (2012). COSMOS: The COsmic-ray Soil Moisture Observing System. *Hydrology and Earth System Sciences*, *16*(11), 4079–4099. https://doi.org/10.5194/hess-16-4079-2012

3. Towards a non-invasive monitoring of the soil-plant-atmosphere interactions: insights from a Mediterranean vineyard case study

Riccardo Mazzoleni[1], Francesco Vinzio[1], Marco Benfenati[1], Ilaria Filippetti[1], Gabriele Baroni[1]

[1]Department of Agricultural and Food Sciences (DISTAL), University of Bologna, Viale Giuseppe Fanin 42-50, 40127 Bologna, Italy.

Note of the Candidate: this chapter is based on a manuscript submitted to Irrigation Science, under the Special Issue "Advances in Irrigation Science: Sensors, Remote Sensing, and Models for Sustainable Agricultural Water Management." The manuscript has been readapted for inclusion in the present Thesis.

Abstract

This study evaluated a non-invasive, integrated monitoring approach to characterize the soil-plant-atmosphere continuum (SPAC) in a commercial vineyard of Pignoletto (PG) and Trebbiano Romagnolo (TR). The approach is based on a cosmic-ray neutron sensor (CRNS) to continuously monitor soil water content (SWC), which was normalized into extractable soil water (ESW) to represent plant-available water. Moreover, vapor pressure deficit (VPD) was calculated based on weather data to characterize the atmospheric demand. Finally, remotely sensed NDVI data were used to detect canopy development and vine physiological responses. Over two growing seasons, measurements of midday stem water potential (Ψ_{stem}) and berry composition complemented the monitoring activities. In 2023, ripening was largely buffered from atmospheric demand, with Ψ_{stem} values between -0.66 and -1.06 MPa, reflecting SWC as a non-limiting factor and uniform ripening. Conversely, the 2024 season showed more negative Ψ_{stem} (-0.95 to -1.12 MPa) and an accelerated ripening process, particularly in TR. Principal Component Analysis (PCA) explained 65% of the variance in 2023 and 81.5% in 2024, revealing that environmental drivers (ESW, VPD) became more tightly linked to physiological and grape composition traits (Ψ_{stem}, TSS, TA). Overall, the results showed the capability of the integrated approach to capture the main interactions within the SPAC, offering a non-invasive and scalable tool for supporting precision and sustainability in Mediterranean viticulture.

3.1. Introduction

In the Mediterranean basin, efficient water use has become a critical concern due to increasing climatic variability, especially considering the recurrent summer droughts

(Büntgen et al., 2024; Seager et al., 2014). In this context, precision agriculture has emerged as a transformative approach in modern agriculture, seeking to optimize crop production and minimize input and costs. Besides, precision agriculture offers promising strategies to enhance sustainability, highlighting the central importance of irrigation management (Bwambale et al., 2022). This is especially relevant in vineyard, where operations depend significantly on effective water management, as water availability can notably impact grape quality and yield (Fuentes and Gago, 2022). In vineyards, for instance, water availability needs to be tailored based on the intended use of the grapes (Bonada et al., 2023), as under a moderate water deficit during the fruit development, it produces grapes with high quality potential for winemaking (Acevedo-Opazo et al., 2010).

In this scenario, soil water content (SWC) is a crucial variable in the soil-plant-atmosphere continuum (SPAC), influencing not only the evapotranspiration process but also being strictly correlated with vine stress and growth (Pellegrino et al., 2005; Seneviratne et al., 2010). Water use in vineyards is a function of available water content of the soil (Lebon et al., 2003), and the occurrence of low SWC may trigger reductions in vegetation productivity driven by drought and heat (Zhou et al., 2019), a scenario particularly critical during the grapes ripening period. Grapevine, although is considered to be highly adaptable to water restrictions (Lovisolo et al., 2010), exhibit however complex physiological responses to water deficits that can influence both vegetative growth and fruit development (Chaves et al., 2010; Valentini et al., 2022). Rainfall during the growing season is often inadequate to meet vine water requirements, making supplemental irrigation increasingly essential. Applied during key phenological stages such as veraison and ripening, irrigation is therefore recognized as an effective adaptive strategy to counteract the negative effects of multiple stresses during summer (Allegro et al., 2023).

Given this, the continuous and accurate monitoring of SWC becomes essential for preventing water stress condition and programming irrigation. Numerous methods for assessing SWC, ranging from point-scale to satellite remote sensing approaches have been devised (Susha Lekshmi et al., 2014).The former has been widely used but applicability and interpretation of the results is limited due to the inherent strong spatial variability of the soil-plant system (Soulis et al., 2015). The latter, even if it has shown an increasing adaptability, it is currently constrained by the relatively small size of the agricultural management units, e.g., lower than 1 km^2 (Massari et al., 2021). Ultimately, research interest was focused on the development and application of non-invasive proximal sensors based on cosmic-ray neutron sensing (CRNS). This approach relies on the inverse relation between neutrons generated by cosmic-ray fluxes and the existence of hydrogen, primarily present in the soil as in the water molecule. Moist soils strongly decelerate and absorb neutrons, leading to a reduced neutron flux at the detector. Conversely, in drier soils, fewer neutrons are absorbed, resulting in a higher detected neutron intensity (Zreda et al., 2008). CRNS probes are installed above the soil surface allowing non-invasive moisture measurements, with a penetration depth ranging from 10 cm to 40 cm and a radius of influence ranging from 100 m to 200 m (Köhli et al., 2015; Schrön et al., 2017). Recent advancements in sensor implementation have enabled the utilization of CRNS probes to monitor SWC fluctuations in agricultural fields, particularly in response to irrigation interventions (Brogi et al., 2023; Gianessi et al., 2024; Mazzoleni et al., 2025). However, the ongoing debate surrounding the use of CRNS for precision irrigation continues to captivate attention, with studies on the topic remaining limited (Li et al., 2019).

In this context, combining CRNS-based SWC monitoring with additional weather-based and plant-based indicators can offer a powerful approach to monitor the SPAC and to assess grapevine growth. Along with soil moisture observations, the monitoring of the atmosphere demand such as vapour water deficit (VPD) can better capture the co-regulation of crop water stress (Novick et al., 2016; J. Zhang et al., 2021). In addition, plant-based measurements provided the key feature to quantify the on-set of the stress and the effect on vegetation growth. In this case, among the different techniques, (Velazquez-Chavez et al., 2024), Normalized Difference Vegetation Index (NDVI) detected by satellite has been widely applied and has become a validated tool to reflect spatio-temporal patterns in vine vigour, water stress, and grape quality (Giovos et al., 2021). For instance, Bolognini et al. (2023) demonstrated that NDVI data from Sentinel-2, collected at key phenological stages in Sangiovese vineyards, could effectively define zones with distinct levels of crop water stress, yield, and grape quality. Pereyra et al. (2022) used NDVI to delineate vigour-based zones in vineyards, enabling variable-rate irrigation and canopy management that led to improved yield and berry composition. Similarly, Ortuani et al. (2024) compared UAV and Sentinel-2-derived NDVI in vineyards in northern Italy, showing that even with coarser resolution, satellite imagery reliably captured the main patterns of variability relevant to vineyard management.

Building on previous work that validated the use of CRNS for SWC monitoring in vineyards (Mazzoleni et al., 2025), this study takes a step further by evaluating its functional integration with plant and atmosphere-based indicators. Rather than focusing solely on SWC dynamics, the analysis seeks to understand how temporal fluctuations in extractable soil water (ESW) interact with atmospheric demand and drive physiological responses in the vine, as expressed by midday stem water potential (Ψ_{stem}) and berry composition parameters. To test this, ESW derived from CRNS was integrated with VPD and remote sensing NDVI, allowing for a combined, non-invasive assessment of soil-plant-atmosphere interactions. The overarching goal is to evaluate the actual contribution and complementarity of these measurements, identifying which indicators are most informative, and how their integration can strengthen irrigation strategies in Mediterranean viticulture

3.2. Materials and methods

3.2.1. Study site overview and setup description

The vineyard (*Vitis vinifera* L.), planted with cv. Trebbiano Romagnolo (TR) and cv. Pignoletto (PG), is located at Imola, Bologna, Italy (44.384954, 11.698439), covering an approximate area of 12 hectares (Figure 1). The vine rows were oriented northeast to southwest, trained to a vertical shoot positioned spur-pruned cordon, and spaced at 1 m within the row and 2.5 m between rows.

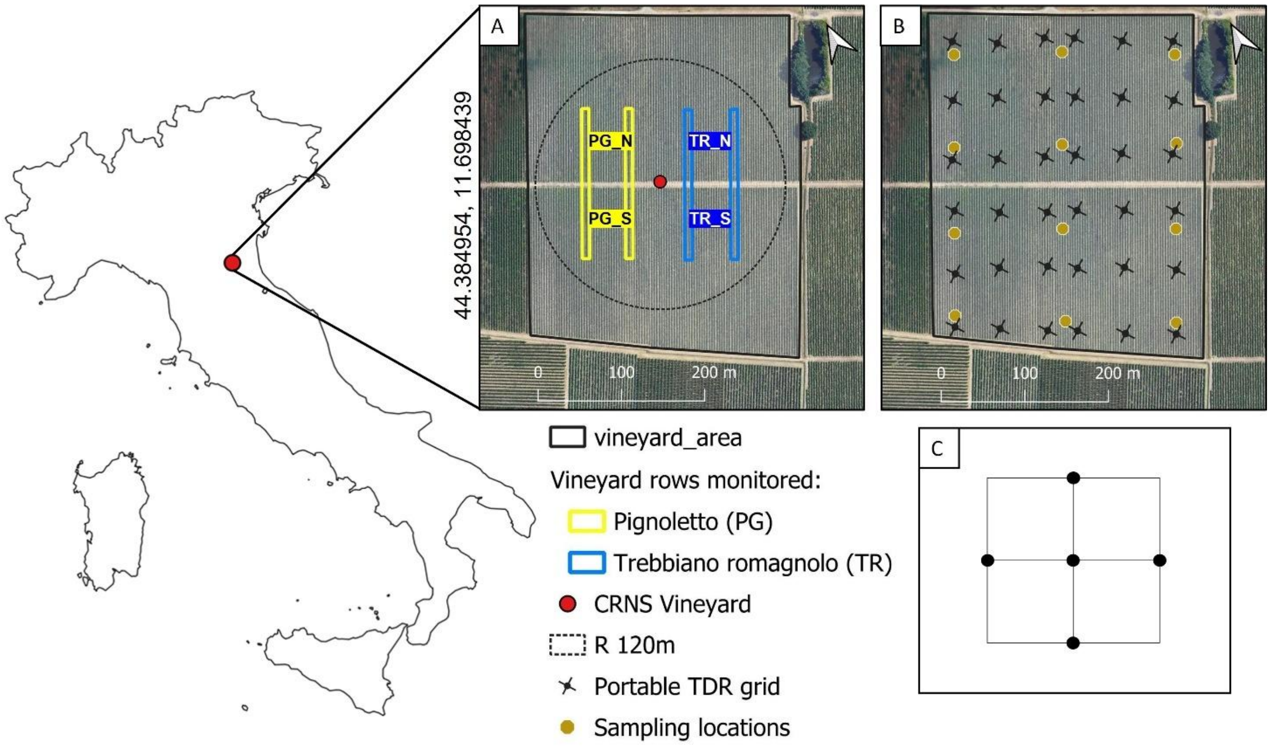

Figure 1: Overview of the experimental vineyard site showing its location in Italy with geographic coordinates and the layout of the instrumentation and sampling design. (A) CRNS sensor installation point and subdivision of monitored vineyard rows between the two cultivars, Pignoletto (PG, yellow) and Trebbiano romagnolo (TR, blue), with corresponding north and south blocks for each variety. R = 120 m indicates the extent of the CRNS detection footprint. (B) Scheme of soil sampling and monitoring layout: 12 locations for soil texture analysis

(yellow circles) and grid of portable TDR measurement points (black crosses). (C) Detail of a single TDR measurement location, where five repeated readings were taken per point.

Irrigation within this area was provided with a sub-surface drip irrigation (SDI) system, and was managed by Società Agricola CACI in Imola, Bologna (Italy). The SDI system is placed at a depth of 25 cm along two lines parallel to each row of plants, and drip system has a water capacity of 0.008 m^3 h^{-1}. Irrigation events and total volume distributed (mm d^{-1}) during the two seasons monitored, together with grape phenological phase (BBCH) according to Lorenz et al. (1995), are resumed in Table 1.

Table 1: Irrigation schedule and estimated phenological stages (BBCH scale) during the 2023 and 2024 growing seasons. Phenological stages were estimated based on field observations, covering berry development (BBCH 75-79), onset of ripening (veraison; BBCH 81-83), and berry maturation (BBCH 85-89).

Irrigation event (DOY)	2023	205	212	222	229	240	259	2024	194	202	209	214	218	233
Total volume distributed (mm d^{-1})		20	18	16	18	16	16		20	18	18	18	18	18
Estimated BBCH stage		75-77	77-79	81-83	83-85	85-87	87-89		75-77	77-79	81-83	83-85	85-87	87-89

3.2.2. Soil characterization and environmental variables

To assess soil physical variability across the vineyard, twelve samples were collected from predefined locations evenly distributed across all sub-parcels, ensuring coverage both along rows and across transects (Figure 1 B). Sampling points were spaced 100 m apart within transects and 130 m between vine rows. Soil samples were taken at 0-50 cm depth using a manual auger and stored in sealed aluminium trays for lab analysis. Particle size distribution (PSD) was determined with a PARIO™ system (METER Group, Pullman, WA, USA), which automatically implements Stokes' Law within the 2-63 μm range to generate continuous PSD curves. Precipitation and weather data were sourced from the network stations of the regional environmental agency ARPAe and were processed following Antolini et al. (2016). Based on these data, the VPD was calculated according to Allen et al. (1998) on an hourly basis for both season.

3.2.3. Soil water content monitoring

A CRNS probe manufactured by Finapp S.r.l (Montegrotto Terme, Padova, Italy) was installed on April 2023 (Figure 1 A). According to Stevanato et al. (2019), the probe is enriched with few centimeters of polyethylene to moderate and slow down epithermal neutrons and enhance the probe's sensitivity to soil moisture (Köhli et al., 2015). Following Zreda et al. (2012), the neutrons measured by the CRNS sensor were corrected to account for changing in air pressure, air humidity and variability in the incoming neutron flux. The CRNS sensor calibration took place on DOY 129 in 2023. The procedure for calibrating the CRNS sensor in this site was previously documented by Mazzoleni et al. (2025), and the protocol is following Franz et al. (2012). The calibration procedure allows to convert corrected neutron counts (Nc) into SWC based on the following equation proposed by Desilets et al. (2010):

$$SWC_v(Nc) = \left(\frac{0.0808}{\frac{Nc}{N_0}-0.372} - 0.115 - SWC_{offset}\right) \cdot \frac{\rho_{bd}}{\rho_w}, \quad \text{Eq. 1}$$

where r_{bd} and r_w are respectively the soil bulk density and water density (kg m^{-3}); SWC_{offset} is the contribution of static hydrogen pools (SHP), which is represented by the lattice water (LW) and soil organic carbon (SOC); $SWC_v\ (N_c)$ is the volumetric SWC average during the calibration day, N_0 is the calibration parameter.

To normalize SWC values throughout the season, extractable soil water (ESW) was calculated based on the method of Gerakis and Zalidis (1998), with modifications following Zhang et al. (2012), to better capture the scale and dynamics of plant-available water. ESW was defined as a dimensionless ratio representing the proportion of available water in the soil, calculated using the current SWC relative to the range between field capacity (FC) and wilting point (WP). The formula applied was:

$$ESW = \frac{SWC-WP}{FC-WP}, \quad \text{Eq. 2}$$

where SWC represents the volumetric soil water content measured hourly by CRNS sensor, FC is the field capacity (0.38 m^3m^{-3}) and WP is the wilting point (0.17 m^3m^{-3}). These values were determined by applying prediction algorithms (pedotransfer functions; PTFs) through the web interface of Szabó et al. (2021), utilizing a mix of the soil samples from the textural analysis described in Section 2.2. Additionally, measurements with a portable TDR sensor (Spectrum Technologies, Inc., Aurora, IL, USA) were carried out in 2023 (DOY 128, 158, and 296) and in 2024 (DOY 194), to characterize the spatial variability of SWC across the vineyard and to assess the consistency of observed patterns (Figure 1 B). The sensor allowed mobile, point-scale, repetitive acquisitions of SWC (%), with a vertical resolution of 15 cm depth. Measurements were evenly distributed across all sub-parcels, ensuring coverage both along vine rows and across transects. At each location, five repeated acquisitions were taken (Figure 1 C), with sampling points spaced 50 m apart within transects and 100 m between vine rows, resulting in approximately 500 individual measurements per survey date.

3.2.4. Plant physiological measurement

The monitored vine rows were divided into two sectors per variety, corresponding to the north and south sections of the vineyard, which are naturally separated by a field road. This subdivision allowed for a more detailed analysis of intra-varietal and spatial variability. Accordingly, the grape varieties are referred to as PG_N and PG_S for Pignoletto, and TR_N and TR_S for Trebbiano Romagnolo (Figure 1 A). A total of 80 vines were randomly selected from the monitored vine rows, 20 in each sector. These vines were monitored throughout the 2023 and 2024 growing seasons to assess their water status and berry composition.

Vine water status was evaluated during both the 2023 and 2024 growing seasons on three dates per year (DOY 201, 215, and 222 in 2023; DOY 194, 218, and 234 in 2024). Measurements were taken at solar midday by determining stem water potential (Ψ_{stem}) with a Scholander pressure chamber (Soilmoisture Corp., Santa Barbara, CA, USA). For each date, a total of 24 leaves were randomly sampled from the vines selected for each variety, 12 in each sector. The leaves were covered with aluminum foil and placed in a plastic bag for 45 minutes prior to measurement.

From each of the 20 selected vines per sector, 50 berries were randomly collected on multiple dates prior to harvest and at harvest. In 2023, sampling occurred on DOY 222, 234, 243, and 249, while in 2024, it was conducted on DOY 220, 235, and 241. The following parameters were analysed: berry weight (g), total soluble solids (°Brix) using a temperature-compensated refractometer (Misure Maselli, Parma, Italy) and must pH and titratable acidity (g L^{-1}), measured with an automatic titrator (Crison Instruments, Barcelona, Spain). In addition, the overall yield at harvest for both varieties was considered to provide a broader context for vine productivity.

3.2.5. Remote sensing data

NDVI maps were generated using level-2A reflectance products from the Sentinel-2 satellite. Data processing and analysis were performed on the Google Earth Engine (GEE) cloud-based platform. Available imagery from the years 2023 and 2024 was first filtered to include only acquisitions captured during the vines growing season, between May 1st and October

1st of each year. Subsequently, the Scene Classification Layer (SCL), provided by the European Space Agency (ESA), was used to generate a filtering mask, which was then applied to the selected images: pixels not classified as vegetation (Class 4) or bare soil (Class 5) were removed. It is well established that the Sen2Cor algorithm, used to elaborate the SCL products, is not always effective in detecting all kinds of cloud coverage, especially close to clouds margins (Baetens et al., 2019). For this reason, images with more than 10% of invalid pixels were also excluded from the analysis. Lastly, a mobile window filter was applied to the mean-values time series, to remove outliers. In the end, a total of 32 acquisitions were used: 17 images from 2023 and 15 from 2024.

3.2.6. Data processing and statistical analysis

The soil textural composition (% of clay, silt, and sand) for each sample, as well as the individual acquisitions of SWC (%) with the portable TDR, were processed using QGIS (LTR version 3.34.10 - Prizren) and interpolated using the Inverse Distance Weighting (IDW) method to generate spatial distribution maps for visual representation. All the correlation and computation analysis presented in this study were conducted using the software R, in RStudio (2024.12.1+563 "Kousa Dogwood" Release). Linear regressions were carried out with the ‘stats’ package, while PCA was performed using the ‘stats’ and ‘ggplot2’ packages for visualization. For multivariate analysis, all variables were standardized (z-scores) and subjected to Principal Component Analysis (PCA) to identify the main gradients of variation and the relative contribution of environmental drivers and physiological traits. The contribution of each variable to PC1 and PC2 was quantified through loadings, and biplots were generated to visualize relationships among variables and vineyard sectors.

3.3. Results

3.3.1. Soil characteristics and intra-field variability

The interpolated soil texture fractions across the vineyard are depicted in Figure 2. The soil texture ranged from clay loam to clay, with localized sandy inclusions. Clay content exhibited the strongest spatial gradient, with markedly higher values (>50%) in the southern and eastern parts of the vineyard, particularly in correspondence with the TR_S sector, whereas lower percentages were observed in the central area. By comparison, silt showed a narrower range of variation, with slightly higher concentrations in the south-western and north-eastern areas, where the PG_S and TR_N sectors are located, respectively. Sand was the least represented fraction but showed localized accumulation in the western, and especially the south-western, zones encompassing the PG_N and PG_S sectors, where the relatively coarser texture is expected to enhance drainage and reduce water storage capacity.

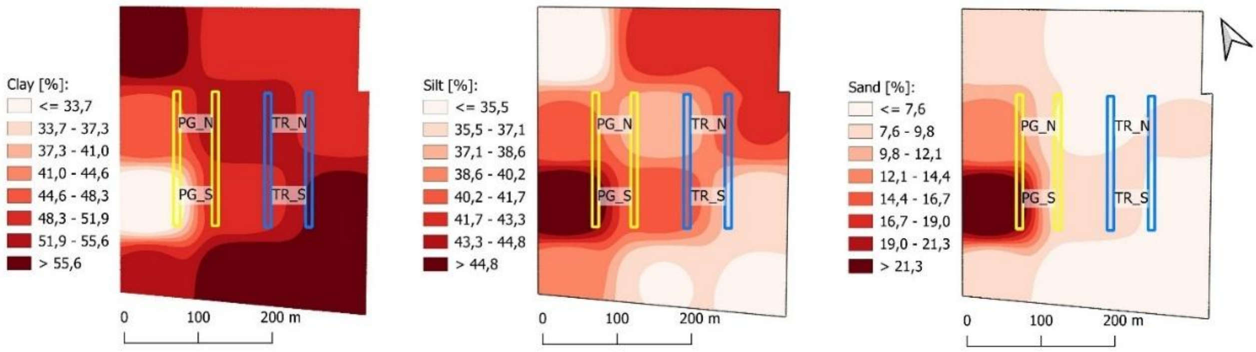

Figure 2: Spatial distribution maps of soil textural fractions (clay, silt, and sand, %) across the experimental vineyard. Yellow and blue boxes indicate monitored vine rows divided into two sectors per variety (N and S) of cv. Pignoletto (PG) and cv. Trebbiano Romagnolo (TR), respectively.

The spatial distribution of SWC measured with a portable TDR sensor at 15 cm depth across the experimental vineyard is shown in Figure 3 (A - D). In 2023, early-season measurements (Figure. 3 A, B) indicated generally high SWC (>40%), with relatively homogeneous patterns across sub-parcels, reflecting mostly the substantial rainfall events occurred in May. By late season (Figure 3 C), SWC decreased markedly, with localized dry patches (<20%) emerging particularly in the western and south-western part of the field, in line with expectations after the warm and dry summer conditions. In 2024 (Figure 3 D), the overall pattern was consistent to what observed in the previous year, with contrasting zones ranging from <25% to >45%, highlighting differences in water retention and depletion across sectors, particularly with a western-eastern gradient. When compared with the textural analysis, these patterns are coherent with the underlying soil heterogeneity. Clay-rich zones in the eastern and southern sectors generally coincide with areas retaining higher SWC (%), whereas sandier areas, particularly in the south-western portion where PG_N and PG_S are located, tended to exhibit lower water contents.

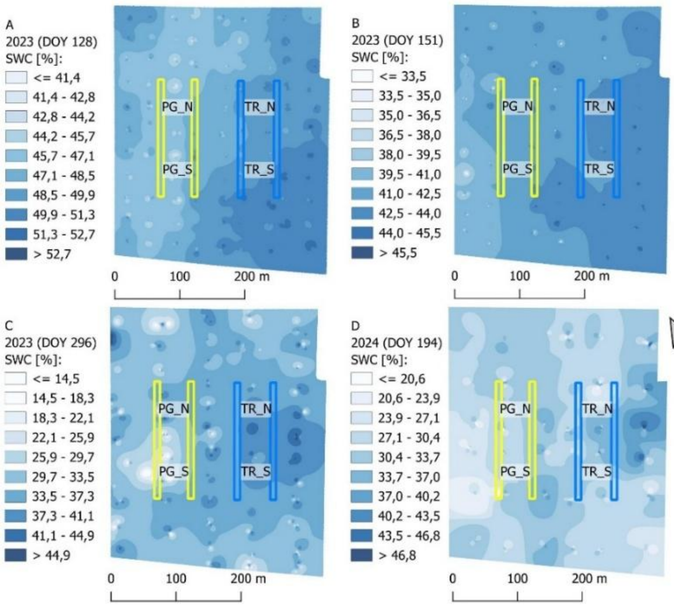

Figure 3: Spatial distribution of SWC (%) measured with a portable TDR sensor at 15 cm depth across the experimental vineyard. Maps correspond to DOY 128 (A), DOY 151 (B), and DOY 296 (C) of 2023, and DOY 194 (D) of 2024. Data represents ~500 measurements per survey date. Yellow and blue boxes indicate monitored vine rows divided into two sectors per variety (N and S) of cv. Pignoletto (PG) and cv. Trebbiano Romagnolo (TR), respectively.

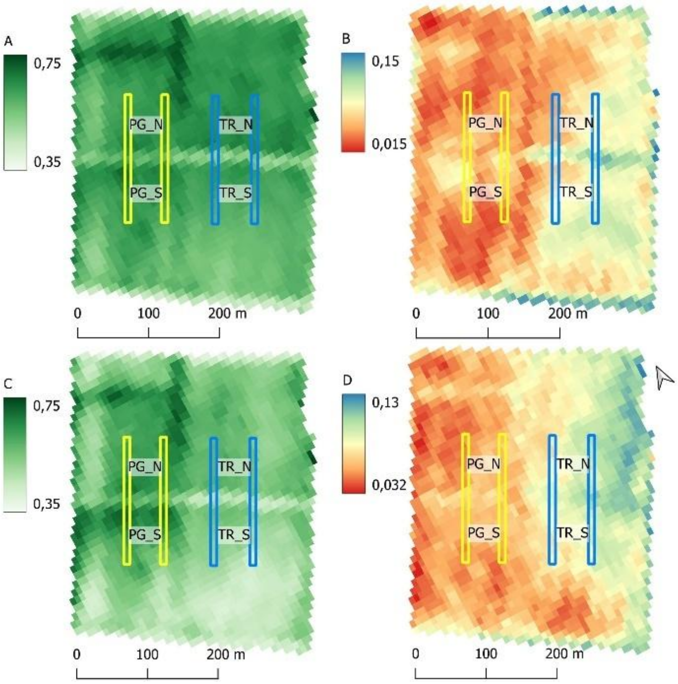

Figure 4: Spatial distribution of average NDVI values and their seasonal variability across the vineyard during the 2023 and 2024 growing seasons (May 1st to October 1st). (A) Mean NDVI for 2023; (B) standard deviation of NDVI for 2023; (C) mean NDVI for 2024; (D) standard deviation of NDVI for 2024. Yellow and blue boxes indicate monitored vine rows divided into two sectors per variety (N and S) of cv. Pignoletto (PG) and cv. Trebbiano Romagnolo (TR), respectively.

The spatial distribution of average NDVI values and their seasonal variability across the vineyard during the 2023 and 2024 growing seasons are depicted in Figure 4 (A - D). In 2023, the vineyard exhibited relatively homogeneous average NDVI values across the entire area (Fig. 4 A), with slightly higher values observed in the north-western sectors compared to the south-eastern ones, where NDVI appeared lower. However, the corresponding NDVI standard deviation map (Fig. 4 B) revealed notable intra-field variability, particularly along an east-west gradient. This pattern may reflect spatial differences in vine growth dynamics throughout the season. In 2024, the average NDVI values appeared to be lower compared to the previous season, especially in the south-western zone, corresponding to TR_S (Fig. 4 C). Comparably to 2023, the trend of NDVI standard deviation appeared even more evident across the east-western gradient (Fig. 4 D).

3.3.2. Seasonal pattern of soil moisture and environmental drivers

The seasonal dynamics of soil water status, expressed as both SWC and normalized ESW, atmospheric evaporative demand represented by VPD, water inputs from precipitation and irrigation and daily average on NDVI are illustrated in Fig. 5 (A - H).

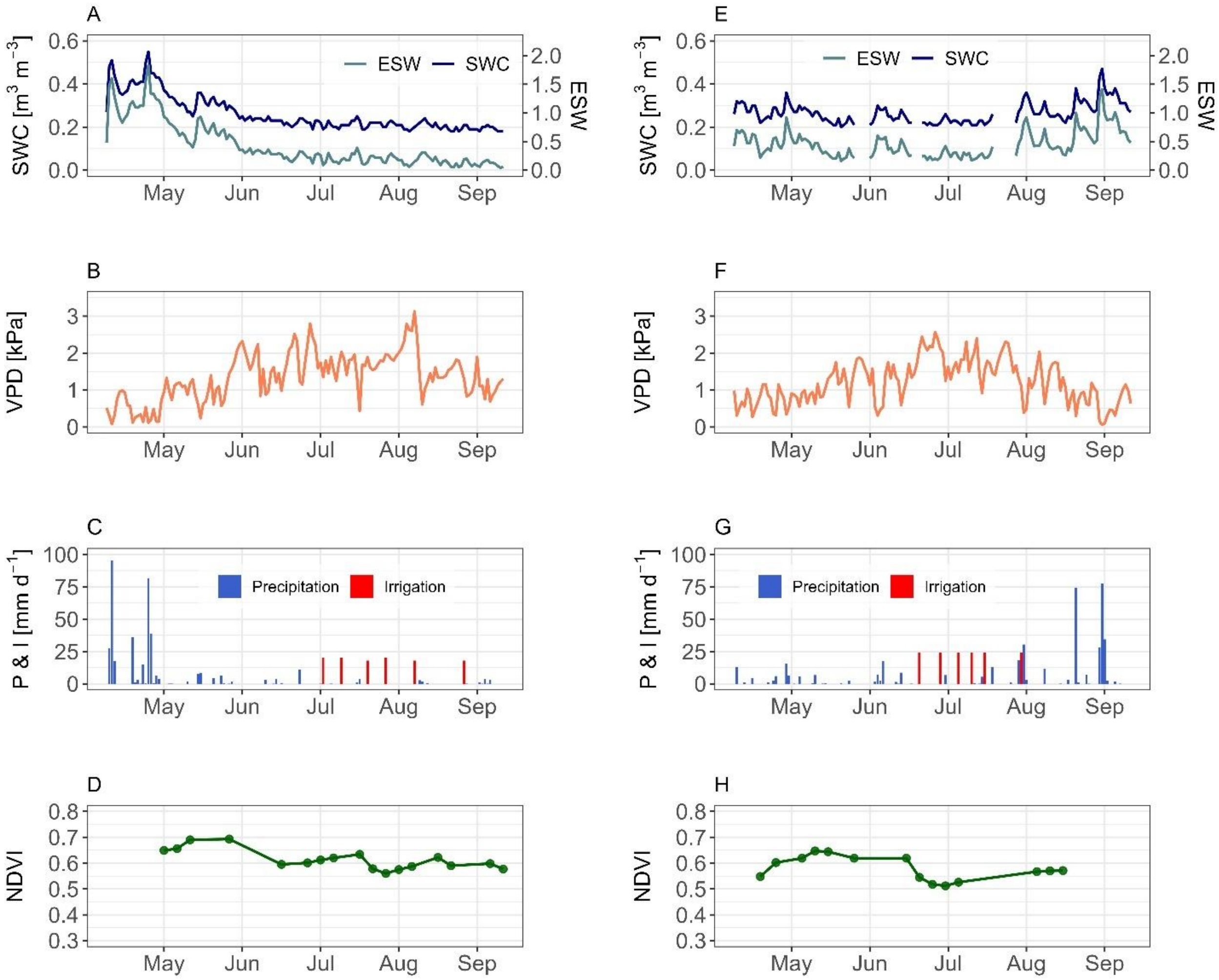

Figure 5: Seasonal dynamics of the monitored variables to assess the SPAC during the 2023 and 2024 growing seasons. Panels A-D refer to the 2023 season; Panels E-H to 2024. (A, E): daily trends of soil water content (SWC, m^3 m^{-3}) measured with the cosmic-ray neutron sensor (CRNS), and extractable soil water (ESW), normalized between field capacity and wilting point. (B, F): daily vapor pressure deficit (VPD, kPa) trends representing atmospheric evaporative demand. (C, G): daily cumulative precipitation (blue bars) and irrigation volumes (red bars) applied to the vineyard (mm d^{-1}). (D, H): interpolated daily average NDVI values registered across the season.

In 2023 (Fig. 5 A - D), the early season was characterized by abundant precipitation events, with a total cumulative precipitation amounting to approximately 300 mm recorded in the Emilia-Romagna region. Consequently, this led to high values of both SWC and ESW. However, from June onward, a sharp decrease in both SWC and ESW was observed, driven by the simultaneous rise in VPD (Fig. 5 B) and the lack of significant rainfall (Fig. 5 C). Despite some irrigation events starting in July, the overall water availability remained low, as shown by the persistently declining ESW values, which approached critical low values in late summer. NDVI values (Fig. 5 D) were initially high, consistent with the expected canopy vigour at onset of vegetative growth. As the season progressed, NDVI gradually declined and then stabilized around 0.60 - 0.55, reflecting a moderate and steady canopy condition during the summer months. The slight decrease was likely associated with canopy management practices (e.g., shoot trimming) and with the senescence or yellowing of inter-row herbaceous cover, which can influence the spectral signal captured by remote sensing (Palazzi et al., 2023).

During 2024, the overall pattern appeared slightly different (Fig. 5 E - H). Although spring rainfall were less intense but more consistent towards the end of June, irrigation inputs were managed consistently from early July (Fig. 5 G). These inputs helped maintain higher SWC and ESW levels throughout most of the season (Fig. 5 E), despite the VPD following a similar seasonal pattern to 2023, with increasing atmospheric demand from May to August. Similar to the previous year, NDVI values rose in mid to late May (Fig. 5 H) with the onset of vegetative growth, followed by a slight decline during the warmer months.

3.3.3. Vine water status and grape berry development

Results of the vine water status measurements, expressed as midday Ψ_{stem}, and grape berry development are depicted in Table 2 and Fig. 6 (A - H), respectively. In 2023, the Ψ_{stem} range (-0.66 to -1.06 MPa) indicated mild to moderate levels of water stress, consistent across grape varieties, with differences among vineyard sectors generally not statistically significant (Table 2). This suggests a rather uniform vine water status, likely due to more consistent SWC availability or effective irrigation, as previously observed in Section 3.2, and as it is visible in Table 1.

In contrast, the 2024 measures revealed more negative Ψ_{stem} values across all dates, consistent with overall higher VPD demand, and despite higher ESW compared to the previous year. Statistical differences among sectors remained limited, while a uniform vine water status was consistent with the previous year. However, a subtle pattern emerged, as PG_S block consistently showed more negative Ψ_{stem} values, particularly on DOY 218 and 234, hinting at a slightly reduced water availability or greater water demand in that block. The observations in the TR_S sector were similar, with slightly significant higher Ψ_{stem} value on DOY 234.

Consistent with the overall midday Ψ_{stem} patterns, berry ripening dynamics also exhibited limited intra-varietal variability in both years (Fig. 6 A - H). Berry weight (Fig. 6 A - E) increased progressively toward harvest, and although average berry size remained comparable between seasons, both varieties showed a decline in yield per hectare in 2024 compared to 2023. Specifically, total yield decreased from 15 t ha^{-1} to 13 t ha^{-1} for Pignoletto and from 21 t ha^{-1} to 18 t ha^{-1} for Trebbiano Romagnolo, corresponding to reductions of approximately 13% and 14%, respectively. Sugar accumulation (Fig. 6 B, F) followed a typical linear trend, reaching about 20 °Brix at harvest in both years for both grape varieties.

Table 2 Midday stem water potential (Ψ_{stem}, MPa) measured in Pignoletto (PG) and Trebbiano Romagnolo (TR) vines across four vineyard sectors (N = North, S = South) during the 2023 and 2024 growing seasons. Values represent means of 20 vines per sector. Different letters within each row indicate statistically significant differences among sectors according to Tukey's HSD test ($p < 0.05$).

cv		PG		TR	
Sector		N	S	N	S
2023					
	201	-0.78 a	-0.82 a	-0.72 a	-0.66 a
DOY	215	-0.88 a	-1.06 a	-0.82 a	-0.80 a
	222	-0.74 a	-0.80 a	-0.72 a	-0.66 a
2024					
	194	-1.07 a	-1.10 a	-1.02 a	-1.06 a
DOY	218	-1.05 b	-1.12 a	-1.02 a	-1.04 a
	234	-1.02 b	-1.10 a	-0.95 b	-1.06 a

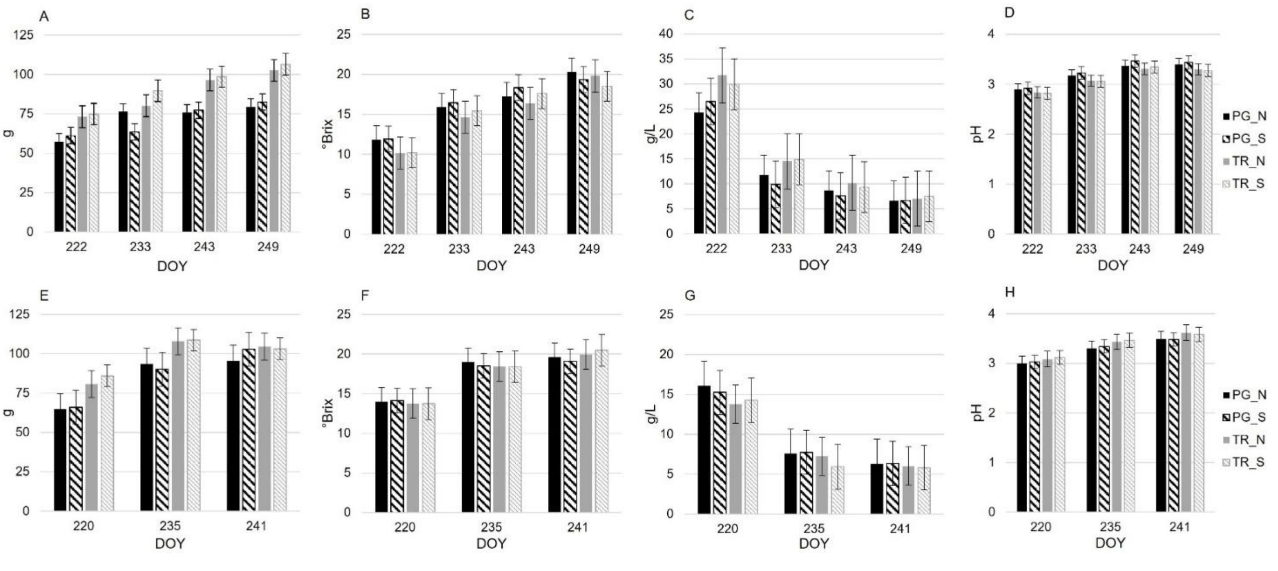

Figure 6 Seasonal evolution of grape berry composition in 2023 (panels A-D) and 2024 (panels E-H) for the four vineyard sectors: PG_N, PG_S, TR_N, and TR_S. Each bar represents the mean of measurements from 50 berries per vine (n = 20 vines per sector), and error bars indicate the standard error of the mean (SEM).

Panels show: (A, E) berry weight (g), (B, F) total soluble solids (°Brix), (C, G) titratable acidity (g L^{-1}), and pH (D, H).

3.3.4. Soil-plant-atmosphere interactions

The relationship between VPD, ESW and NDVI are further analysed to identify possible interactions among these variables (Fig. 7 A, B). The relationship between ESW and VPD (Fig. 7 A, B) exhibited a clear non-linear pattern in both seasons, with ESW decreasing as VPD increased, reflecting the progressive depletion of extractable soil water under higher evaporative demand. This inverse relationship was well captured by the fitted curves, with determination coefficients (R2 = 0.63 in 2023; R2 = 0.66 in 2024) indicating that a substantial portion of ESW variability was explained by atmospheric demand. The NDVI gradient, shown by the color scale, further revealed how canopy vigour co-varied with these dynamics: higher NDVI values corresponded to intermediate ESW and lower VPD, highlighting periods of balanced water availability, while lower NDVI values occurred under higher evaporative conditions.

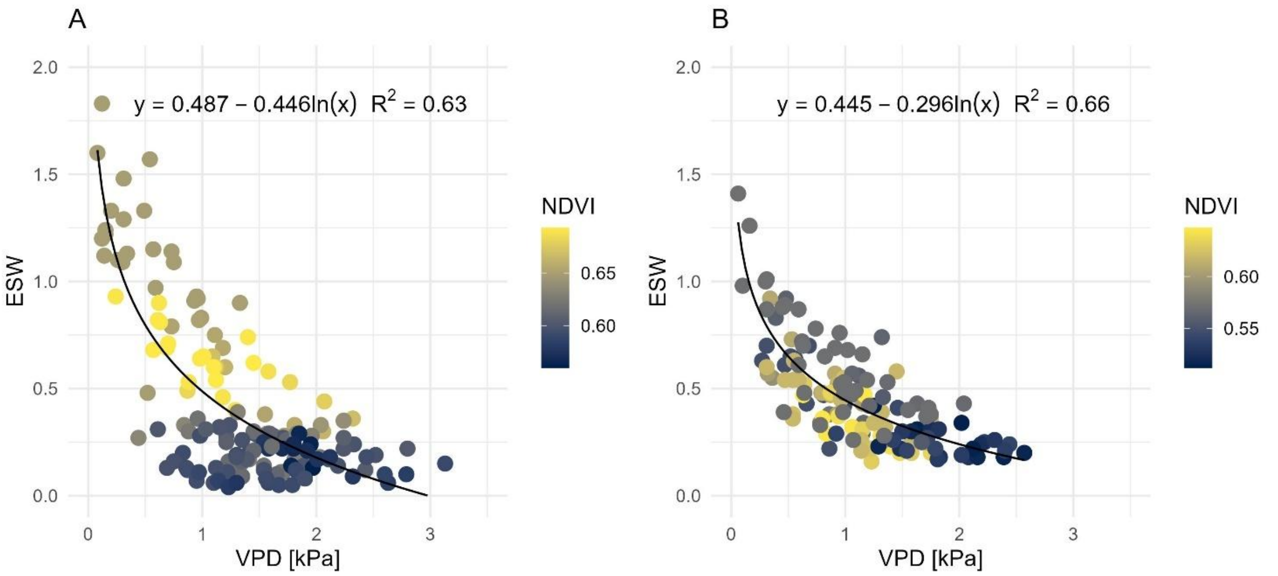

Figure 7 Relationship between vapor pressure deficit (VPD) and extractable soil water (ESW) for the 2023 (A) and 2024 (B) seasons. The regression line highlights the logarithmic relationship between the two variables, and the coefficients of determination were fitted for both 2023 and 2024 (R2 = 0.63 and 0.66, respectively). Point colors represent the normalized difference vegetation index (NDVI).

A Principal Component Analysis (PCA) was carried out using ESW, VPD, NDVI, and the average values of midday Ψ_{stem}, TSS and TA for the two monitored grapevine varieties during the 2023 and 2024 seasons (Fig. 8 A, B). In 2023 (Fig. 8 A), the first two components explained 65.1% of the total variance (PC1: 46.0%, PC2: 19.1%). PC1 was dominated by berry composition traits, with strong and opposite loadings of TSS and TA, while VPD contributed negatively along the same axis. This pattern indicates that the ripening process was inversely related to atmospheric evaporative demand. PC2 was mainly driven by NDVI and, to a lesser extent, by VPD and Ψ_{stem}, suggesting a secondary gradient linked to canopy vigour and vine water status. The overall distribution of the two varieties revealed a relatively homogeneous pattern, consistent with the moderate water stress and uniform ripening conditions recorded in 2023. The functional grouping of variables further supports this interpretation: the environmental ellipse was positioned near the centre of the biplot, reflecting the buffering effect of adequate soil water availability and irrigation, whereas the physiological ellipse extended along the PC1 axis, illustrating the dominant role of ripening dynamics over climatic influence during this season. In contrast, the 2024 PCA (Fig. 8 B) explained 81.5% of the total variance (PC1: 55.8%, PC2: 25.7%), showing a clearer separation among variables and between varieties. PC1 was strongly driven by TSS and TA and VPD, indicating a pronounced ripening gradient influenced by atmospheric conditions, and in less extent from ESW. PC2 was mainly determined by Ψ_{stem} and NDVI, with a moderate contribution from ESW, revealing a secondary axis associated with vine water potential and canopy development. Compared with 2023, the 2024 biplot showed a tighter coupling between fruit ripening traits and environmental drivers. The relative displacement of the ellipses further emphasized this pattern: the environmental ellipse shifted along PC1, capturing the strong influence of VPD and ESW, while the physiological ellipse extended diagonally across both components, indicating that grape composition traits were more closely linked to Ψ_{stem} and NDVI.

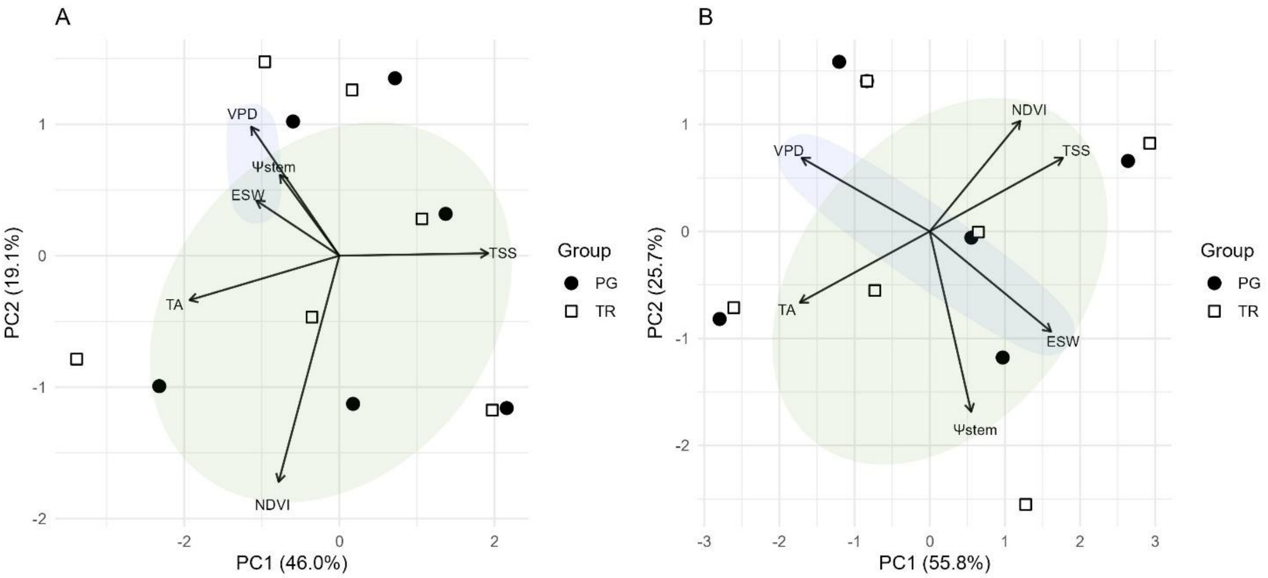

Figure 8 Principal Component Analysis (PCA) biplots of monitored variables for 2023 (A) and 2024 (B). The analysis was conducted on standardized (z-score) data of extractable soil water (ESW), normalized difference vegetation index (NDVI), vapor pressure deficit (VPD), midday Ψstem (Ψstem), total soluble solids (TSS), and titratable acidity (TA). Colored ellipses delineate functional groups of variables: environmental drivers (blue) and physiological/fruit-related traits (green). Each symbol represents the average position of a grapevine variety in the multivariate space: circles correspond to Pignoletto (PG) and squares to Trebbiano Romagnolo (TR). Data from the vineyard sectors were averaged, and the two grapevine varieties are displayed as separate groups.

3.4. Discussion and conclusions

This study provided an integrated assessment of soil-plant-atmosphere interactions in a commercial vineyard, combining soil texture characterization, remote sensing indicators (NDVI), vine physiology, and grape composition across two contrasting seasons.

The spatial pattern of soil texture (Fig. 3) indicated clear differences in soil water-holding capacity, with clay-rich zones likely providing greater moisture retention and sandier areas promoting faster drainage. Such within-field variability can influence soil water dynamics and vine water status even over short distances (Brillante et al., 2018; Tang et al., 2022). Soil texture strongly determines soil hydraulic properties and thus grapevine hydraulics (Lavoie-Lamoureux et al., 2017; Tramontini et al., 2013). Because soil properties can vary markedly within a single vineyard, they play a key role in vine performance through growth and water supply (Arnó et al., 2012; Gatti et al., 2022). The spatial and temporal patterns of SWC derived from portable TDR measurements were consistent across seasons and with soil texture variability, showing coherent patterns despite differences in mean SWC levels. NDVI and its inter-annual relative standard deviation (Fig. 4) provided complementary information on intra-field variability and its linkage with soil properties. The overall stability of NDVI values between years suggests that canopy vigour remained relatively uniform, with minor differences likely associated with seasonal soil water availability and atmospheric conditions rather than major changes in vegetation cover. Considering canopy spatial dynamics together with edaphic data reinforces the rationale for zone-specific management approaches in vineyards (Alliaume et al., 2024; von Hebel et al., 2021). Despite temporal fluctuations, the spatial variability of vine water status within the vineyard remained limited across both seasons, likely due to the homogenizing effect of irrigation. Given the stability of soil properties and the fixed irrigation layout, this uniformity is not expected to change substantially over short time scales. Consequently, a single, dedicated survey may be sufficient to characterize the spatial variability and to delineate potential management zones within the vineyard.

In contrast, temporal variability was more pronounced, reflecting differences in rainfall and atmospheric demand between seasons and requiring a precise temporal assessment. The combined monitoring of ESW, NDVI, and VPD effectively captured these temporal dynamics, showing how soil water availability, canopy vigour, and atmospheric demand interact throughout the growing cycle. Incorporating CRNS-derived ESW allowed the seasonal evolution of soil water availability to be linked directly with atmospheric demand and vine response. The relationship between VPD and ESW in both years highlighted a strong coupling between atmospheric demand and soil water dynamics: as VPD increased, ESW declined non-linearly, reflecting progressive depletion of available water under higher evaporative demand. This pattern agrees with previous observations in other agro-ecosystems, where increasing VPD exerts dominant control on soil-plant water fluxes (Novick et al., 2016; J. Zhang et al., 2021). The negative association between VPD and ESW observed across both years (Singh and Apurv, 2025), together with the relatively high coefficients of determination (R^2 = 0.63-0.66), confirms that atmospheric demand was a primary driver of vineyard water dynamics. Seasonal contrasts further illustrated this control. In 2023, abundant early rainfall and timely irrigation buffered vines against evaporative demand, leading to moderate water stress (Ψ_{stem} = -0.66 to -1.06 MPa) and a steady ripening progression with limited varietal differentiation. In 2024, lower soil water availability and higher VPD resulted in more negative Ψ_{stem} values (-0.95 to -1.12 MPa), and an earlier harvest (DOY 241 vs 249 in 2023). Sampling followed phenological development from veraison to harvest, revealing that atmospheric drivers, especially VPD, exerted a stronger influence on ripening in 2024, consistent with earlier findings linking elevated VPD and temperature to faster sugar accumulation and acid degradation (Di Carlo et al., 2019; Fila et al., 2014; Jones et al., 2005; Menzel, 2005). The slightly earlier plateau in 2024 indicates that ripening was not delayed despite the shorter season, potentially due to higher VPD, which is closely linked to elevated air temperatures and known to accelerate sugar accumulation (Mira de Orduña, 2010; Sadras and Petrie, 2011). Besides, higher temperature and VPD may have promoted the degradation of organic acids, as described by Rienth et al. (2016). This could explain why, despite the earlier harvest in 2024, titratable acidity levels at harvest were comparable between years (Fig. 9 C, G).

The PCA analysis confirmed these contrasting seasonal controls. In 2023, variance was mainly driven by berry ripening traits that were largely decoupled from atmospheric variables, whereas in 2024, environmental drivers (ESW, VPD) were more closely linked to physiological traits, underscoring a stronger climatic influence on vine functioning. This divergence indicates that under conditions of high evaporative demand and adequate soil water supply, vine physiology and ripening become increasingly responsive to atmospheric drivers, partially overriding the buffering role of SWC. Despite the restricted number of variables included in the PCA, these findings are consistent with previous studies showing that soil-plant-atmosphere interactions exert cascading effects on vine physiology and fruit composition (Beauchet et al., 2020; Suter et al., 2019; Yu et al., 2020) and that intra-block variability in water status affects berry development (Jasse et al., 2021). In this case, however, such effects were modest, likely due to irrigation maintaining generally adequate water availability.

Overall, this study proved how CRNS-derived SWC is a robust integrative indicator of soil-plant water relations and a valuable complement to plant-based and remote-sensing observations. As such, this integration can offer a non-invasive solution to enhance the temporal and functional understanding of crop water relations, supporting more adaptive and sustainable water management. Future work should extend this approach to other crops, incorporate additional physiological variables, and explore CRNS scalability within decision-support systems

3.5. References

Acevedo-Opazo, C., Ortega-Farias, S., & Fuentes, S. (2010). Effects of grapevine (*Vitis vinifera* L.) water status on water consumption, vegetative growth and grape quality: An irrigation scheduling application to achieve regulated deficit irrigation. *Agricultural Water Management*, *97*(7), 956–964. https://doi.org/10.1016/j.agwat.2010.01.025

Allegro, G., Pastore, C., Valentini, G., Mazzoleni, R., & Filippetti, I. (2023). Irrigation during ripening may reduce sunburn damages on berries of *Vitis vinifera* L. 'Sangiovese.' *Acta Horticulturae*, *1366*, 377–384. https://doi.org/10.17660/ActaHortic.2023.1366.46

Allen, R. G., Pereira, L., Raes, D., & Smith, M. (Eds.). (1998). *Crop evapotranspiration: Guidelines for computing crop water requirements* (repr). Food and Agriculture Organization of the United Nations.

Alliaume, F., Echeverria, G., Ferrer, M., & González Barrios, P. (2024). A Study of the Multivariate Spatial Variability of Soil Properties, and their Association with Vine Vigour Growing on a Clayish Soil. *Journal of Soil Science and Plant Nutrition*, *24*(2), 3282–3297. https://doi.org/10.1007/s42729-024-01751-8

Antolini, G., Auteri, L., Pavan, V., Tomei, F., Tomozeiu, R., & Marletto, V. (2016). A daily high-resolution gridded climatic data set for Emilia-Romagna, Italy, during 1961-2010: EMILIA-ROMAGNA DAILY GRIDDED CLIMATIC DATA SET. *International Journal of Climatology*, *36*(4), 1970–1986. https://doi.org/10.1002/joc.4473

Arnó, J., Rosell, J. R., Blanco, R., Ramos, M. C., & Martínez-Casasnovas, J. A. (2012). Spatial variability in grape yield and quality influenced by soil and crop nutrition characteristics. *Precision Agriculture*, *13*(3), 393–410. https://doi.org/10.1007/s11119-011-9254-1

Babaeian, E., Sadeghi, M., Jones, S. B., Montzka, C., Vereecken, H., & Tuller, M. (2019). Ground, Proximal, and Satellite Remote Sensing of Soil Moisture. *Reviews of Geophysics*, *57*(2), 530–616. https://doi.org/10.1029/2018RG000618

Baetens, L., Desjardins, C., & Hagolle, O. (2019). Validation of Copernicus Sentinel-2 Cloud Masks Obtained from MAJA, Sen2Cor, and FMask Processors Using Reference Cloud Masks Generated with a Supervised Active Learning Procedure. *Remote Sensing*, *11*(4), 433. https://doi.org/10.3390/rs11040433

Beauchet, S., Cariou, V., Renaud-Gentie, C., Meunier, M., Siret, R., Thiollet-Scholtus, M., & Jourjon, F. (2020). Modeling grape quality by multivariate analysis of viticulture practices, soil and climate. *OENO One*. https://doi.org/10.20870/oeno-one....1067

Bolognini, M., Modina, D., Bianchi, D., Cavallaro, L., Carnevali, P., & Brancadoro, L. (2023). Using a vegetation index to define homogeneous zones for variable rate irrigation in vineyard. In *Precision agriculture '23* (pp. 75–82). Wageningen Academic. https://doi.org/10.3920/978-90-8686-947-3_7

Bonada, M., Petrie, P. R., Phogat, V., Collins, C., & Sadras, V. O. (2023). Benchmarking Water-Limited Yield Potential and Yield Gaps of Shiraz in the Barossa and Eden Valleys. *Australian Journal of Grape and Wine Research*, *2023*(1), 5807266. https://doi.org/10.1155/2023/5807266

Brillante, L., Mathieu, O., Lévêque, J., van Leeuwen, C., & Bois, B. (2018). Water status and must composition in grapevine cv. Chardonnay with different soils and topography and a mini meta-analysis of the δ13C/water potentials correlation. *Journal of the Science of Food and Agriculture*, *98*(2), 691–697. https://doi.org/10.1002/jsfa.8516

Brogi, C., Pisinaras, V., Köhli, M., Dombrowski, O., Hendricks Franssen, H.-J., Babakos, K., Chatzi, A., Panagopoulos, A., & Bogena, H. R. (2023). Monitoring Irrigation in Small Orchards with Cosmic-Ray Neutron Sensors. *Sensors*, *23*(5), Article 5. https://doi.org/10.3390/s23052378

Büntgen, U., Reinig, F., Verstege, A., Piermattei, A., Kunz, M., Krusic, P., Slavin, P., Štěpánek, P., Torbenson, M., del Castillo, E. M., Arosio, T., Kirdyanov, A., Oppenheimer, C., Trnka, M., Palosse, A., Bebchuk, T., Camarero, J. J., & Esper, J. (2024). Recent summer warming over the western Mediterranean region is unprecedented since medieval times. *Global and Planetary Change*, *232*, 104336. https://doi.org/10.1016/j.gloplacha.2023.104336

Bwambale, E., Abagale, F. K., & Anornu, G. K. (2022). Smart irrigation monitoring and control strategies for improving water use efficiency in precision agriculture: A review. *Agricultural Water Management*, *260*, 107324. https://doi.org/10.1016/j.agwat.2021.107324

Chaves, M. M., Zarrouk, O., Francisco, R., Costa, J. M., Santos, T., Regalado, A. P., Rodrigues, M. L., & Lopes, C. M. (2010). Grapevine under deficit irrigation: Hints from physiological and molecular data. *Annals of Botany*, *105*(5), 661–676. https://doi.org/10.1093/aob/mcq030

Desilets, D., Zreda, M., & Ferré, T. P. A. (2010). Nature's neutron probe: Land surface hydrology at an elusive scale with cosmic rays. *Water Resources Research*, *46*(11). https://doi.org/10.1029/2009WR008726

Di Carlo, P., Aruffo, E., & Brune, W. H. (2019). Precipitation intensity under a warming climate is threatening some Italian premium wines. *Science of The Total Environment*, *685*, 508–513. https://doi.org/10.1016/j.scitotenv.2019.05.449

Fila, G., Gardiman, M., Belvini, P., Meggio, F., & Pitacco, A. (2014). A comparison of different modelling solutions for studying grapevine phenology under present and future climate scenarios. *Agricultural and Forest Meteorology*, *195–196*, 192–205. https://doi.org/10.1016/j.agrformet.2014.05.011

Franz, T. E., Zreda, M., Rosolem, R., & Ferre, T. P. A. (2012). Field Validation of a Cosmic-Ray Neutron Sensor Using a Distributed Sensor Network. *Vadose Zone Journal*, *11*(4). https://doi.org/10.2136/vzj2012.0046

Fuentes, S., & Gago, J. (2022). Chapter 7—Modern approaches to precision and digital viticulture. In J. M. Costa, S. Catarino, J. M. Escalona, & P. Comuzzo (Eds.), *Improving Sustainable Viticulture and Winemaking Practices* (pp. 125–145). Academic Press. https://doi.org/10.1016/B978-0-323-85150-3.00015-3

Gatti, M., Garavani, A., Squeri, C., Diti, I., De Monte, A., Scotti, C., & Poni, S. (2022). Effects of intra-vineyard variability and soil heterogeneity on vine performance, dry matter and nutrient partitioning. *Precision Agriculture*, *23*(1), 150–177. https://doi.org/10.1007/s11119-021-09831-w

Gerakis, A., & Zalidis, G. (1998). Estimating field-measured, plant extractable water from soil properties: Beyond statistical models. *Irrigation and Drainage Systems*, *12*, 311–322.

Gianessi, S., Polo, M., Stevanato, L., Lunardon, M., Francke, T., Oswald, S. E., Said Ahmed, H., Toloza, A., Weltin, G., Dercon, G., Fulajtar, E., Heng, L., & Baroni, G. (2024). Testing a novel sensor design to jointly measure cosmic-ray neutrons, muons and gamma rays for non-invasive soil moisture estimation. *Geoscientific Instrumentation, Methods and Data Systems*, *13*(1), 9–25. https://doi.org/10.5194/gi-13-9-2024

Giovos, R., Tassopoulos, D., Kalivas, D., Lougkos, N., & Priovolou, A. (2021). Remote Sensing Vegetation Indices in Viticulture: A Critical Review. *Agriculture*, *11*(5), Article 5. https://doi.org/10.3390/agriculture11050457

Grolemund, G., & Wickham, H. (2011). Dates and Times Made Easy with lubridate. *Journal of Statistical Software*, *40*, 1–25. https://doi.org/10.18637/jss.v040.i03

Jasse, A., Berry, A., Aleixandre-Tudo, J. L., & Poblete-Echeverría, C. (2021). Intra-block spatial and temporal variability of plant water status and its effect on grape and wine parameters. *Agricultural Water Management*, *246*, 106696. https://doi.org/10.1016/j.agwat.2020.106696

Jones, G. V., White, M. A., Cooper, O. R., & Storchmann, K. (2005). Climate Change and Global Wine Quality. *Climatic Change*, *73*(3), 319–343. https://doi.org/10.1007/s10584-005-4704-2

Kassambara, A., & Mundt, F. (2016). *factoextra: Extract and Visualize the Results of Multivariate Data Analyses*. https://rpkgs.datanovia.com/factoextra/index.html

Köhli, M., Schrön, M., Zreda, M., Schmidt, U., Dietrich, P., & Zacharias, S. (2015). Footprint characteristics revised for field-scale soil moisture monitoring with cosmic-ray neutrons. *Water Resources Research*, *51*(7), 5772–5790. https://doi.org/10.1002/2015WR017169

Lavoie-Lamoureux, A., Sacco, D., Risse, P.-A., & Lovisolo, C. (2017). Factors influencing stomatal conductance in response to water availability in grapevine: A meta-analysis. *Physiologia Plantarum*, *159*(4), 468–482. https://doi.org/10.1111/ppl.12530

Lê, S., Josse, J., & Husson, F. (2008). FactoMineR: An R Package for Multivariate Analysis. *Journal of Statistical Software*, *25*, 1–18. https://doi.org/10.18637/jss.v025.i01

Lebon, E., Dumas, V., Pieri, P., & Schultz, H. R. (2003). Modelling the seasonal dynamics of the soil water balance of vineyards. *Functional Plant Biology*, *30*(6), 699. https://doi.org/10.1071/FP02222

Li, D., Schrön, M., Köhli, M., Bogena, H., Weimar, J., Jiménez Bello, M. A., Han, X., Martínez Gimeno, M. A., Zacharias, S., Vereecken, H., & Hendricks Franssen, H. (2019). Can Drip Irrigation be Scheduled with Cosmic-Ray Neutron Sensing? *Vadose Zone Journal*, *18*(1), 190053. https://doi.org/10.2136/vzj2019.05.0053

Lorenz, D. h., Eichhorn, K. w., Bleiholder, H., Klose, R., Meier, U., & Weber, E. (1995). Growth Stages of the Grapevine: Phenological growth stages of the grapevine (Vitis vinifera L. ssp. vinifera)—Codes and descriptions according to the extended BBCH scale. *Australian Journal of Grape and Wine Research*, *1*(2), 100–103. https://doi.org/10.1111/j.1755-0238.1995.tb00085.x

Lovisolo, C., Perrone, I., Carra, A., Ferrandino, A., Flexas, J., Medrano, H., & Schubert, A. (2010). Drought-induced changes in development and function of grapevine (Vitis spp.) organs and in their hydraulic and non-hydraulic interactions at the whole-plant level: A physiological and molecular update. *Functional Plant Biology*, *37*(2), 98–116. https://doi.org/10.1071/FP09191

Massari, C., Modanesi, S., Dari, J., Gruber, A., De Lannoy, G. J. M., Girotto, M., Quintana-Seguí, P., Le Page, M., Jarlan, L., Zribi, M., Ouaadi, N., Vreugdenhil, M., Zappa, L., Dorigo, W., Wagner, W., Brombacher, J., Pelgrum, H., Jaquot, P., Freeman, V., … Brocca, L. (2021). A Review of Irrigation Information Retrievals from Space and Their Utility for Users. *Remote Sensing*, *13*(20), 4112. https://doi.org/10.3390/rs13204112

Mazzoleni, R., Emamalizadeh, S., & Baroni, G. (2025). *Cosmic-ray neutron sensing to monitor soil moisture across various irrigation methods* (Preprint No. VZJ-2025-06-0057-OA.R1). ESS Open Archive. https://doi.org/10.22541/essoar.176097443.35022248/v1

Menzel, A. (2005). A 500 year pheno-climatological view on the 2003 heatwave in Europe assessed by grape harvest dates. *Meteorologische Zeitschrift*, *14*(1), 75–77. https://doi.org/10.1127/0941-2948/2005/0014-0075

Mira de Orduña, R. (2010). Climate change associated effects on grape and wine quality and production. *Food Research International*, *43*(7), 1844–1855. https://doi.org/10.1016/j.foodres.2010.05.001

Novick, K. A., Ficklin, D. L., Stoy, P. C., Williams, C. A., Bohrer, G., Oishi, A. C., Papuga, S. A., Blanken, P. D., Noormets, A., Sulman, B. N., Scott, R. L., Wang, L., & Phillips, R. P. (2016). The increasing importance of atmospheric demand for ecosystem water and carbon fluxes. *Nature Climate Change*, *6*(11), 1023–1027. https://doi.org/10.1038/nclimate3114

Ortuani, B., Mayer, A., Bianchi, D., Sona, G., Crema, A., Modina, D., Bolognini, M., Brancadoro, L., Boschetti, M., & Facchi, A. (2024). Effectiveness of Management Zones Delineated from UAV and Sentinel-2 Data for Precision Viticulture Applications. *Remote Sensing*, *16*(4), 635. https://doi.org/10.3390/rs16040635

Palazzi, F., Biddoccu, M., Borgogno Mondino, E. C., & Cavallo, E. (2023). Use of Remotely Sensed Data for the Evaluation of Inter-Row Cover Intensity in Vineyards. *Remote Sensing*, *15*(1), 41. https://doi.org/10.3390/rs15010041

Pellegrino, A., Lebon, E., Voltz, M., & Wery, J. (2005). Relationships between plant and soil water status in vine (Vitis vinifera L.). *Plant and Soil*, *266*(1), 129–142. https://doi.org/10.1007/s11104-005-0874-y

Pereyra, G., Pellegrino, A., Gaudin, R., & Ferrer, M. (2022). Evaluation of site-specific management to optimise *Vitis vinifera* L. (cv. Tannat) production in a vineyard with high heterogeneity. *OENO One*, *56*(3), Article 3. https://doi.org/10.20870/oeno-one.2022.56.3.5485

Rienth, M., Torregrosa, L., Sarah, G., Ardisson, M., Brillouet, J.-M., & Romieu, C. (2016). Temperature desynchronizes sugar and organic acid metabolism in ripening grapevine fruits and remodels their transcriptome. *BMC Plant Biology*, *16*(1), 164. https://doi.org/10.1186/s12870-016-0850-0

Robinson, D. A., Campbell, C. S., Hopmans, J. W., Hornbuckle, B. K., Jones, S. B., Knight, R., Ogden, F., Selker, J., & Wendroth, O. (2008). Soil Moisture Measurement for Ecological and Hydrological Watershed-Scale Observatories: A Review. *Vadose Zone Journal*, *7*(1), 358–389. https://doi.org/10.2136/vzj2007.0143

Sadras, V. o., & Petrie, P. r. (2011). Quantifying the onset, rate and duration of sugar accumulation in berries from commercial vineyards in contrasting climates of Australia. *Australian Journal of Grape and Wine Research*, *17*(2), 190–198. https://doi.org/10.1111/j.1755-0238.2011.00135.x

Schrön, M., Köhli, M., Scheiffele, L., Iwema, J., Bogena, H. R., Lv, L., Martini, E., Baroni, G., Rosolem, R., Weimar, J., Mai, J., Cuntz, M., Rebmann, C., Oswald, S. E., Dietrich, P., Schmidt, U., & Zacharias, S. (2017). Improving calibration and validation of cosmic-ray neutron sensors in the light of spatial sensitivity. *Hydrology and Earth System Sciences*, *21*(10), 5009–5030. https://doi.org/10.5194/hess-21-5009-2017

Seager, R., Liu, H., Henderson, N., Simpson, I., Kelley, C., Shaw, T., Kushnir, Y., & Ting, M. (2014). Causes of Increasing Aridification of the Mediterranean Region in Response to Rising Greenhouse Gases. *Journal of Climate*, *27*(12), 4655–4676. https://doi.org/10.1175/JCLI-D-13-00446.1

Seneviratne, S. I., Corti, T., Davin, E. L., Hirschi, M., Jaeger, E. B., Lehner, I., Orlowsky, B., & Teuling, A. J. (2010). Investigating soil moisture–climate interactions in a changing climate: A review. *Earth-Science Reviews*, *99*(3), 125–161. https://doi.org/10.1016/j.earscirev.2010.02.004

Singh, V., & Apurv, T. (2025). An Analytical Approach for Quantifying the Role of Vapor Pressure Deficit in Soil Moisture Depletion During Flash Droughts. *Water Resources Research*, *61*(6), e2024WR038995. https://doi.org/10.1029/2024WR038995

Soulis, K. X., Elmaloglou, S., & Dercas, N. (2015). Investigating the effects of soil moisture sensors positioning and accuracy on soil moisture based drip irrigation scheduling systems. *Agricultural Water Management*, *148*, 258–268. https://doi.org/10.1016/j.agwat.2014.10.015

Stevanato, L., Baroni, G., Cohen, Y., Fontana, C. L., Gatto, S., Lunardon, M., Marinello, F., Moretto, S., & Morselli, L. (2019). A Novel Cosmic-Ray Neutron Sensor for Soil Moisture Estimation over Large Areas. *Agriculture*, *9*(9), Article 9. https://doi.org/10.3390/agriculture9090202

Susha Lekshmi, S. U., Singh, D. N., & Shojaei Baghini, M. (2014). A critical review of soil moisture measurement. *Measurement*, *54*, 92–105. https://doi.org/10.1016/j.measurement.2014.04.007

Suter, B., Triolo, R., Pernet, D., Dai, Z., & Van Leeuwen, C. (2019). Modeling Stem Water Potential by Separating the Effects of Soil Water Availability and Climatic Conditions on Water Status in Grapevine (Vitis vinifera L.). *Frontiers in Plant Science*, *10*. https://doi.org/10.3389/fpls.2019.01485

Szabó, B., Weynants, M., & Weber, T. K. D. (2021). Updated European hydraulic pedotransfer functions with communicated uncertainties in the predicted variables (euptfv2). *Geoscientific Model Development*, *14*(1), 151–175. https://doi.org/10.5194/gmd-14-151-2021

Tang, Z., Jin, Y., Alsina, M. M., McElrone, A. J., Bambach, N., & Kustas, W. P. (2022). Vine water status mapping with multispectral UAV imagery and machine learning. *Irrigation Science*, *40*(4), 715–730. https://doi.org/10.1007/s00271-022-00788-w

Tramontini, S., van Leeuwen, C., Domec, J.-C., Destrac-Irvine, A., Basteau, C., Vitali, M., Mosbach-Schulz, O., & Lovisolo, C. (2013). Impact of soil texture and water availability on the hydraulic control of plant and grape-berry development. *Plant and Soil*, *368*(1), 215–230. https://doi.org/10.1007/s11104-012-1507-x

Valentini, G., Pastore, C., Allegro, G., Mazzoleni, R., Chinnici, F., & Filippetti, I. (2022). Vine Physiology, Yield Parameters and Berry Composition of Sangiovese Grape under Two Different Canopy Shapes and Irrigation Regimes. *Agronomy*, *12*(8), Article 8. https://doi.org/10.3390/agronomy12081967

Velazquez-Chavez, L. J., Daccache, A., Mohamed, A. Z., & Centritto, M. (2024). Plant-based and remote sensing for water status monitoring of orchard crops: Systematic review and meta-analysis. *Agricultural Water Management*, *303*, 109051. https://doi.org/10.1016/j.agwat.2024.109051

von Hebel, C., Reynaert, S., Pauly, K., Janssens, P., Piccard, I., Vanderborght, J., van der Kruk, J., Vereecken, H., & Garré, S. (2021). Toward high-resolution agronomic soil information and management zones delineated by ground-based electromagnetic induction and aerial drone data. *Vadose Zone Journal*, *20*(4), e20099. https://doi.org/10.1002/vzj2.20099

Wickham, H. (2011). Ggplot2. *WIREs Computational Statistics*, *3*(2), 180–185. https://doi.org/10.1002/wics.147

Yu, R., Brillante, L., Martínez-Lüscher, J., & Kurtural, S. K. (2020). Spatial Variability of Soil and Plant Water Status and Their Cascading Effects on Grapevine Physiology Are Linked to Berry and Wine Chemistry. *Frontiers in Plant Science*, *11*. https://doi.org/10.3389/fpls.2020.00790

Zhang, J., Guan, K., Peng, B., Pan, M., Zhou, W., Jiang, C., Kimm, H., Franz, T. E., Grant, R. F., Yang, Y., Rudnick, D. R., Heeren, D. M., Suyker, A. E., Bauerle, W. L., & Miner, G. L. (2021). Sustainable irrigation based on co-regulation of soil water supply and atmospheric evaporative demand. *Nature Communications*, *12*(1), 5549. https://doi.org/10.1038/s41467-021-25254-7

Zhang, Y., Oren, R., & Kang, S. (2012). Spatiotemporal variation of crown-scale stomatal conductance in an arid Vitis vinifera L. cv. Merlot vineyard: Direct effects of hydraulic properties and indirect effects of canopy leaf area. *Tree Physiology*, *32*(3), 262–279. https://doi.org/10.1093/treephys/tpr120

Zhou, S., Zhang, Y., Park Williams, A., & Gentine, P. (2019). Projected increases in intensity, frequency, and terrestrial carbon costs of compound drought and aridity events. *Science Advances*, *5*(1), eaau5740. https://doi.org/10.1126/sciadv.aau5740

Zreda, M., Desilets, D., Ferré, T. P. A., & Scott, R. L. (2008). Measuring soil moisture content non-invasively at intermediate spatial scale using cosmic-ray neutrons. *Geophysical Research Letters*, *35*(21). https://doi.org/10.1029/2008GL035655

Zreda, M., Shuttleworth, W. J., Zeng, X., Zweck, C., Desilets, D., Franz, T., & Rosolem, R. (2012). COSMOS: The COsmic-ray Soil Moisture Observing System. *Hydrology and Earth System Sciences*, *16*(11), 4079–4099. https://doi.org/10.5194/hess-16-4079-2012

4. Integrating multi-sensor monitoring to characterize vine water dynamics under semi-arid environments

Riccardo Mazzoleni[1], Beng Umali[2,3], Gabriele Valentini[1], Ilaria Filippetti[1], Gabriele Baroni[1]

[1]Department of Agricultural and Food Sciences (DISTAL), University of Bologna, Viale Giuseppe Fanin 42-50, 40127 Bologna, Italy.

[2]University of South Australia – STEM, Adelaide, SA 5000 Australia.

[3]ICT International Pty Ltd, 211 Mann St, Armidale NSW 2350 Australia.

Abstract

Water scarcity poses increasing challenges to viticulture in semi-arid regions such as South Australia, where grapevine production depends almost entirely on irrigation. This study combined continuous multi-sensor monitoring of the soil-plant-atmosphere continuum (SPAC), integrating soil water content (SWC) measured by cosmic-ray neutron sensing (CRNS), stem water potential (Ψ_{stem}) recorded with psychrometers, and vine sap flow total flow rate (TFR) measured by sap-flow meters, to evaluate vine hydraulic responses to atmospheric drivers (vapour pressure deficit, VPD). The monitoring was carried out in a Syrah vineyard located in Renmark, South Australia, employing daily drip irrigation. Daytime Ψ_{stem} values indicated overall non-stressed conditions, while TFR exhibited regular diurnal cycles. Spearman and PCA analyses revealed a dominant atmospheric control (VPD-TFR-Ψ_{stem} axis explaining ~85 % of total variance), with SWC contributing on an orthogonal axis. Linear Mixed Models (LMMs) further confirmed VPD as the primary driver of vine water status ($p < 0.001$), whereas SWC had a significant positive effect only on nighttime Ψ_{stem}, suggesting enhanced stem rehydration under higher SWC. Model performance was stronger during daytime (R^2 = 0.55-0.71) than nighttime (R^2 = 0.22-0.38). The integration of continuous monitoring and LMMs effectively quantified SPAC interactions and supports data-driven, adaptive vineyard water management in semi-arid systems.

4.1. Introduction

Water scarcity represents a major challenge for viticulture in semi-arid areas such as South Australia, where increasingly hot and dry conditions are placing growing pressure on grape production. Within this context, the Riverland stands as a central contributor in the Australian's wine industry, relying almost entirely on irrigation supplied by the Murray River (Prosser et al., 2021; Robinson & Song, 2023). The region is characterized by a

Mediterranean climate, featuring hot, extremely dry summers and mild winters, and is further limited by a significant rainfall deficit, with average annual precipitation ranging from just 230 to 270 mm (Bureau of Meteorology, 2025). In contrast, grapevines grown in hot climates typically require between 400 and 800 mm of water over the course of the growing season (Williams and Baeza, 2007).

Grapevines exhibit complex strategies to cope with such sever water restrictions that can influence both vegetative growth and fruit development (Chaves et al., 2010). Yet, translating these physiological responses into actionable vineyard water management remains difficult because of the high spatiotemporal variability in soil and atmospheric drivers, and the need to integrate measurements across the soil-plant-atmosphere continuum (SPAC). Within the SPAC, the atmospheric component is largely governed by evaporative demand, quantified as vapor pressure deficit (VPD), which exerts a major influence on vine water status (Gambetta et al., 2020). High VPD levels are often more closely associated with critical water stress conditions than temperature or precipitation anomalies considered individually (Cogato et al., 2022). Recent experimental evidence by Valentini et al. (2024) demonstrated that mitigation of evaporative demand through localized misting systems can substantially alleviate the effects of high VPD on vine physiology. This finding underscores the critical role of atmospheric regulation in maintaining vine hydraulic balance and highlights the potential of microclimate management as a complementary strategy to irrigation. Moreover, vine growth and productivity remain tightly linked to SWC, which represents a primary driver of vegetative and reproductive performance, making irrigation often essential in semi-arid viticultural systems (Lebon et al., 2003).

Recent ecohydrological frameworks highlight the central role of plants as regulators of water fluxes, operating across scales from leaves to catchments (Asbjornsen et al., 2011). Hence, monitoring seasonal vine water status is a critical step in selecting appropriate management strategies to safeguard grape yield and quality (Rienth and Scholasch, 2019). Vine water potential (Ψ) represents the tension or negative pressure required by the plant to extract water from the soil. As SWC declines, the vine lowers its Ψ to maintain water uptake and sustain photosynthesis. For this reason, Ψ serves as a reliable tool for evaluating the vine's water status (Choné, 2001). Among the direct or plant-based measurements of Ψ, measurements relative to the pre-dawn (Ψ_{PD}), leaf (Ψ_{leaf}) or stem (Ψ_{stem}) are the most widely used by growers and eco-physiological studies (Rienth and Scholasch, 2019), with Ψ_{stem} considered as showing the best correlations with vine transpiration (Choné, 2001; Choné et al., 2000). The most common used tool for measuring Ψ remains the Scholander's pressure chamber (Scholander et al., 1965). Although its operating principle is relatively straightforward, the need for time-consuming, high-frequency measurements poses significant limitations for routine or large-scale monitoring (Benyahia et al., 2023). Advances in monitoring technologies offer new opportunities for viticulture (Fuentes and Gago, 2022). Technologies such as sap flow sensors and psychrometers offer continuous, direct measurements of plant water uptake and Ψ, providing valuable insights into the vine's hydraulic functioning (Mancha et al., 2021; Martinez et al., 2011).

Given the inherent complexity and spatiotemporal variability of water fluxes within the SPAC, no single indicator or sensor can fully capture the dynamics of vine water use under field conditions. Therefore, integrating continuous data from multiple sensing platforms is essential to build a more comprehensive picture of vine water status (Brillante et al., 2016). This multi-sensor approach not only enhances our capacity to interpret plant-environment interactions in real time but also lays the foundation for the development of dynamic, data-driven irrigation models tailored to semi-arid viticultural systems.

In light of these considerations, this chapter presents a field study aimed at assessing vine water status through the integrated monitoring of soil, plant, and atmospheric components in a commercial vineyard. The main objective was to evaluate how continuous multi-sensor data, combining SWC from a CRNS sensor with sap flow and Ψ_{stem} measurements, can be used to characterize vine hydraulic behaviour and its environmental drivers, ultimately supporting more adaptive and efficient irrigation strategies under semi-arid conditions in South Australia. The specific objectives of this chapter were to:

i. Quantify the relationships between key environmental variables, particularly SWC and VPD, and physiological indicators of the sap flow rate (Total Flow Rate, TFR) and Ψ_{stem}.

ii. Assess the potential of hierarchical mixed-effects models for integrating multi-sensor datasets and interpreting water dynamics across the SPAC.

By linking ecohydrological principles with continuous, sensor-based monitoring, this work contributes to the development of a data-driven framework to support advanced irrigation scheduling and adaptive stress management strategies in viticulture.

4.2. Materials and methods

4.2.1. Experimental site characteristics and sensors setup

The experimental site consists of a commercial vineyard located in Renmark, South Australia (34.22071° S, 140.7153° E), cultivated with *Vitis vinifera* L. cv. Syrah. The vines are trained to a box-hedge pruning system fully managed through mechanized operations, with a planting layout of 3.6 m between rows and 2 m within rows. The study area encompasses approximately 7 hectares. (Figure 1).

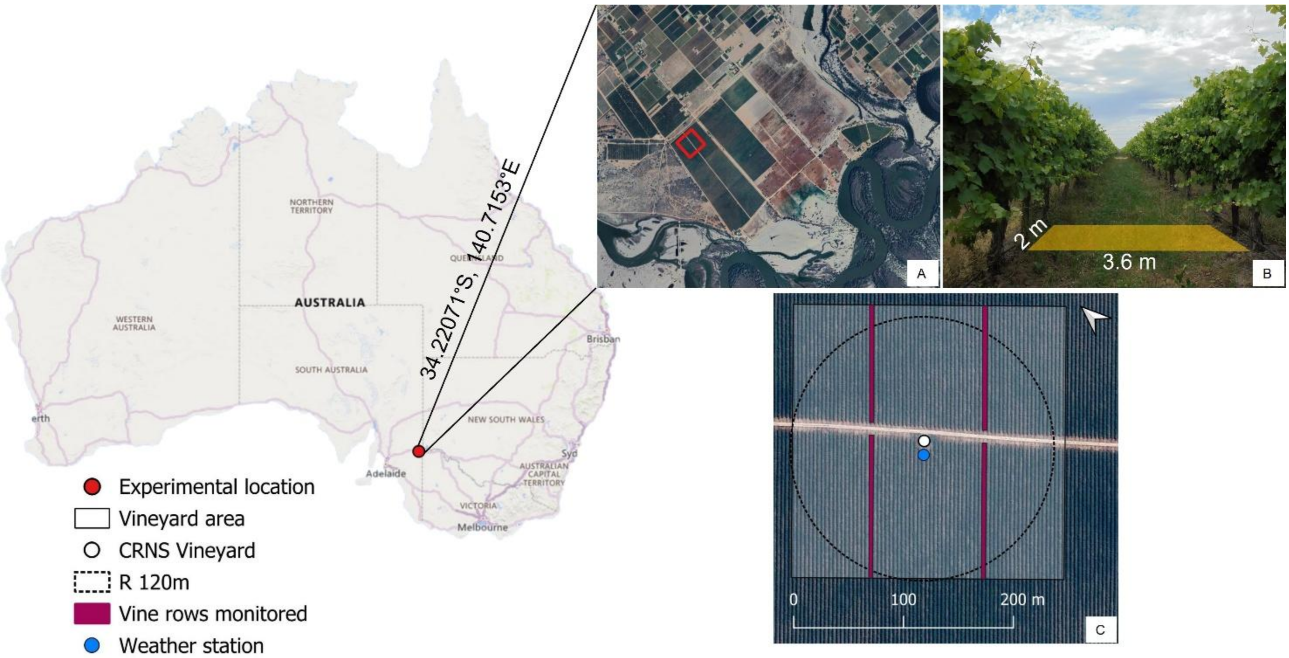

Figure 1: Overview of the vineyard's location in Renmark, South Australia (34.22071° S, 140.7153° E). (A) Aerial view of the study site and surrounding agricultural area and the Murray River in proximity. (B) Vineyard layout showing the planting spacing of 2.5 m between rows and 1.0 m within rows. (C) Spatial configuration of the monitoring setup: the CRNS sensor was installed at the centre of the monitored area, with a detection footprint radius of 120 m (R 120m). Four vine rows, named according to their geographic position (NW, NE, SW, SE), were instrumented with sap flow sensors (SFM1x) and stem psychrometers (PSY1). A weather station was also installed within the same area to record local climatic conditions.

The vineyard is managed under a fully drip-irrigated system. During the monitoring period (27th November 2024 - 4th February 2025), irrigation was applied uniformly by a drip irrigation (DI) system daily in 8/10-hour cycles. Drippers are spaced at 1.5 m intervals along the vine rows, each delivering water at a nominal discharge rate of 0.006 m^3h^{-1}. According to South Australian soil type classifications, the site is characterized by deep friable gradational clay loam (~35%), with an overall clay-loam texture prevailing across the upper 1 m of the soil profile (~60%).

To continuously monitor the SWC, a CRNS probe (Finapp S.r.l., Montegrotto Terme, Padova, Italy) was installed in November 2024. To quantify the average SWC within the sensor's footprint area, soil samples have been collected on 27th November and, subsequently, analysed in the laboratory for assessing average gravimetric SWCg (g g^{-1}), bulk density ρ_{bd} (g m^{-3}) and static hydrogen pools (SHP, g g^{-1}), which is represented by the lattice water (LW, g g^{-1}) and soil organic carbon (SOC, g g^{-1}). The technical details of the sensor as well as the calibration procedure have already been discussed in Section 2.2.2 and Section 2.2.3. In this study, the local muon-based incoming correction (F_i Muons) approach was implemented for the CRNS signal (Stevanato et al., 2022) and considering the unique characteristics of Australia, following the findings of McJannet et al. (2025). A weather station (ATH-2S, ICT International, Armidale, NSW, Australia) continuously recorded air temperature (T_{air}, °C), air relative humidity (RH, %) and pressure (hPa), Photosynthetic Active Radiation (PAR, µmol m^{-2} s^{-1}) and rainfall (mm h^{-1}). Based on temperature and air relative humidity, the vapour pressure deficit (VPD, kPa) has been calculated, following Allen et al. (1998).

A network of sensors was deployed to monitor vine water status across the site, with three vines randomly selected along each monitored row (NW, NE, SW, and SE), for a total of twelve vines (Figure 1). Xylem sap flow TFR was quantified using 12 Sap Flow Meters (SFM1x, ICT International, Armidale, NSW, Australia) operating with the Heat Ratio Method (HRM), which derives xylem sap velocity from the differential temperature response to a short heat pulse (Burgess et al., 1998). Probes (heater and thermocouples) were inserted into the trunk after bark removal, aligned in parallel, and thermally insulated. Continuous measurements were recorded at fixed intervals, and final outputs were expressed as TFR (L h^{-1}). In parallel, 12 Psychrometers (PSY1, ICT International, Armidale, NSW, Australia) were installed on the vine trunks to provide continuous measurements of Ψ_{stem}. The psychrometer measures the Ψ_{stem} by detecting vapour pressure equilibrium within a sealed chamber containing fine thermocouples. A Peltier cooling pulse induces condensation on the wet junction, and the subsequent evaporation produces a wet-bulb depression that is converted into Ψ values (MPa). All installations were insulated to reduce thermal gradients and ensure stable readings. Both sensors were installed on the same vine trunk, allowing the deployment of 24 sensors on 12 vines. A schematic illustration of the sensor installation and their main operating features is provided in Figure 2.

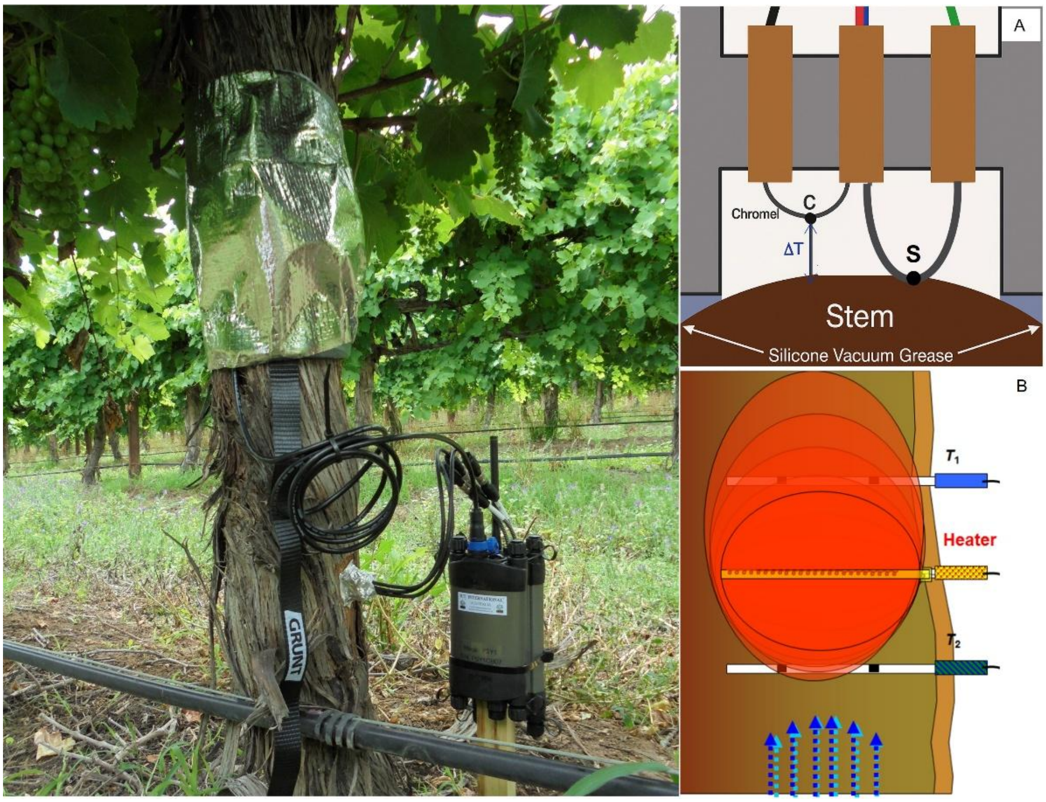

Figure 2: Instrumentation setup for continuous monitoring of vine water status (left panel). Both sensors were installed on the same vine trunk to enable simultaneous and coordinated measurements of plant water status and sap flow. A stem psychrometer (PSY1) was installed on the trunk to measure stem water potential (Ψ_{stem}) based on vapor pressure equilibrium within a sealed chamber. The schematic inset (A) illustrates the sensor configuration, showing the thermocouples - one ('S') in direct contact with the plant tissue and the other ('C') suspended in the chamber air space - and the temperature difference (ΔT) generated during the Peltier cooling cycle, which is directly proportional to Ψ_{stem}. A sap-flow meter (SFM1) was mounted below the psychrometer to measure whole-plant water uptake using the Heat Ratio Method (HRM). The schematic (B) depicts the configuration of the heater and thermocouples (T_1 downstream and T_2 upstream) positioned around the xylem tissue.

4.2.2. Statistical and data analysis framework

All data processing and statistical analyses were performed using software R, in RStudio (2024.12.1+563 "Kousa Dogwood" Release), employing specific packages according to the analysis type: *ggplot2* (Wickham, 2011) for the graphs and plots, *lubridate* (Grolemund & Wickham, 2011) to manage temporal data, *FactoMineR* (Lê et al., 2008) and *factoextra* (Kassambara and Mundt, 2016) for multi-variate analysis, *lme4* (Bates et al., 2003) and *MuMIn* (Bartoń, 2010) for mixed models, *lmerTest* (Kuznetsova et al., 2017) for significance of predictors in mixed models. Prior to the analyses, datasets were quality-checked for missing or outlier values, time-synchronized across sensor types, and partitioned into daytime (PAR > 50 µmol m^{-2} s^{-1}) and nighttime (PAR < 50 µmol m^{-2} s^{-1}) subsets to separate periods of active photosynthesis and transpiration from nocturnal recovery (Campbell and Norman, 1998; Monteith and Unsworth, 2013).

To identify pairwise associations among physiological and environmental variables, Spearman's rank correlation coefficients were computed. This method was chosen because it is robust to non-linear relationships and non-normally distributed data. The correlation matrices were accompanied by significance tests (p-values). The variables included in the analysis were stem water potential (Ψ_{stem}, MPa), total sap flow rate (TFR, L h^{-1}), soil volumetric water content (SWC, m^3 m^{-3}), vapor pressure deficit (VPD, kPa), photosynthetically active radiation (PAR, µmol m^{-2} s^{-1}), and an irrigation proxy variable (Proxy_irr; 0 = no irrigation, 1 = irrigation). This latter variable was defined consistently with the approach described in Section 2.2.4, where irrigation events were assigned a value of 1 during irrigation and for the following 12 hours, and 0 for the 12 hours preceding each event.

A Principal Component Analysis (PCA) was conducted to explore the multivariate structure of the dataset and to identify the most influential environmental and physiological drivers of Ψ_{stem} and TFR. For each subset (daytime and nighttime), the first two components (PC1 and PC2) were analysed, as they accounted for the majority of total variance (>50%). Variable contributions (loading coefficients) were interpreted to identify dominant gradients, and cosine similarity (cos ϑ) between variable loadings was calculated to quantify how strongly each factor was aligned with Ψ_{stem} and TFR, respectively (Korenius et al., 2007).

To quantify the relative influence of VPD and SWC on Ψ_{stem} and TFR, Linear Mixed-Effects Models (LMMs) were fitted (Yang, 2010). The LMMs followed this general model equation:

$$Y = X\beta + Z\gamma + \varepsilon \qquad \text{Eq. 1}$$

Where Y is the vector of response variable (either Ψ_{stem} or TFR), X is the designed matrix for fixed effects, β are the fixed-effect coefficients for the predictors (VPD and SWC), Z is the random effect associated with date (to account for temporal autocorrelation and day-specific conditions), γ are random effects, assumed normal distributed with mean 0 and variance σ^2, ε is the residual error, assumed normal distributed with mean 0 and variance σ^2. Consequently, separate models were fitted for daytime and nighttime datasets. Effect sizes and their 95% confidence intervals (CIs) were visualized as point-range coefficient plots, where significant predictors ($p < 0.05$) were marked with asterisks. Additionally, marginal effect plots were produced to show the predicted influence of each predictor (VPD and SWC) on Ψ_{stem} and TFR, keeping the other variable constant at its median. Model performance was further evaluated by comparing observed versus predicted values, including Pearson's R^2 as a measure of model goodness-of-fit.

4.3. Results and discussion

4.3.1. Vineyard soil features and seasonal environmental conditions

The results of the soil analyses conducted on the same day as the deployment and calibration of the CRNS sensor are presented in Table 1.

Table 1: Results of the soil sample analyses for CRNS sensor calibration at Renmark's experimental vineyard.

Site	Renmark
calibration date	2024/11/27
SOC [a]	0.040
LW [b]	0.015
SWCg [c]	0.22 ± 0.04
SWCg (wt) [d]	0.26
ρ_{bd} [e]	1.18
Nc (Fi Muons) [f]	845
N_0 (Muons) [g]	1486

[a] Soil organic carbon (g g^{-1}); [b] Lattice water (g g^{-1}); [c] Gravimetric soil water content (g g^{-1}); [d] Weighted average gravimetric soil water content (g g^{-1}); [e] soil bulk density (g cm^{-3}); [f] Neutron counts during the calibration campaign corrected using in-situ muon particles (cph); [g] Calibrated parameter based using incoming muon correction (cph) based on Desilets et al. (2010).

These measurements provided the reference values required for the site-specific calibration and characterization of the soil profile. It is important to note that at the time of the CRNS deployment and subsequent soil sampling, the vineyard was already under irrigation. Consequently, the standard deviation observed among soil samples reflected the natural spatial variability in SWC across the site, with wetter samples collected beneath drip-irrigated rows and drier ones originating from the non-irrigated inter-row areas. This variability is consistent with the expected heterogeneity in soil moisture distribution under localized irrigation conditions

The main environmental dynamics observed at the experimental site during the monitoring period (27th November 2024 – 5th February 2025), corresponding to the pre-veraison to preharvest stages (approximately BBCH 77 – 85 according to Lorenz et al. 1995), are depicted in Figure 3.

Figure 3: Seasonal dynamics of soil and atmospheric variables recorded at the experimental vineyard between 27th November 2024 – 5th February 2025. A: hourly trends of SWC (m^3 m^{-3}) measured with the CRNS sensor. B): hourly VPD (kPa) trends representing atmospheric evaporative demand. C): cumulative daily precipitation (P, mm d^{-1}).

Hourly SWC (Figure 3 A), derived from CRNS measurements, displayed some variability throughout the season, with a gradual decline from early December to mid-summer and distinct short-term fluctuations. These fluctuations reflect both the daily soil-atmosphere equilibrium and the temporal sensitivity of the CRNS signal to near-surface temperature dynamics, as previously discussed concerning the muon-calibrated signal in Section 2.3.1. Considering that irrigation was homogeneously provided on a daily 8/10 hour-base across the monitored period, SWC showed evident day-night variations, with lower values generally coinciding with high evaporative demand, expressed by VPD (Figure 3 B). The limited rainfall events recorded during the period (Figure 3 C) caused short-term but visible increases in SWC, confirming the responsiveness of the CRNS probe to these events. However, these transient peaks were followed by rapid declines, indicating high evaporative losses and limited infiltration under hot and dry summer conditions.

The VPD exhibited a strong diurnal pattern, with midday peaks frequently exceeding 5 kPa and lower peaks approaching zero during nighttime hours. Although VPD values above 5 kPa are not representative of average daily conditions, they occur with high frequency and predictability during the afternoon peaks of intense summer heatwaves in the Riverland region (Cogato et al., 2021).

4.3.2. Observations of vine water status dynamics

The temporal patterns observed in Ψ_{stem} and sap flow TFR (Figure 4) align closely with the environmental trends described in Figure 3, underscoring the strong coupling between vine water status and both soil and atmospheric conditions. A visual inspection of the time-series and variance among the four monitored vine rows (NE, NW, SE, SW) did not reveal any consistent differences in either Ψ_{stem} or TFR. The responses were comparable across all sectors, suggesting uniform vine behaviour and irrigation distribution throughout the vineyard. Therefore, the values were averaged across rows to represent mean vine water status in the subsequent analyses.

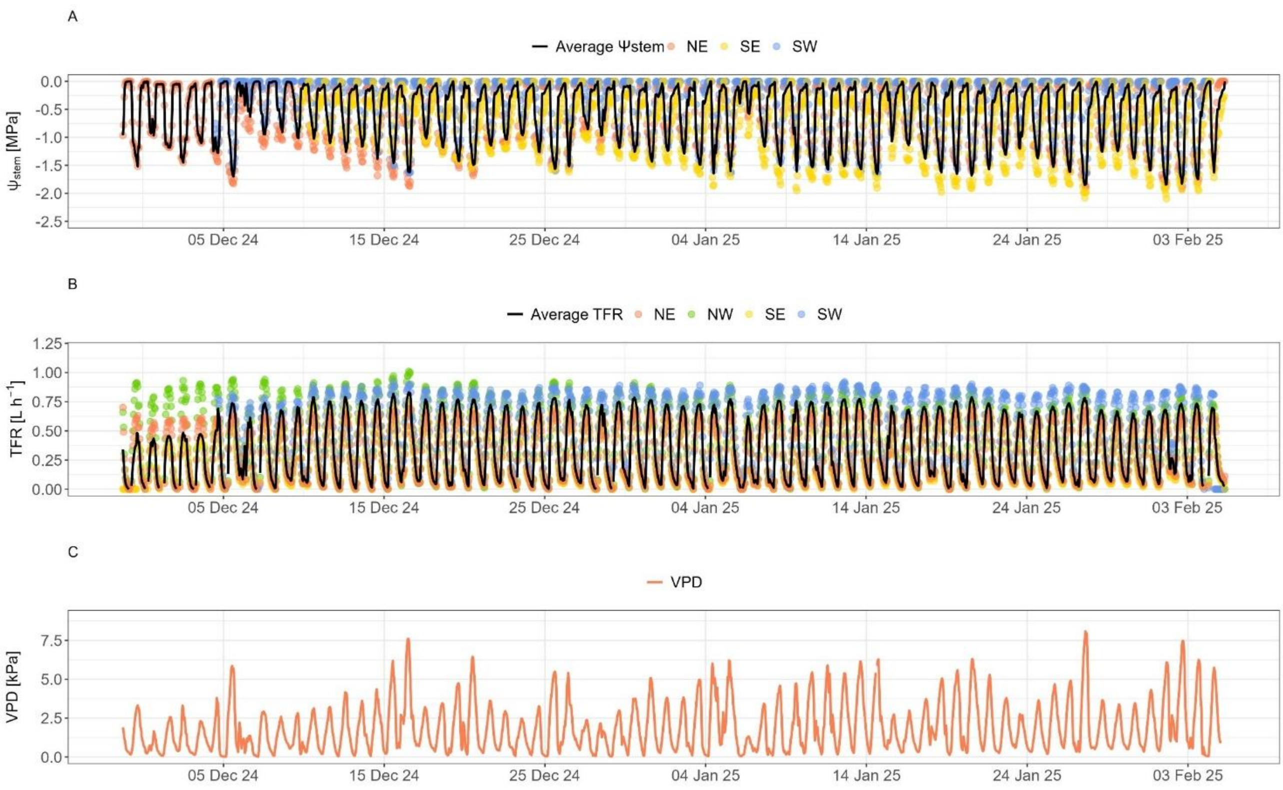

Figure 4: Seasonal dynamics of vine water status variables recorded at the experimental vineyard between 27 November 2024 and 5 February 2025. (A) Hourly measurements of stem water potential (Ψ_{stem}, MPa) acquired with psychrometers and (B) hourly total sap flow rate (TFR, L h^{-1}) measured with sap-flow meters across all monitored vine rows (NE, NW, SE, SW). (C) Hourly vapor pressure deficit (VPD, kPa) trends representing atmospheric evaporative demand. Black lines indicate the mean values across monitored vines.

Consistent with the day-night variability detected in SWC, Ψ_{stem} (Figure 4 A) displayed a coherent diel pattern aligned with VPD dynamics, with minima intensifying under peak evaporative demand. A consistent pattern was also observed across the monitored vine rows, with average Ψ_{stem} values generally above -1.5 MPa, confirming that vines remained within a well-watered physiological range throughout the season. Sap flow TFR exhibited highly regular diurnal cycles, with daily maxima remaining stable despite extreme VPD values, suggesting that irrigation fully met vine water demand and prevented significant hydraulic limitation (Benyahia et al., 2023; Wei et al., 2020).

Interestingly, both Ψ_{stem} and sap flow TFR values during nighttime did not always drop to zero, potentially indicating that, despite continuous irrigation, vines may relocate water or nutrients during nocturnal hours. While this hypothesis requires further validation, comparable observations of non-zero nighttime sap flow TFR have been reported in grapevines (Fuentes et al., 2014; Wei et al., 2020). In grapevines grown under semi-arid conditions, nocturnal transpiration or root-driven flow has been documented by Montoro et al. (2020), although Dayer et al. (2021) suggested that nighttime water loss constitutes only a small fraction of daily water use.

Overall, the amplitude of Ψ_{stem} oscillations was greater than that of sap flow TFR (Figure 4 B), indicating that Ψ_{stem} responded more directly to short-term VPD fluctuations, while sap flow TFR integrated the overall water flux over longer time scales. During some particularly intense VPD peaks, Ψ_{stem} values temporarily dropped below -1.5 MPa. Indeed, irrigated vineyards generally maintain Ψ_{stem} > -1.5 MPa to avoid cavitation and loss of turgor (Gambetta et al., 2020). While brief dips below this threshold can occur under extreme evaporative demand, they typically do not lead to sustained physiological damage unless prolonged (Shtai et al., 2024; Wenter et al., 2022).

To further support the interpretation of periods characterized by elevated VPD, Figure 5 depicts the diurnal evolution of VPD, SWC, Ψ_{stem}, and sap flow TFR, highlighting their synchronized responses under extreme atmospheric demand.

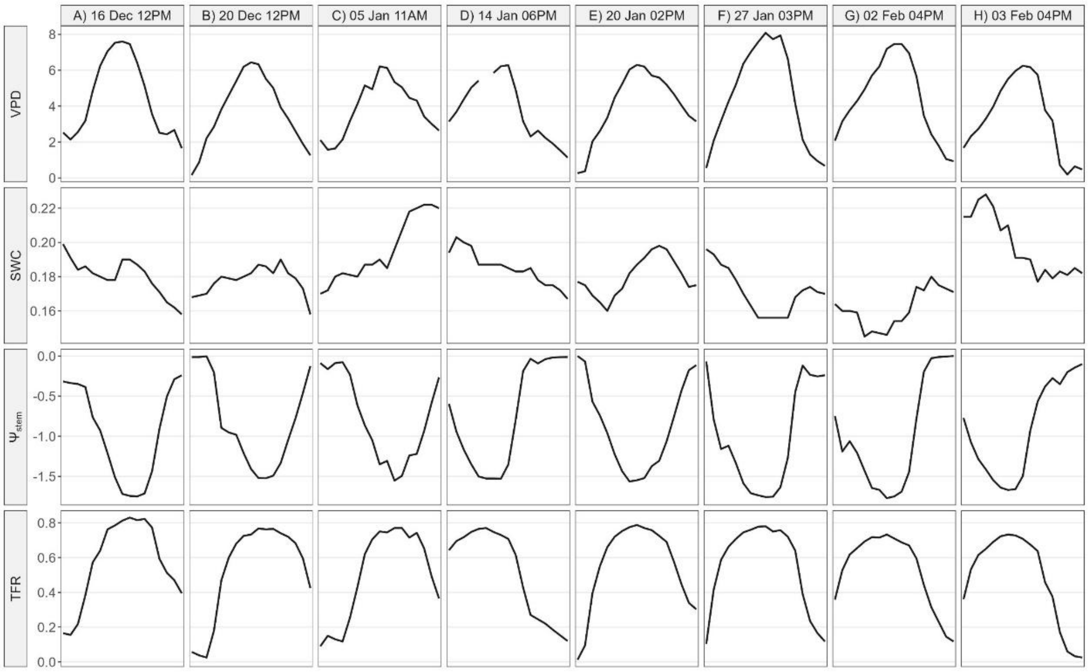

Figure 5: Intra-hour dynamics of VPD (kPa), SWC (m^3 m^{-3}), Ψ_{stem} (MPa), and sap flow TFR (L h^{-1}) on eight selected dates characterized by peak VPD values exceeding 5 kPa. Each panel represents a four-hour window centered around the daily VPD maximum (± 2 hours).

On days when VPD reached extreme afternoon peaks above 6-7 kPa, corresponding short-term depressions in Ψ_{stem} were observed, while SWC exhibited minor but detectable intra-hour fluctuations consistent with near-surface drying and re-equilibration processes.

In grapevines, Ψ_{stem} and sap flow TFR often exhibit strong diurnal cycles tightly coupled to environmental drivers such as VPD, although correlations with SWC are weaker in non-limiting conditions. However, Wei et al. (2020) observed lagged responses between sap flow TFR and environmental variables, indicating that sap flow TFR does not always instantaneously follow external forcing. Moreover, earlier work by Patakas et al. (2005) anticipated that sap flow TFR in grapevines does not increase indefinitely with increasing VPD and, beyond certain thresholds, the relationship plateaus. The high-frequency monitoring presented here supports the conclusions of Rienth and Scholasch (2019), who underlined the importance of continuous, high-resolution measurements to capture transient Ψ_{stem} fluctuations that are often overlooked by coarser sampling intervals.

4.3.3. Statistical analysis of vine water status and environmental drivers

To further explore the interrelationships among vine physiological responses and environmental drivers, Spearman's rank correlations among variables have been computed (Figure 6). This nonparametric approach allowed to detect monotonic associations without requiring linearity or normal distributions. Hence, this represented a methodological advantage, especially when dealing with ecological or plant-physiological data that frequently exhibit nonlinear responses or threshold behaviour (McDonald, 2014).

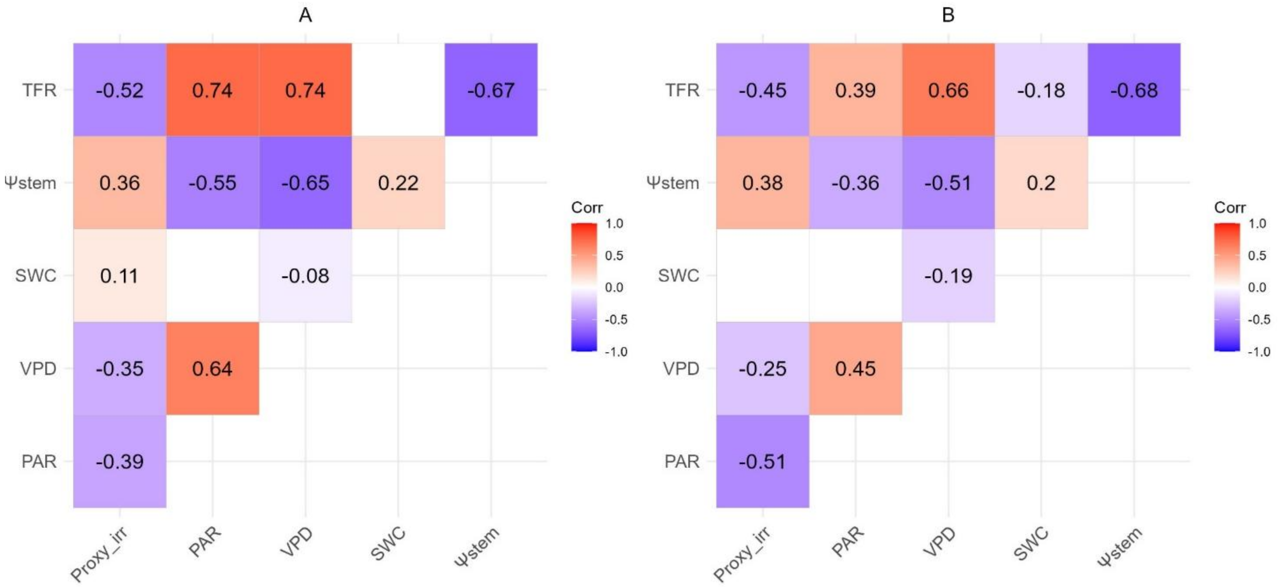

Figure 6: Spearman rank correlation heatmaps among key variables: total flow rate (TFR), stem water potential (Ψ_{stem}), soil water content (SWC), vapor pressure deficit (VPD), photosynthetically active radiation (PAR), and irrigation proxy (Proxy_irr). Panels A and B represent correlation matrices computed for daytime (A; PAR > 50 μmol m^{-2} s^{-1}) and nighttime (B; PAR < 50 μmol m^{-2} s^{-1}) conditions, respectively. The colour scale indicates correlation strength, with red denoting positive and blue negative associations, while blank cells indicated no correlation.

During daytime (Figure 6 A), TFR exhibited strong positive correlations with both VPD (r = 0.74) and PAR (r = 0.74), confirming that sap flow TFR is primarily driven by atmospheric evaporative demand and radiation, consistent with the diurnal dynamics previously discussed. Conversely, Ψ_{stem} showed moderate to strong negative correlations with VPD (r = -0.65) and PAR (r = -0.55), reflecting the expected midday decline in Ψ_{stem} as evaporative demand increases. The observed relationship between Ψ_{stem} and TFR (r = -0.67) indicates that higher sap flow TFR are associated with more negative Ψ_{stem} values, an expected consequence of greater transpiration pull during high VPD episodes (Suter et al., 2019). SWC exhibited a weak negative correlation with VPD and was not significantly correlated with TFR, further confirming that under constant irrigation, SWC played a minor role in regulating sap flow TFR. This observation is consistent with previous findings in semi-arid vineyards, where atmospheric conditions dominate the short-term variability in sap flow TFR when SWC is maintained above critical thresholds (Mancha et al., 2021; Montoro et al., 2016).

At nighttime (Figure 6 B), the correlation matrix highlights a substantial weakening of most relationships compared to daytime, reflecting the expected decoupling between vine water status and atmospheric drivers. The strong positive correlation between TFR and VPD (r = 0.66) suggests that even during the night, sap flow did not completely drop to zero, reinforcing what observed in Figure 4 and the hypothesis that such behaviour likely reflects nighttime hydraulic adjustments and stem refilling. To further sustain this, a negative correlation between TFR and Ψ_{stem} (r = -0.68) was observable, consistent with momentary internal redistribution of water during absence of photosynthesis activity and refilling cycles (Fuentes et al., 2014; Suter et al., 2019). Ψ_{stem} itself showed negative correlations with VPD (r = -0.51) and PAR (r = -0.36), implying that warm, dry nights with higher residual VPD tended to limit complete stem rehydration. Despite in other grape varieties and environment, high nocturnal VPD is a known constraint to full recovery, especially in our climate context, where air humidity remains low even after sunset (Zufferey et al., 2011). Conversely, the positive correlation between Ψ_{stem} and SWC (r = 0.20) suggests that adequate SWC availability supported overnight mitigation of still high VPD.

It is worth noting that SWC and Proxy_irr weakly correlated only during daytime (r = 0.11). Because of that and considering what already observed and discussed in Section 2.3.4, further comparison of SWC changes in response to irrigation events is presented (Figure 7). A possible estimation of the irrigation contribution to the SWC was also performed assuming a soil layer of 30 cm, based on average CRNS penetration depth.

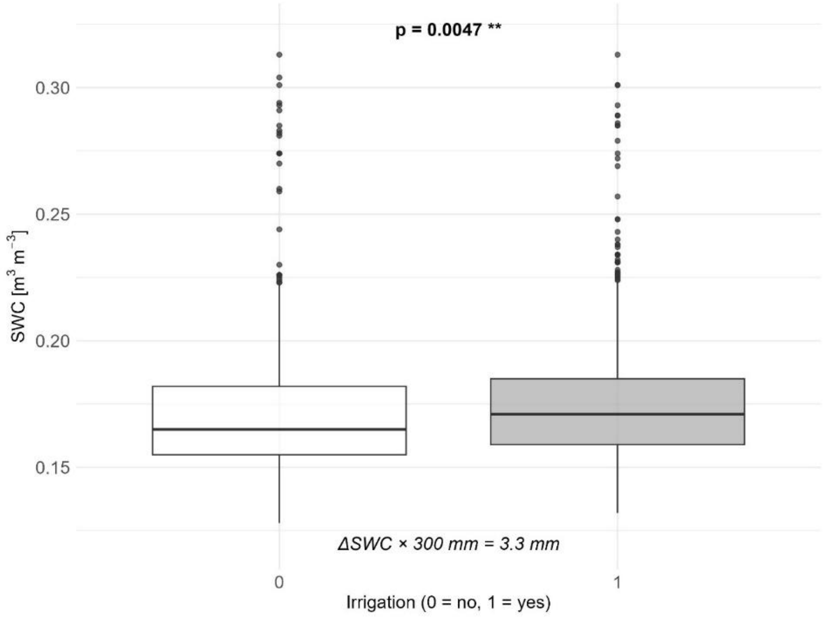

Figure 7: Boxplots showing SWC (m^3 m^{-3}) measured with CRNS under irrigated (1) and non-irrigated (0) conditions, based on a binary irrigation proxy (Proxy_irr) assigned to 12 hours before and after each irrigation event. Statistical comparisons were conducted using linear models to assess the significance of SWC differences between the two conditions. Significance levels were assigned based on conventional p-values thresholds ($p < 0.05$, 0.01, and 0.001). In addition, the equivalent change in SWC was estimated as ΔSWC × 300 mm and reported within each panel to provide an integrated measure of CRNS sensitivity to irrigation in 30 cm depth.

In contrast to the patterns observed in the Spearman rank correlation, Proxy_irr exhibited a significant and measurable effect on SWC ($p < 0.01$; ΔSWC = 3.3 mm), indicating that the CRNS sensor effectively captured increases in SWC associated with irrigation events. Consequently, SWC was retained as the representative variable for irrigation in the subsequent analyses, while Proxy_irr was excluded to avoid collinearity. Similarly, PAR values were also excluded from further analytical steps, as they had already been used to segment the dataset into daytime and nighttime periods, and their inclusion could introduce redundancy in the multivariate structure.

To further explore the joint variability among environmental and physiological variables, a PCA (Principal Component Analysis) was conducted (Figure 8). This multivariate approach allowed the identification of patterns and dominant axes of variation across the monitored period, highlighting how vine water status responds to concurrent fluctuations in soil and atmospheric drivers.

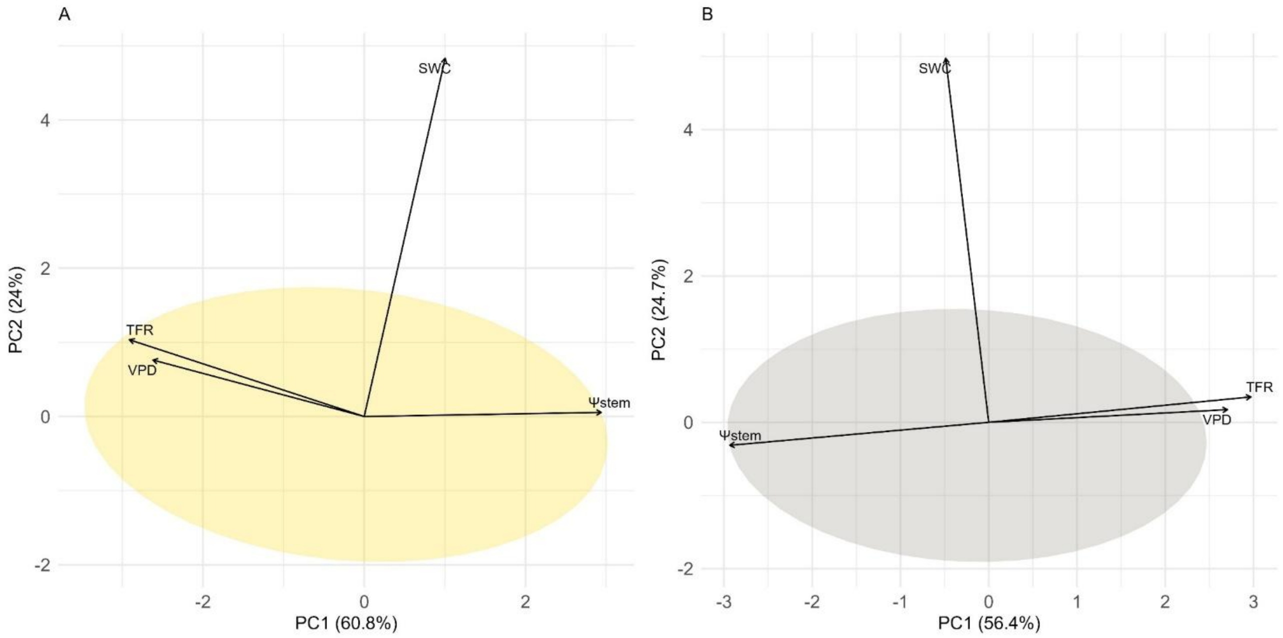

Figure 8: Principal Component Analysis (PCA) biplots of environmental and physiological variables during (A) daytime and (B) nighttime. Vectors indicate variable loadings: total flow rate (TFR), stem water potential (Ψstem), soil water content (SWC), and vapor pressure deficit (VPD). The ellipses represent the 95 % confidence region of vine measurements. Loading coefficients were interpreted to identify dominant gradients, and cosine similarity (cos ϑ) between variable loadings was calculated to quantify how strongly each factor was aligned with Ψ_{stem} and TFR, respectively (Korenius et al., 2007).

During the daytime (Figure 8 A), the first two components explained 84.8 % of the total variance (PC1 = 60.8 %, PC2 = 24.0 %). PC1 captured the primary gradient of vine water status under evaporative demand, with strong and oppositely directed loadings of Ψ_{stem} and VPD - TFR, indicating that the latter were closely coupled. Besides, Ψ_{stem} aligned positively with PC1 (Ψ_{stem} – VPD cos $\vartheta \approx -0.98$; Ψ_{stem} – TFR cos ≈ -0.95), whereas VPD and TFR pointed in the opposite direction (cos $\vartheta \approx 0.99$), confirming that increases in evaporative demand and sap flow TFR corresponded to more negative Ψ_{stem}. PC2 was largely driven by SWC, positioned almost orthogonally to other variables (cos $\theta \approx 0$), showing that short-term variation in SWC was relatively independent from daily fluctuations in VPD and vine water status. This structure suggests that, during the day, vine hydraulics were dominated by atmospheric forcing rather than by SWC variability, consistent with the daily irrigation regime and limited range of SWC observations.

At night (Figure 8 B), the first two components explained 81.1 % of the total variance (PC1 = 56.4 %, PC2 = 24.7 %). The loading pattern maintained a similar orientation but with reduced separation among variables, reflecting the partial decoupling of the SPAC when photosynthesis activity ceased, also showing a generally weaker relationship (Ψ_{stem} – VPD cos $\vartheta \approx -0.85$; Ψ_{stem} – TFR cos $\vartheta \approx -0.82$). VPD, TFR and Ψ_{stem} remained mainly associated with the PC1 axis, but their vectors were more closely aligned. This might be interpreted as a slightly weaker hydraulic gradient, as expected. SWC continued to dominate PC2, confirming that SWC variations did not directly constrained nighttime physiological processes.

Building on the relationships revealed by the PCA, which highlighted and confirmed the dominant atmospheric control over vine water dynamics and the secondary role of SWC, the subsequent analysis focused on quantifying the magnitude and direction of these effects. To this end, LMMs (Linear Mixed Models) were employed to statistically evaluate how VPD and SWC influenced Ψ_{stem} and TFR, while accounting for temporal variability across dates (Figure 9).

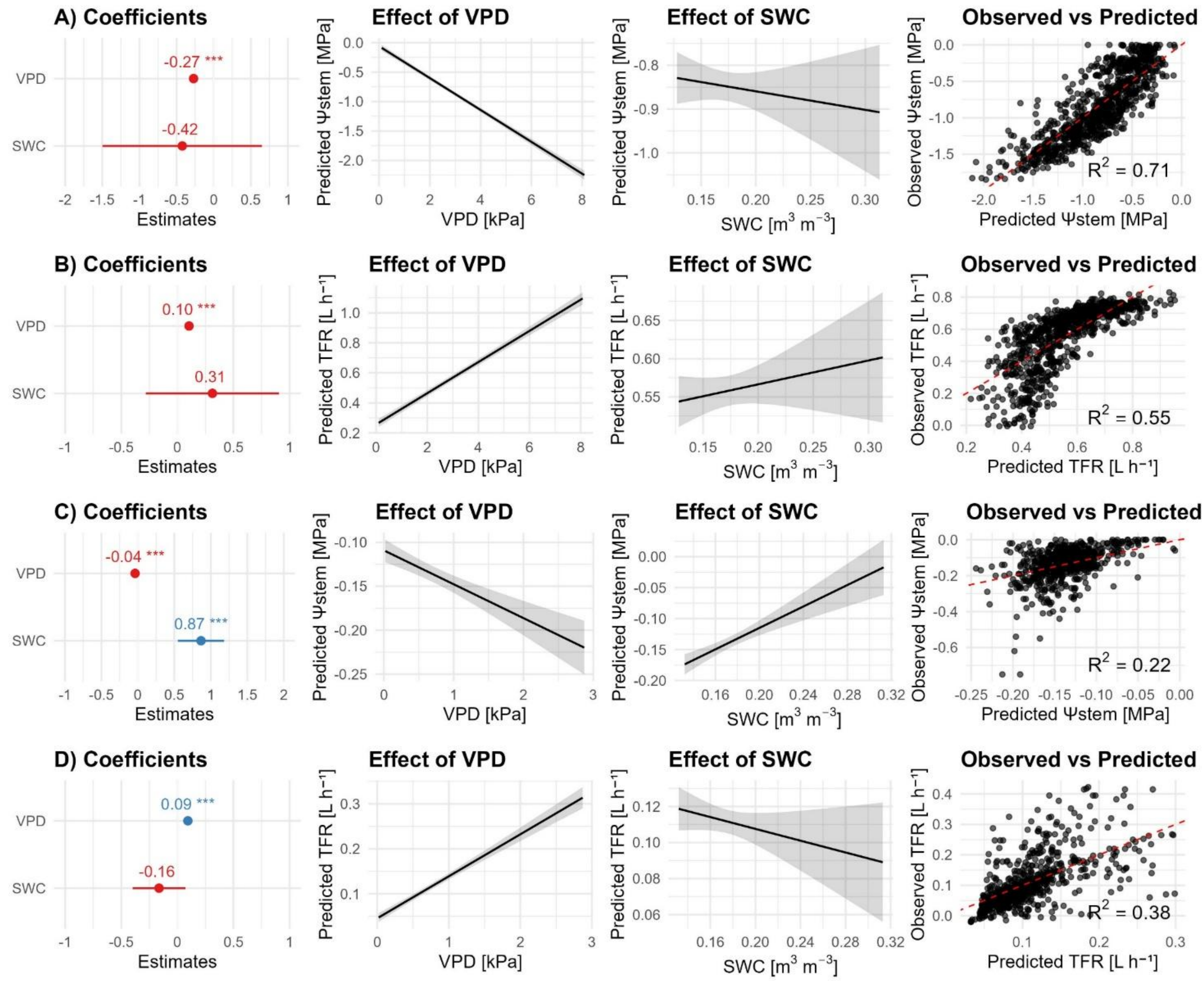

Figure 9: Linear mixed-effect models (LMMs) estimate for daytime and nighttime. A) Daytime effects on Ψ_{stem}. (B) Daytime effects on TFR. C) Nighttime effects on Ψ_{stem}. D) Nighttime effects on TFR. Left column: fixed-effect coefficients with 95% Cis and significance levels, assigned based on conventional p-values thresholds ($p < 0.05$, 0.01, and 0.001); middle columns: partial effects of VPD and SWC with 95% CIs; right column:

observed vs. model-predicted values with coefficient of determination (R^2). Models included date as a random effect.

Across all models, VPD showed a consistent and highly significant effect ($p < 0.001$), exerting a strong negative influence on Ψ_{stem} and a positive one on TFR, confirming that atmospheric demand was the primary driver of vine hydraulic responses in our context. This coupling between VPD, sap flow TFR, and Ψ_{stem} is further confirmed from this analysis and in agreement with previous studies demonstrating that, when SWC is adequate, atmospheric factors dominate diurnal fluctuations in vine water status (Kokkotos et al., 2025; Suter et al., 2019; Wei et al., 2020). In contrast, SWC displayed limited and often non-significant effects, except for a positive and significant influence on nighttime Ψ_{stem} (Figure 9 C, left panel), reinforcing the hypothesis that higher SWC might have favoured nocturnal rehydration and partial recovery of Ψ_{stem}. The relatively large standard errors associated with SWC (Figure 9, middle panels) are plausibly related to the natural variability of SWC at the field scale and to the broader spatial footprint of the CRNS system compared with the vine-level physiological measurements. Nevertheless, the CRNS sensor successfully detected SWC fluctuations and irrigation-related increases in SWC across the monitored period, confirming what observed in the previous chapters about its suitability for capturing soil water dynamics in relatively uniform fields. The observed-versus-predicted plots further showed stronger model performance during daytime (Figure 9 A, B, right panels. $R^2 = 0.55 - 0.71$) than nighttime (Figure 9 C, D, right panels. $R^2 = 0.22 - 0.38$), which is expected given that vines are photosynthetically active and hydraulically coupled with the atmosphere during the day, while at night water fluxes are largely governed by internal processes and weaker vapor gradients (Montoro et al., 2020; Steppe et al., 2015).

4.4. Summary and conclusions

This chapter provided an integrated, high-resolution assessment of vine water dynamics under semi-arid conditions by combining continuous soil, plant, and atmospheric monitoring with advanced statistical modelling. Seasonal observations revealed that the vineyard experienced persistently high evaporative demand, with frequent VPD peaks above 5 kPa during summer heatwaves. Despite this, daily drip irrigation maintained the vines in non-stress conditions, as indicated by Ψ_{stem} values generally above -1.5 MPa and stable diurnal sap flow TFR patterns. SWC derived from the CRNS system exhibited clear day-night oscillations and consistent irrigation-driven increases, confirming its sensitivity and reliability as a field-scale proxy for water inputs.

Spearman correlation and PCA both highlighted the dominant role of atmospheric forcing on vine hydraulics. During daytime, strong positive correlations between VPD and TFR, coupled with negative correlations with Ψ_{stem}, revealed a tight coupling between transpiration demand and water potential dynamics. PCA results confirmed this structure, with the first principal component (explaining ~60 % of the variance) defined by an inverse VPD-Ψ_{stem} relationship, while SWC loaded orthogonally on the second component, reflecting its background influence independent of atmospheric fluctuations. The nighttime PCA showed a partial decoupling of these relationships, consistent with reduced transpiration and the onset of hydraulic recovery processes.

LMMs quantified these relationships, confirming VPD as the principal driver of vine water status across all conditions ($p < 0.001$). The significant positive effect of SWC on nighttime Ψ_{stem} further supported the hypothesis that higher SWC values promotes nocturnal rehydration once stomata close. Model performance was stronger during the day (R^2 = 0.55-0.71) than at night (R^2 = 0.22-0.38), in line with the diurnal predominance of photosynthetic activity and atmospheric coupling. Integrating continuous field monitoring with robust statistical approaches such as LMMs provided significant advantages for advancing in data-driven vineyard management. By simultaneously estimating fixed effects of environmental drivers (e.g., VPD, SWC) and accounting for random temporal variability, LMMs increased the reliability of inferences compared with traditional regression approaches. In viticulture, reviews of data-driven irrigation methods emphasized that monitoring tools (soil moisture sensors, stem or trunk water potential measurements, sap flow sensors) are foundational, but their integration with robust statistical models and control logics remains rather unexplored (Jenkins and Block, 2024). Recent applications in grapevine systems have demonstrated that data-driven irrigation scheduling based on real-time physiological and soil monitoring systems can substantially improve water-use efficiency. For instance, Schlank et al. (2024) reported that in *Vitis vinifera* cv. Cabernet Sauvignon, irrigation scheduling derived from data-based thresholds reduced applied water volumes by up to 65 % without compromising yield or fruit quality. Similarly, Garofalo et al., (2023) found that a decision-support system based on continuous SWC monitoring preserved productive performance while achieving 10-17 % water savings. Thus, although direct case studies applying LMMs to sensor-based grapevine water datasets are sparse, the success of analogous modelling frameworks and the physiological rationale for continuous monitoring strongly suggest that this methodology could provide further advancements.

Overall, the integration of continuous CRNS, sap-flow, and psychrometric monitoring with correlation, multivariate, and mixed-model analyses proved highly effective in quantifying SPAC interactions under semi-arid vineyard conditions. Beyond the scientific insights, this framework also shows strong potential for data-driven irrigation management, offering a scalable and adaptable approach for optimizing water use, enhancing vineyard resilience, and improving sustainability in semi-arid viticultural regions.

4.5. References

Allen, R. G., Pereira, L., Raes, D., & Smith, M. (Eds.). (1998). *Crop evapotranspiration: Guidelines for computing crop water requirements* (repr). Food and Agriculture Organization of the United Nations.

Asbjornsen, H., Goldsmith, G. R., Alvarado-Barrientos, M. S., Rebel, K., Van Osch, F. P., Rietkerk, M., Chen, J., Gotsch, S., Tobón, C., Geissert, D. R., Gómez-Tagle, A., Vache, K., & Dawson, T. E. (2011). Ecohydrological advances and applications in plant–water relations research: A review. *Journal of Plant Ecology*, *4*(1–2), 3–22. https://doi.org/10.1093/jpe/rtr005

Bartoń, K. (2010). *MuMIn: Multi-Model Inference* (p. 1.48.11) [Dataset]. https://doi.org/10.32614/CRAN.package.MuMIn

Bates, D., Maechler, M., Bolker, B., & Walker, S. (2003). *lme4: Linear Mixed-Effects Models using "Eigen" and S4* (p. 1.1-37) [Dataset]. https://doi.org/10.32614/CRAN.package.lme4

Benyahia, F., Bastos Campos, F., Ben Abdelkader, A., Basile, B., Tagliavini, M., Andreotti, C., & Zanotelli, D. (2023). Assessing Grapevine Water Status by Integrating Vine Transpiration, Leaf Gas Exchanges, Chlorophyll Fluorescence and Sap Flow Measurements. *Agronomy*, *13*(2), 464. https://doi.org/10.3390/agronomy13020464

Brillante, L., Bois, B., Lévêque, J., & Mathieu, O. (2016). Variations in soil-water use by grapevine according to plant water status and soil physical-chemical characteristics—A 3D spatio-temporal analysis. *European Journal of Agronomy*, *77*, 122–135. https://doi.org/10.1016/j.eja.2016.04.004

Bureau of Meteorology. (2025). *Climate statistics for Australian locations*. https://www.bom.gov.au/climate/averages/tables/cw_024048_All.shtml#rainfall

Burgess, S. S. O., Adams, M. A., Turner, N. C., & Ong, C. K. (1998). The redistribution of soil water by tree root systems. *Oecologia*, *115*(3), 306–311. https://doi.org/10.1007/s004420050521

Campbell, G. S., & Norman, J. M. (1998). *Introduction to environmental biophysics* (2nd ed). Springer.

Chaves, M. M., Zarrouk, O., Francisco, R., Costa, J. M., Santos, T., Regalado, A. P., Rodrigues, M. L., & Lopes, C. M. (2010). Grapevine under deficit irrigation: Hints from physiological and molecular data. *Annals of Botany*, *105*(5), 661–676. https://doi.org/10.1093/aob/mcq030

Choné, X. (2001). Stem Water Potential is a Sensitive Indicator of Grapevine Water Status. *Annals of Botany*, *87*(4), 477–483. https://doi.org/10.1006/anbo.2000.1361

Choné, X., Trégoat, O., Leeuwen, C. van, & Dubourdieu, D. (2000). Vine water deficit: Among the 3 applications of pressure chamber, stem water potential is the most sensitive indicator. *OENO One*, *34*(4), 169–176. https://doi.org/10.20870/oeno-one.2000.34.4.996

Cogato, A., Jewan, S. Y. Y., Wu, L., Marinello, F., Meggio, F., Sivilotti, P., Sozzi, M., & Pagay, V. (2022). Water Stress Impacts on Grapevines (Vitis vinifera L.) in Hot Environments: Physiological and Spectral Responses. *Agronomy*, *12*(8), 1819. https://doi.org/10.3390/agronomy12081819

Cogato, A., Wu, L., Jewan, S. Y. Y., Meggio, F., Marinello, F., Sozzi, M., & Pagay, V. (2021). Evaluating the Spectral and Physiological Responses of Grapevines (Vitis vinifera L.) to Heat and Water Stresses under Different Vineyard Cooling and Irrigation Strategies. *Agronomy*, *11*(10), 1940. https://doi.org/10.3390/agronomy11101940

Dayer, S., Herrera, J. C., Dai, Z., Burlett, R., Lamarque, L. J., Delzon, S., Bortolami, G., Cochard, H., & Gambetta, G. A. (2021). Nighttime transpiration represents a negligible part of water loss and does not increase the risk of water stress in grapevine. *Plant, Cell & Environment*, *44*(2), 387–398. https://doi.org/10.1111/pce.13923

Desilets, D., Zreda, M., & Ferré, T. P. A. (2010). Nature's neutron probe: Land surface hydrology at an elusive scale with cosmic rays. *Water Resources Research*, *46*(11). https://doi.org/10.1029/2009WR008726

Fuentes, S., De Bei, R., Collins, M. J., Escalona, J. M., Medrano, H., & Tyerman, S. (2014). Night-time responses to water supply in grapevines (*Vitis vinifera* L.) under deficit irrigation and partial root-zone drying. *Agricultural Water Management*, *138*, 1–9. https://doi.org/10.1016/j.agwat.2014.02.015

Fuentes, S., & Gago, J. (2022). Chapter 7—Modern approaches to precision and digital viticulture. In J. M. Costa, S. Catarino, J. M. Escalona, & P. Comuzzo (Eds.), *Improving Sustainable Viticulture and Winemaking Practices* (pp. 125–145). Academic Press. https://doi.org/10.1016/B978-0-323-85150-3.00015-3

Gambetta, G. A., Herrera, J. C., Dayer, S., Feng, Q., Hochberg, U., & Castellarin, S. D. (2020). The physiology of drought stress in grapevine: Towards an integrative definition of drought tolerance. *Journal of Experimental Botany*, *71*(16), 4658–4676. https://doi.org/10.1093/jxb/eraa245

Garofalo, S. P., Intrigliolo, D. S., Camposeo, S., Alhajj Ali, S., Tedone, L., Lopriore, G., De Mastro, G., & Vivaldi, G. A. (2023). Agronomic Responses of Grapevines to an Irrigation Scheduling Approach Based on Continuous Monitoring of Soil Water Content. *Agronomy*, *13*(11), 2821. https://doi.org/10.3390/agronomy13112821

Grolemund, G., & Wickham, H. (2011). Dates and Times Made Easy with lubridate. *Journal of Statistical Software*, *40*, 1–25. https://doi.org/10.18637/jss.v040.i03

Jenkins, M., & Block, D. E. (2024). A Review of Methods for Data-Driven Irrigation in Modern Agricultural Systems. *Agronomy*, *14*(7), Article 7. https://doi.org/10.3390/agronomy14071355

Kassambara, A., & Mundt, F. (2016). *factoextra: Extract and Visualize the Results of Multivariate Data Analyses*. https://rpkgs.datanovia.com/factoextra/index.html

Kokkotos, E., Zotos, A., Tsesmelis, D. E., Petrakis, E. A., & Patakas, A. (2025). Estimating Grapevine Transpirational Losses Using Models Under Different Conditions of Soil Moisture. *Horticulturae*, *11*(6), 665. https://doi.org/10.3390/horticulturae11060665

Korenius, T., Laurikkala, J., & Juhola, M. (2007). On principal component analysis, cosine and Euclidean measures in information retrieval. *Information Sciences*, *177*(22), 4893–4905. https://doi.org/10.1016/j.ins.2007.05.027

Kuznetsova, A., Brockhoff, P. B., & Christensen, R. H. B. (2017). lmerTest Package: Tests in Linear Mixed Effects Models. *Journal of Statistical Software*, *82*, 1–26. https://doi.org/10.18637/jss.v082.i13

Lê, S., Josse, J., & Husson, F. (2008). FactoMineR: An R Package for Multivariate Analysis. *Journal of Statistical Software*, *25*, 1–18. https://doi.org/10.18637/jss.v025.i01

Lebon, E., Dumas, V., Pieri, P., & Schultz, H. R. (2003). Modelling the seasonal dynamics of the soil water balance of vineyards. *Functional Plant Biology*, *30*(6), 699. https://doi.org/10.1071/FP02222

Lorenz, D. h., Eichhorn, K. w., Bleiholder, H., Klose, R., Meier, U., & Weber, E. (1995). Growth Stages of the Grapevine: Phenological growth stages of the grapevine (Vitis vinifera L. ssp. vinifera)—Codes and descriptions according to the extended BBCH scale. *Australian Journal of Grape and Wine Research*, *1*(2), 100–103. https://doi.org/10.1111/j.1755-0238.1995.tb00085.x

Mancha, L. A., Uriarte, D., & Prieto, M. del H. (2021). Characterization of the Transpiration of a Vineyard under Different Irrigation Strategies Using Sap Flow Sensors. *Water*, *13*(20), 2867. https://doi.org/10.3390/w13202867

Martinez, E., Cancela, J. J., Cuesta, T., & Neira, X. (2011). Review. Use of psychrometers in field measurements of plant material: Accuracy and handling difficulties. *SPANISH JOURNAL OF AGRICULTURAL RESEARCH*, *9*, 313–328.

McDonald, J., H. (2014). *Handbook of Biological Statistics* (3rd ed.). Sparky House Publishing. https://www.biostathandbook.com/spearman.html?utm_source=chatgpt.com

McJannet, D., Rasche, D., Marano, J., Hawdon, A., Stenson, M., & Schrön, M. (2025). Over-Water Low-Energy Neutron Observations for Intensity Corrections Across Cosmic-Ray Soil Moisture Sensor Networks. *Water Resources Research*, *61*(9), e2024WR039727. https://doi.org/10.1029/2024WR039727

Monteith, J. L., & Unsworth, M. H. (2013). *Principles of environmental physics: Plants, animals, and the atmosphere* (4th edition). Elsevier/Academic Press.

Montoro, A., Mañas, F., & López-Urrea, R. (2016). Transpiration and evaporation of grapevine, two components related to irrigation strategy. *Agricultural Water Management*, *177*, 193–200. https://doi.org/10.1016/j.agwat.2016.07.005

Montoro, A., Torija, I., Mañas, F., & López-Urrea, R. (2020). Lysimeter measurements of nocturnal and diurnal grapevine transpiration: Effect of soil water content, and phenology. *Agricultural Water Management*, *229*, 105882. https://doi.org/10.1016/j.agwat.2019.105882

Patakas, A., Noitsakis, B., & Chouzouri, A. (2005). Optimization of irrigation water use in grapevines using the relationship between transpiration and plant water status. *Agriculture, Ecosystems & Environment*, *106*(2), 253–259. https://doi.org/10.1016/j.agee.2004.10.013

Prosser, I. P., Chiew, F. H. S., & Stafford Smith, M. (2021). Adapting Water Management to Climate Change in the Murray–Darling Basin, Australia. *Water*, *13*(18), 2504. https://doi.org/10.3390/w13182504

Rienth, M., & Scholasch, T. (2019). State-of-the-art of tools and methods to assess vine water status. *OENO One*, *53*(4). https://doi.org/10.20870/oeno-one.2019.53.4.2403

Robinson, G. M., & Song, B. (2023). Managing Water for Environmental Provision and Horticultural Production in South Australia's Riverland. *Sustainability*, *15*(15), 11546. https://doi.org/10.3390/su151511546

Schlank, R., Kidman, C. M., Gautam, D., Jeffery, D. W., & Pagay, V. (2024). Data-driven irrigation scheduling increases the crop water use efficiency of Cabernet Sauvignon grapevines. *Irrigation Science*, *42*(1), 29–44. https://doi.org/10.1007/s00271-023-00866-7

Scholander, P. F., Bradstreet, E. D., Hemmingsen, E. A., & Hammel, H. T. (1965). Sap Pressure in Vascular Plants. *Science*, *148*(3668), 339–346. https://doi.org/10.1126/science.148.3668.339

Shtai, W., Asensio, D., Kadison, A. E., Schwarz, M., Raifer, B., Andreotti, C., Hammerle, A., Zanotelli, D., Haas, F., Niedrist, G., Wohlfahrt, G., & Tagliavini, M. (2024). Soil water availability modulates the response of grapevine leaf gas exchange and PSII traits to a simulated heat wave. *Plant and Soil*, *501*(1), 537–554. https://doi.org/10.1007/s11104-024-06536-7

Steppe, K., Vandegehuchte, M. W., Tognetti, R., & Mencuccini, M. (2015). Sap flow as a key trait in the understanding of plant hydraulic functioning. *Tree Physiology*, *35*(4), 341–345. https://doi.org/10.1093/treephys/tpv033

Stevanato, L., Baroni, G., Oswald, S. E., Lunardon, M., Mares, V., Marinello, F., Moretto, S., Polo, M., Sartori, P., Schattan, P., & Ruehm, W. (2022). An Alternative Incoming Correction for Cosmic-Ray Neutron Sensing Observations Using Local Muon Measurement. *Geophysical Research Letters*, *49*(6), e2021GL095383. https://doi.org/10.1029/2021GL095383

Suter, B., Triolo, R., Pernet, D., Dai, Z., & Van Leeuwen, C. (2019). Modeling Stem Water Potential by Separating the Effects of Soil Water Availability and Climatic Conditions on Water Status in Grapevine (Vitis vinifera L.). *Frontiers in Plant Science*, *10*. https://doi.org/10.3389/fpls.2019.01485

Valentini, G., Allegro, G., Pastore, C., Sangiorgio, D., Noferini, M., Muzzi, E., & Filippetti, I. (2024). Use of an automatic fruit-zone cooling system to cope with multiple summer stresses in Sangiovese and Montepulciano grapes. *Frontiers in Plant Science*, *15*. https://doi.org/10.3389/fpls.2024.1391963

Wei, X., Fu, S., Chen, D., Zheng, S., Wang, T., & Bai, Y. (2020). Grapevine Sap Flow in Response to Physio-Environmental Factors under Solar Greenhouse Conditions. *Water*, *12*(11), 3081. https://doi.org/10.3390/w12113081

Wenter, A., Zanotelli, D., Tagliavini, M., & Andreotti, C. (2022). Thresholds of soil and plant water availability that affect leaf transpiration, stomatal conductance and photosynthesis in grapevines. *Acta Horticulturae*, *1335*, 605–612. https://doi.org/10.17660/ActaHortic.2022.1335.76

Wickham, H. (2011). Ggplot2. *WIREs Computational Statistics*, *3*(2), 180–185. https://doi.org/10.1002/wics.147

Williams, L. E., & Baeza, P. (2007). Relationships among Ambient Temperature and Vapor Pressure Deficit and Leaf and Stem Water Potentials of Fully Irrigated, Field-Grown Grapevines. *American Journal of Enology and Viticulture*, *58*(2), 173–181. https://doi.org/10.5344/ajev.2007.58.2.173

Yang, R.-C. (2010). Towards understanding and use of mixed-model analysis of agricultural experiments. *Canadian Journal of Plant Science*, *90*(5), 605–627. https://doi.org/10.4141/CJPS10049

Zufferey, V., Cochard, H., Ameglio, T., Spring, J.-L., & Viret, O. (2011). Diurnal cycles of embolism formation and repair in petioles of grapevine (Vitis vinifera cv. Chasselas). *Journal of Experimental Botany*, *62*(11), 3885–3894. https://doi.org/10.1093/jxb/err081

5. Concluding remarks

The research presented in this thesis was developed within the broader effort to improve SWC monitoring in agricultural systems through the integration of innovative technologies and analytical approaches. Building on the objectives defined at the outset, the work progressively advanced from sensor validation to a comprehensive interpretation of SPAC interactions.

Through continuous monitoring of SWC across distinct sites and irrigation systems, the research demonstrated the robustness and versatility of CRNS as non-invasive method for quantifying SWC dynamics. The comparative evaluation of neutron incoming correction factors contributed new insights into how local and global factors affect neutron-derived signals. These results reinforced the sensor's reliability under irrigated conditions, while also highlighting the need for refined calibration procedures to improve temporal responsiveness and accuracy. The findings are particularly relevant for hydrological applications in intensively managed agricultural landscapes, where the characterization of water inputs and redistribution remains a major challenge.

By combining CRNS measurements with plant-level and atmospheric observations, the research moved beyond single-variable analysis toward a systemic and integrative representation of the SPAC. The combined use of continuous SWC and plant physiological measurements, together with atmospheric evaporative demand (VPD) and NDVI-based canopy information from remote sensing, provided a detailed understanding of how soil water availability and atmospheric conditions interact to regulate plant water status. The application of mixed models provided a statistically rigorous framework to quantify these relationships, accounting for both fixed environmental effects and random temporal variability. This modelling approach proved particularly effective in distinguishing day-night physiological responses and in quantifying the transition between soil-driven and atmosphere-driven control of plant water fluxes. Finally, the incorporation of CRNS into a continuous monitoring network that included psychrometers, sap flow meters, and meteorological instruments represents a methodological advancement toward a real-time, data-driven approach to irrigation and hydrological decision-making.

This thesis underscores the value of interdisciplinary approaches that merge environmental physics, plants physiology, sensor technology, and data analysis. In this sense, the research contributed to the emerging paradigm of precision management of water resources in agriculture and hydrology, where continuous environmental observation forms the backbone of predictive management.

The outcomes also carry practical implications. Conducting research under real agricultural conditions, across different irrigation layouts, climates, and soil types, provided empirical evidence of how these technologies perform outside controlled environments. The experiments confirmed that the success of innovative sensing systems depends not only on technological performance but also on their adaptability to operational contexts. The experience gained through field implementation strengthens the potential of CRNS and associated sensors to support both research and on-farm applications, bridging the gap between scientific innovation and practical water management.

Looking ahead, several avenues for further research emerge from this work. Increasing the spatial resolution of CRNS networks through multi-detector arrays would enhance the representation of SWC variability at the sub-field scale. Integrating plant physiological feedbacks into automated irrigation control systems also represents a promising direction, potentially leading to closed-loop irrigation frameworks where soil and plant signals jointly regulate water supply. Additionally, establishing standardized calibration, correction, and data-fusion protocols would facilitate the assimilation of CRNS data into hydrological and crop models at regional or even broader scales.

Beyond the specific experiments and case studies, this thesis contributes to a conceptual and methodological evolution in agricultural hydrology. The results obtained across the experimental sites converge toward a key conclusion: multi-scale and multi-sensor integration is essential for understanding and managing water fluxes in agricultural systems. However, while this approach has proven highly valuable from a research perspective, allowing a more complete interpretation of SPAC interactions, it also highlights the challenges of applying such complex monitoring frameworks at the operational farm scale. The practical adoption of advanced sensing systems is still constrained by costs, maintenance requirements, and data management complexity. Future research should therefore focus not only on technological innovation and scientific accuracy, but also on developing simplified monitoring solutions that retain the core benefits of sensor integration while remaining accessible and manageable within real agricultural settings.